Draft version 0.2

ATLAS NOTE

April 17, 2017

Search for Higgs pair production in the final state of $\gamma\gamma WW^*(\rightarrow l\nu jj)$ using 36.5 fb^{-1} pp collision data at $\sqrt{s}$ = 13 TeV with the ATLAS detector

Yaquan Fang[1], Douglas Gingrich[3], Qi Li[1], Xinchou Lou[1,2], Bruce Mellado Garcia[4], Abdualazem Fadol Mohammed[4], Tshidiso Sydwell Molupe[4], Xifeng Ruan[4], Xiaohu Sun[3], Jin Wang[5], Maosen Zhou[1], Yu Zhang[1]

[1.] *Institute of High Energy Physics, Chinses Academy of Siences, Beijing, China*
[2.] *University of Texas at Dallas, USA*
[3.] *University of Alberta, Canada*
[4.] *University of the Witwatersrand, ZA*
[5.] *University of Sydney, AU*

Abstract

A search is performed for resonant and non-resonant Higgs pair production with one Higgs boson decaying to semi-leptonic WW and the other to $\gamma\gamma$ using proton-proton collision data corresponding to an integrated luminosity of 36.5 fb^{-1} at a 13 TeV centre-of-mass energy recorded with the ATLAS detector. The observed (expected) upper limit at 95% confidence level on the cross section for $gg \rightarrow hh$ is XXX pb (7.78 pb) for the non-resonant Higgs pair production. For resonant Higgs pair production, the observed (expected) upper limits at 95% confidence level on cross section times the branching ratio of $X \rightarrow hh$ range from XXX pb (13.5 pb) to XXX pb (7.09 pb) as a function of the resonant mass from 260 GeV to 500 GeV assuming that the narrow-width approximation holds.

Contents

1 Statements **3**
1.1 List of contributions . . . 3
1.2 Version 0.2 . . . 4
1.3 Version 0.1 . . . 4
1.4 Version 0.0 . . . 4

2 Introduction **5**

3 Data and Monte Carlo samples **6**
3.1 Data samples . . . 6
3.2 Monte Carlo samples . . . 6
3.2.1 MC samples for signals . . . 6
3.2.2 MC samples for SM single Higgs backgrounds . . . 7
3.2.3 MC samples for continuum backgrounds . . . 9

4 Object definition **11**
4.1 Photons . . . 11
4.2 Jets . . . 11
4.3 Electrons . . . 11
4.4 Muons . . . 12
4.5 Overlap removal . . . 12

5 Event selection **13**
5.1 Selection and efficiency . . . 13

6 Selection optimizations **15**
6.1 Optimal b-tagging working point . . . 15
6.2 Cuts optimization . . . 15

7 Signal and background estimations **16**
7.1 Signal estimation . . . 16
7.2 Single Higgs background estimation . . . 19
7.3 Continuum background estimation . . . 19
7.3.1 Function form . . . 21
7.3.2 Lepton dependence . . . 25
7.3.3 Spurious signal . . . 27

8 Systematic uncertainties **32**
8.1 Luminosity uncertainties . . . 32
8.2 Theoretical uncertainties . . . 32
8.3 Experimental Uncertainties . . . 32
8.4 Uncertainty on the continuum background modeling . . . 33

9 Statistical interpretation **35**

Appendices **52**

59 **A MadGraphs5 cards used for signals** **52**

60 **B Systematic uncertainties in details** **55**

61 **C Cut optimizations** **84**

1 Statements

1.1 List of contributions

Yaquan Fang	Paper editor, supervision of IHEP students
Douglas Gingrich	Supervisor
Qi Li	Supporting note editor, main analyzer (signal, background estimations, systematics and statistics), plot production
Xinchou Lou	Supervision of Yu Zhang
Bruce Mellado Garcia	Supervision of Witwatersrand students
Abdualazem Fadol Mohammed	Cross check of the cutflow
Tshidiso Sydwell Molupe	Continuum background decomposition
Xifeng Ruan	Background decomposition, supirous signal, supervision of Witwatersrand students
Xiaohu Sun	Supporting note/paper editor, analyzer, statistics, supervision of IHEP students
Jin Wang	Statistics, background modeling
Maosen Zhou	Signal and background sample validation, Wh uncertainties from jet multiplicity
Yu Zhang	Photon purity checks, derivations of MC samples, cross check of the data

1.2 Version 0.2

- Upgrade to the shape fit
- Include combination and introduce orthogonal cuts between the fully hadronic and this analysis.
- Explore additional kinematic cuts besides what have been applied; no one shows promising reuslts.

1.3 Version 0.1

Almost all the results and plots are updated to 36.47 fb^{-1}.

1.4 Version 0.0

This version is based on ICHEP INT note

2 Introduction

A Higgs boson was discovered by the ATLAS and CMS collaborations [1, 2] in 2012 and has been subsequently studied by spin and coupling measurements [3, 4, 5], which have established that its properties are very similar to the ones of the Standard Model (SM) Higgs boson. These measurements are mainly based on Higgs production via gluon-fusion, vector-boson-fusion and in association with a W or Z boson. Higgs pair production has not been measured and, if its cross section is similar to the SM predicted value 33.41 fb [6], it is impossible to measure with the current data. However, the non-resonant Higgs pair production can be significantly enhanced either by altering the Higgs boson self-coupling λ_{HHH} [7] or in extended Higgs sectors such as 2-Higgs-Doublet Models (2HDM) [8] where a heavy resonance decaying into a pair of SM-like Higgs bosons could exist. In RUN I, various channels were explored with the ATLAS detector, such as $bb\gamma\gamma$ [9], $bbbb$ [10], $bb\tau\tau$ and $WW\gamma\gamma$ [11]. In RUN II, $bb\gamma\gamma$ [], $bbbb$ [] and $WW\gamma\gamma$ [] continue searching for the Higgs boson pair production.

This note provides supporting material for the search of Higgs pair either from the non-resonant production or from the resonant one, with the subsequent decay chain of $hh \to WW\gamma\gamma \to lvjj\gamma\gamma$, namely one of the W bosons decays hadronically while the other decays leptonically, leading to a final state with two jets, one charged lepton (either electron or muon), missing transverse momentum and two photons. In terms of the mass scan on the resonant search, we start from 260 GeV and stop at 500 GeV based on our RUN I sensitivity [11]. The object and event selections inherits the ICHEP analysis as much as possible. With a set of similar selections, around two times more data are accumulated and examined for the Higgs pair search. The featured update is that a shape fit on $m_{\gamma\gamma}$ is adopted rather than the simple event counting method given more sufficient statistics.

Section 3 introduces the data and MC samples used in this analysis. Section 4 defines the objects used in the event selection. Section 5 gives the event selection definitions and relevant cut efficiencies. Section 6 describes the optimization on selection criteria. Section 7 discusses the signal and background estimations in the non-resonant and resonant Higgs pair searches. Section 8 describes the systematic uncertainties. In Section 9, statistical interpretation and relevant checks are done, followed by Section **??** where the combination of $WW\gamma\gamma \to jjjj\gamma\gamma$ and $WW\gamma\gamma \to jjlv\gamma\gamma$ is presented.

Appendix A gives the details of MG5 cards used for signal event generation. Appendix B records the details of systematic uncertainties related to detectors. Appendix C provides the discussions on the cuts optimizations.

3 Data and Monte Carlo samples

3.1 Data samples

The data samples used in this analysis correspond to the data recorded by ATLAS in the whole 2015 and 2016, which sums up to an inegrated luminosity of 36.5 fb^{-1}. The whole dataset is recorded with all subsystems of ATLAS operational [1].

3.2 Monte Carlo samples

SM single Higgs bacgkrounds and signals are estimated with MC samples that are documented in this section, while the continuum photon background of the SM processes with multiphotons and multijets is determined with the data in sideband [2] with the data-driven method. Nevertheless, two relevant MC samples are used to check and consolidate the modelling of the continuum photon background and they are described in this section.

The simulation under MC15c configuration is used in the analysis. The samples are generated with the consideration of multiple interactions per bunch crossing by introducing pileup noise at the stage of digitization. MC15c configuration incorporates the pileup condition that is an average of the actual pileup condition in 2015 data and an estimation for 2016 data.

3.2.1 MC samples for signals

Signal samples are generated with MadGraph5_aMC@NLO [12]. For both non-resonant and resonant productions, the event generation is performed using a next-to-leading-order SM Higgs pair model developped by the Cosmology, Particle Physics and Phenomenology (CP3) theory group [13]. Events are generated with a Higgs Effective Field Theory (HEFT) using aMC@NLO method [14] and are reweighted to take into account top quark mass dependence. The top mass can become an important effect [15], particularly for the non-resonant case. The shower is implemented by Herwig++ [16] with UEEE5 underlying-event tune [17], and the PDF set CTEQ6L1 [18] is used. The heavy scalar, H, is assumed to have a narrow width. Technically its decay width is set to 10 MeV in the event generation for the following masses: 260 GeV, 300 GeV, 400 GeV and 500 GeV. The card used in MadGraph5 for signal event generations is attached in Appendix A. Subsequently, the H boson is required to decay into a pair of SM Higgs bosons, one of which decays into a pair of photons and the other into two W bosons. The generator level filter *ParentChildFilter* implements the selection of these decay products. Details on the signal samples are listed in Table 1. All signal samples are produced with the Atlas fast simulation framework (AF2).

The kinematic distributions after hadronization and parton shower before interacting with the materials in the detector are shown for non-resonant and resonant Higgs pair productions. In Figure 1 and Figure 2, the transverse momentum p_T and pseudorapidity η distributions are shown for each object in the final state. The p_T spectrum of the decay products get harder as the resonant mass rises and the non-resonant one is the most hardest under the centre-of-mass energy of 13 TeV.

[1] Good Run Lists are data15_13TeV.periodAllYear_DetStatus-v79-repro20-02_DQDefects-00-02-02_PHYS_StandardGRL_All_Good_25ns.xml for 2015 data and data16_13TeV.periodAllYear_DetStatus-v83-pro20-15_DQDefects-00-02-04_PHYS_StandardGRL_All_Good_25ns.xml for 2016 data

[2] The sideband is defined as $m_{\gamma\gamma} \in [105, 125.09 - 2\sigma_{\gamma\gamma}] \cap [125.09 + 2\sigma_{\gamma\gamma}, 160]$ GeV orthogonal to the signal region defined in Section 5.

DSID	Processes	Generators, tunes and PDFs	Tags
342621	non-resonance	MadGraph + Herwigpp UEEE5 CTEQ6L1	*e*4419_*a*766_*a*821_*r*7676_*p*2691
343756	$X \to hh$, 260 GeV	MadGraph + Herwigpp UEEE5 CTEQ6L1	*e*5153_*a*766_*a*821_*r*7676_*p*2691
343758	$X \to hh$, 300 GeV	MadGraph + Herwigpp UEEE5 CTEQ6L1	*e*5153_*a*766_*a*821_*r*7676_*p*2691
343761	$X \to hh$, 400 GeV	MadGraph + Herwigpp UEEE5 CTEQ6L1	*e*5153_*a*766_*a*821_*r*7676_*p*2691
343763	$X \to hh$, 500 GeV	MadGraph + Herwigpp UEEE5 CTEQ6L1	*e*5153_*a*766_*a*821_*r*7676_*p*2691

Table 1: Simulated signal samples

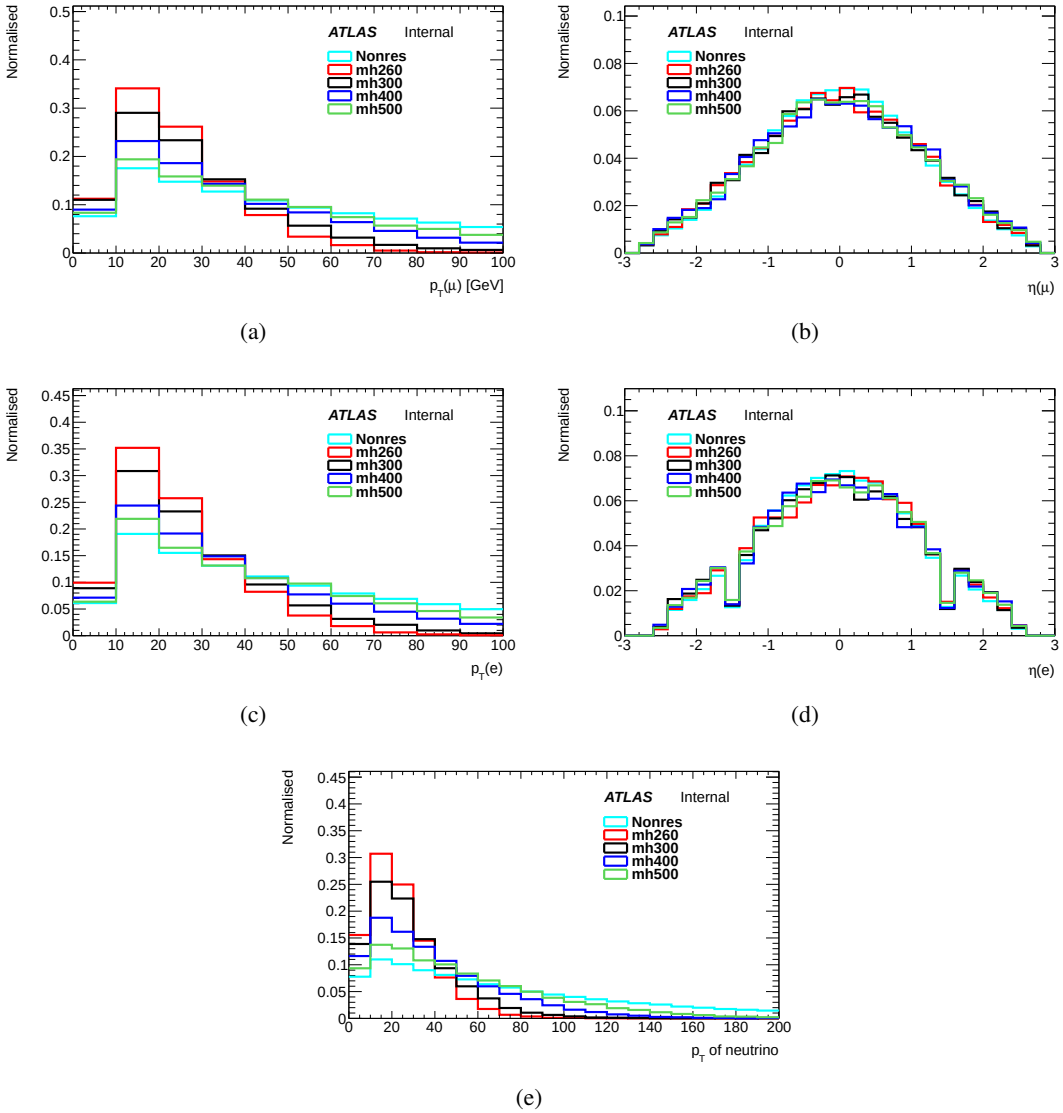

(a) (b) (c) (d) (e)

Figure 1: Kinematic distributions for the production of $hh \to WW\gamma\gamma$: (a) p_T of muons, (b) η of muons, (c) p_T of electrons, (d) η of electrons, (e) p_T of neutrino. Distributions are normalized to unity.

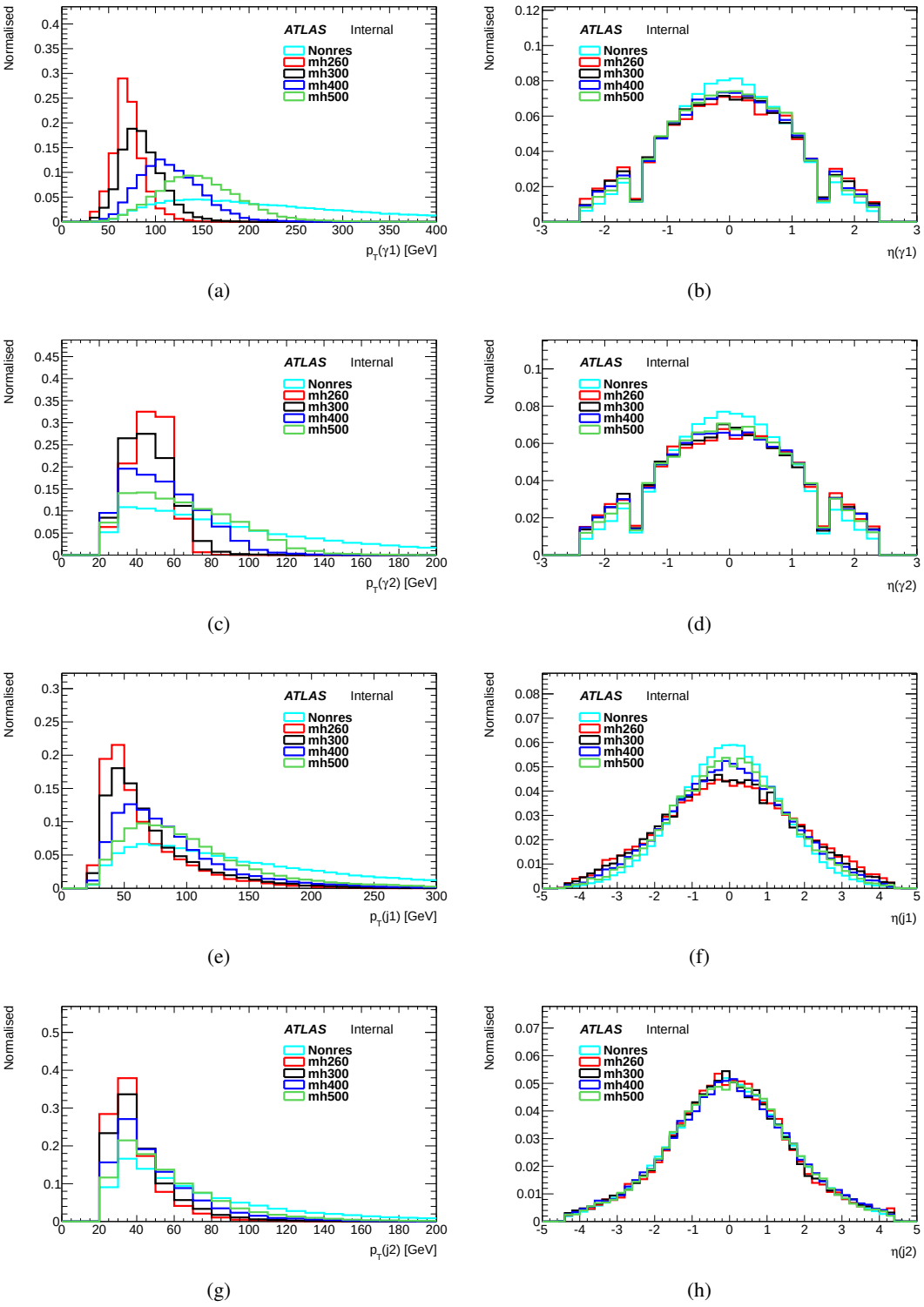

Figure 2: Kinematic distributions for the production of $hh \to WW\gamma\gamma$: (a) p_T of leading photon, (b) η of leading photon, (c) p_T of subleading photon, (b) η of subleading photon, (e) p_T of leading jet, (f) η of leading jet, (g) p_T of subleading jet, (h) η of subleading jet. Distributions are normalized to unity.

3.2.2 MC samples for SM single Higgs backgrounds

Simulated samples for SM single Higgs background are produced to investigate the components of this background in $m_{\gamma\gamma}$ and to estimate their contributions. The SM single Higgs background considered here is assumed to be produced via five production modes: ggh, VBF, Wh, Zh and tth, where h is the light (SM-like) 125 GeV Higgs boson. These samples are simulated using the full ATLAS simulation and reconstruction chain. The mass of the SM Higgs boson is set to 125 GeV. More details on generator, parton shower and simulation tags are listed in Table 2.

The cross sections at $\sqrt{s}$ = 13 TeV corresponding to each production mode are listed in Table 3. In the analysis, these cross sections will be multiplied by the $h \to \gamma\gamma$ branching ratio of 0.00227, since all simulated samples are produced with SM Higgs decaying into photon pairs.

DSID	Processes	Generators, tunes and PDFs	Tags
341000	ggh	Powheg+Pythia8 AZNLO CTEQ6L1	*e*3806_*s*2608_*r*7772_*r*7676_*p*2669
341001	VBF	Powheg+Pythia8 AZNLO CTEQ6L1	*e*3806_*s*2608_*r*7772_*r*7676_*p*2669
341067	Wh	Pythia8 A14 NNPDF2.3LO	*e*3796_*s*2608_*s*2183_*r*7772_*r*7676_*p*2669
341068	Zh	Pythia8 A14 NNPDF2.3LO	*e*3796_*s*2608_*s*2183_*r*7772_*r*7676_*p*2669
341069	tth	Pythia8 A14 NNPDF2.3LO	*e*3796_*s*2608_*s*2183_*r*7772_*r*7676_*p*2669

Table 2: Simulated SM single Higgs background samples.

production	cross sections
ggh	48.52 pb
VBF	3.779 pb
Wh	1.369 pb
Zh	0.8824 pb
tth	0.5065 pb
$gg \to hh$	33.41 fb

Table 3: Cross sections for SM single Higgs processes at $\sqrt{s}$ = 13 TeV with m_h = 125.09 GeV and the SM Higgs pair productions, $gg \to hh$.

3.2.3 MC samples for continuum backgrounds

The simulated sample of the $pp \to lvjj\gamma\gamma$ background is used to study the components with the SM background with the same final states of signal. The backgound sample $pp \to jj\gamma\gamma$ is generated by HGam group. The $pp \to jj\gamma\gamma$ as well as $pp \to lvjj\gamma\gamma$ is used to validate the $m_{\gamma\gamma}$ modeling. These processes are listed in Table 4.

DSID	Processes	Generators, tunes and PDFs	Tags
343363	$pp \to lvjj\gamma\gamma$	MadGraph + Pythia8 AU2 NN23LO1ME	e4852_a766_a821_r7676_p2691
341065	$pp \to jj\gamma\gamma$	MadGraph + Pythia8 A14 NNPDF23LO	e4292_a766_a821_r7676_p2691

Table 4: The simulated samples for continuum background.

4 Object definition

The photon selections follow the recommendations in HGam analyses and are exactly the same as what $bb\gamma\gamma$ uses. This analysis additionally requires leptons and jets. The analysis framework of $hh \to WW\gamma\gamma$ is based on the HGamAnalysisFramework that is centrally developed by HGam group. The tag of the framework is HGamAnalysisFramework-00-02-55-18 which is used to produce official MxAOD samples of version h013.

4.1 Photons

- The E_T of leading (sub-leading) photon is required to be large than 35% (25%) of the invariant mass of the leading two photons.
- The $|\eta|$ of photon is considered up to 2.37, vetoing the crack region $1.37 < |\eta| < 1.52$.
- Tight photons are required as is the default in HGam group. The photon identification algorithm is based on the lateral and longitudinal energy profiles of the shower measured in the electromagnetic calorimeter.
- The isolation working point FixedCutLoose is used. It is one of the recommended points from the isolation forum. Photons are required to pass both calorimeter-based and track-based isolation requirements.
- The neutral network photon pointing information that is default in HGam is used to select the primary vertex (PV) and recalculate the photons' four momenta and other quantities including JVT and track isolation. The NN training takes into account the inputs from the weighted average of the z position obtained from photon pointing, the beam spot position, the conversion vertex for converted photons, $log(\Sigma p_T$ of tracks), $log(\Sigma p_T^2$ of tracks), and $\Delta\phi(\gamma\gamma$,PV).
- The invariant mass of two leading photons is required to be within [105,160] GeV.

4.2 Jets

- The Anti-k_t algorithm [19] with the distance parameter of $R = 0.4$ is used.
- Jets are required to have $p_T > 25$ GeV and $|\eta| < 2.5$.
- Jets from pileup are rejected by applying a JVT (Jet Vertex Tagger) cut. The jet is rejected if JVT< 0.59 for $p_T < 60$ GeV and $|\eta| < 2.4$.
- Events with a jet passing the LooseBad cut are rejected. The LooseBad jet quality requirement is designed to reject fake jets caused by detector readout problems and non-collision backgrounds.

4.3 Electrons

Electrons are reconstructed from energy clusters in the EM calorimeter matched with tracks reconstructed in the inner detector.

- E_T is required to be larger than 10 GeV.
- $|\eta|$ is required to be less than 2.47 vetoing the transition region with $1.37 < |\eta| < 1.52$.

- The $|d_0|$ significance ($d_0/\sigma(d_0)$) with respect to the primary vertex in the event is required to be less than 5.
- The $|z_0|$ with respect to the primary vertex in the event is required to be less than 0.5mm.
- Identification: Medium quality electrons are used.
- Isolation: Loose electrons are used.

4.4 Muons

Muons are reconstructed from tracks in the inner detector and the muon spectrometer.

- p_T is required to be larger than 10 GeV.
- $|\eta|$ is required to be less than 2.7.
- The $|d_0|$ significance with respect to the primary vertex in the event is required to be less than 3.
- The $|z_0|$ with respect to the primary vertex in the event is required to be less than 0.5mm.
- Identification: Medium quality muons are used.
- Isolation: GradientLoose is used.

4.5 Overlap removal

Since objects are reconstructed with different algorithms in parallel, i.e. no check to see if a same set of clusters or tracks are used for reconstructing two different object, one needs to implement a set of rules to remove objects close to each other to avoid double counting. The rule is defined as below:

- The two leading photons are always kept.
- Electrons with $\Delta R(e, \gamma) < 0.4$ are removed.
- Jets with $\Delta R(jet, \gamma) < 0.4$ are removed.
- Jets with $\Delta R(jet, e) < 0.2$ are removed.
- Muons with $\Delta R(\mu, \gamma) < 0.4$ or $\Delta R(\mu, jet) < 0.4$ are removed
- Electrons with $\Delta R(e, jet) < 0.4$ are removed.

5 Event selection

5.1 Selection and efficiency

The event selection procedure identifies two photons and then applies requirements on the multiplicities of jets and leptons in order to increase the signal purity and background rejection for events with at least 2 jets, at least 1 lepton and at least 2 photons. The event selection for the analysis starts with the full di-photon selection from the $h \to \gamma\gamma$ analysis in RUN II to select two high p_T isolated photons.

- **Trigger**: di-photon trigger *HLT_g35_loose_g25_loose* is used.
- **Good Run List and Detector Quality**: Events must belong to the luminosity blocks specified in the Good Run Lists:
  - data15_13TeV.periodAllYear_DetStatus-v79-repro20-02_DQDefects-00-02-02_PHYS_StandardGRL_All_Good_25ns.xml for 2015 data
  - data16_13TeV.periodAllYear_DetStatus-v83-pro20-15_DQDefects-00-02-04_PHYS_StandardGRL_All_Good_25ns.xml for 2016 data

  Events with data integrity errors in the calorimeters and incomplete events where some detector information is missing are rejected, as well as events which are corrupted due to power supply trips in the tile calorimeter.
- **Primary Vertex**: The primary vertex is selected using the neural network algorithm form HGam group. The photons' four momenta, JVT and track isolation are corrected with respect to this origin, and the mass of the diphoton system is accordingly rescalculated.
- **2 loose photons**: At least two loose photons with $E_T > 25$ GeV and within the detector acceptance are selected.
- The other cuts on photons involving **Identification (tight ID), Isolation, Rel.Pt cuts** and $m_{\gamma\gamma} \in [105, 160]$ **GeV** have been discussed in Section 4.1
- **Number of jets**: At least two jets.
- **b-veto**: In order to suppress bacgkrounds with top quarks and keep orthogonality to other hh channels $bb\gamma\gamma$, $bbbb$, $bb\tau\tau$ etc, the event is rejected if there is any b-jet. The b-tagger is MV2c10 with a b-tagging efficiency of 70%. The optimization is discussed in Section 6.1.
- **Number of leptons**: At least one muon or electron.
- **Tight mass window**: The tight mass window is used to define the final signal region which is blinded till the background estimation is consolidated. In the final fit on the shape of $m_{\gamma\gamma}$ 7, the events both in the window and out are used.

The efficiencies of event selection are listed in Table 5. These efficiencies are derived for signals from simulated samples. After the selection of the two photons, the signal efficiencies range from 35.9% to 42.5%, while after the additional selection on the jets, the leptons and the tight mass window on the di-photon, the signal efficiencies range from 5.54% to 10.5%, for a resonant mass from 260 to 500 GeV.

	SM	Resonant			
	Higgs pair	260 GeV	300 GeV	400 GeV	500 GeV
All Events	100.0%	100.0%	100.0%	100.0%	100.0%
Duplicate	100.0%	100.0%	100.0%	100.0%	100.0%
GRL	100.0%	100.0%	100.0%	100.0%	100.0%
Pass Trigger	73.8%	68.4%	69.4%	71.8%	74.5%
Detector Quality	73.8%	68.4%	69.4%	71.8%	74.5%
has PV	73.8%	68.4%	69.4%	71.8%	74.5%
2 loose photons	59.3%	56.6%	56.1%	57.5%	59.7%
Trig Match	59.0%	56.3%	55.8%	57.2%	59.4%
Tight ID	49.3%	46.2%	45.5%	47.5%	50.2%
Isolation	44.6%	39.3%	39.3%	42.6%	45.7%
Rel.Pt cuts	41.0%	36.6%	35.6%	38.8%	42.4%
$105 < m_{\gamma\gamma} < 160$ GeV	40.9%	36.6%	35.6%	38.6%	42.2%
At least 2 central jets	29.7%	17.7%	20.1%	26.5%	32.1%
B-veto	27.8%	16.7%	19.0%	25.0%	30.2%
At least 1 lepton	11.1%	6.56%	7.60%	10.4%	12.0%
Tight mass window	9.62%	5.54%	6.48%	8.91%	10.5%

Table 5: Efficiencies for event selection

ϵ(btag)	ggh	VBF	Wh	Zh	tth	Cont.	Non-res	ϵ(non-res)	Sig.
60%	0	0.001	0.042	0.016	0.093	1.60	0.128	8.7%	0.09556σ
70%	0	0.001	0.042	0.012	0.067	1.60	0.127	8.6%	0.09568σ
77%	0	0.001	0.042	0.012	0.050	1.60	0.126	8.5%	0.09548σ
85%	0	0.001	0.039	0.012	0.035	1.60	0.100	7.1%	0.07625σ

Table 6: The event yields (SM single Higgs, continuum background and non-resonant signal), signal efficiencies and the expected significance for difference b-tagging working points. Non-resonant signal is used as a benchmark. Events pass all selections defined for signal region. The backgrounds in this table were estimated with the luminosity from 2015 data.

6 Selection optimizations

Optimizations on object or event selection are discussed in this section. In general, the expected significance formula for low-statistical analyses is used as a figure-of-merit.

$$Z = \sqrt{2 \times [(S+B) \times (\ln \frac{S+B}{B}) - S]} \quad (1)$$

where S is the signal yield and B is the background yield after a set of selections. The higher the significance is, the better the expected sensitivity would be. Normally, we choose the selections that give the highest expected significance. When doing the optimization, the cross section $\sigma(gg \to hh)$ for non-resonance and $\sigma(gg \to H) \times BR(X \to hh)$ for resonances are assumed to be 1 pb.

6.1 Optimal b-tagging working point

As recommended by the performance groups, the btagger MV2c10 is used for b-veto to suppress tth background. Several working points corresponding to difference b-tagging efficiencies are tested as shown in Table 6. As expected, the b-tagging working point only affects the SM tth process significantly. Eventually, we choose working point with 70% b-tagging efficiency based on the expected significane.

6.2 Cuts optimization

Additonal optimizations are attached in the Appdendix C. Since the statistics are relatively low and the improvement is very limited, there is no more cut applied finally in this analysis except $p_T(\gamma\gamma)$ that will be discussed later.

7 Signal and background estimations

Previously a cut-and-count method was used given a limit statistics, while now a shape fit on $m_{\gamma\gamma}$ is performed to capture the features of signal events. The signal region is defined with all the cuts described in Section 5 for both non-resonant and resonant searches, while the background region (sideband region) is defined with the same selections but reversing the Tight mass window cut in Table 5. A control region is defined by asking exactly no lepton and exactly 2 jets to constain the shape and the normalization of the continuum background. This control region is orthogonal to the signal and background regions as well as the fully hadronic channel. In the end, events in any of the above regions are used in the final fit of $m_{\gamma\gamma}$. Given no mass-dependent selections, the background estimation are exactly same for non-resonance and resonances with masses larger than 400 GeV (inclusive), and the same for all lower masses less than 400 GeV (exclusive), respectively.

7.1 Signal estimation

The contributions are estimated with MC for both non-resonant and resonant signals. The expected signal yields of non-resonance with the recommended cross section $\sigma(gg \to hh)$ [6] and the ones of resonance at each mass point with the assumption of $\sigma(gg \to H) \times BR(X \to hh) = 1pb$ are listed in Table 7.

Signal yields	non-resonance	260 GeV	300 GeV	400 GeV	500 GeV
At least one leptons	-	0.964	1.12	-	-
$pT_{\gamma\gamma} > 100$ GeV	1.357	-	-	1.233	1.631

Table 7: Event yields assuming the cross section $\sigma(gg \to hh)$ or $\sigma(gg \to H) \times BR(X \to hh)$ of 1 pb,with the integrated luminosity of 36.5 fb^{-1}.

Important kinematic distributions are shown in Figure 3, 4 and 5 for comparisons among non-resonant, 260 GeV, 300 GeV, 400GeV, 500 GeV resonant signals and the continuum background.

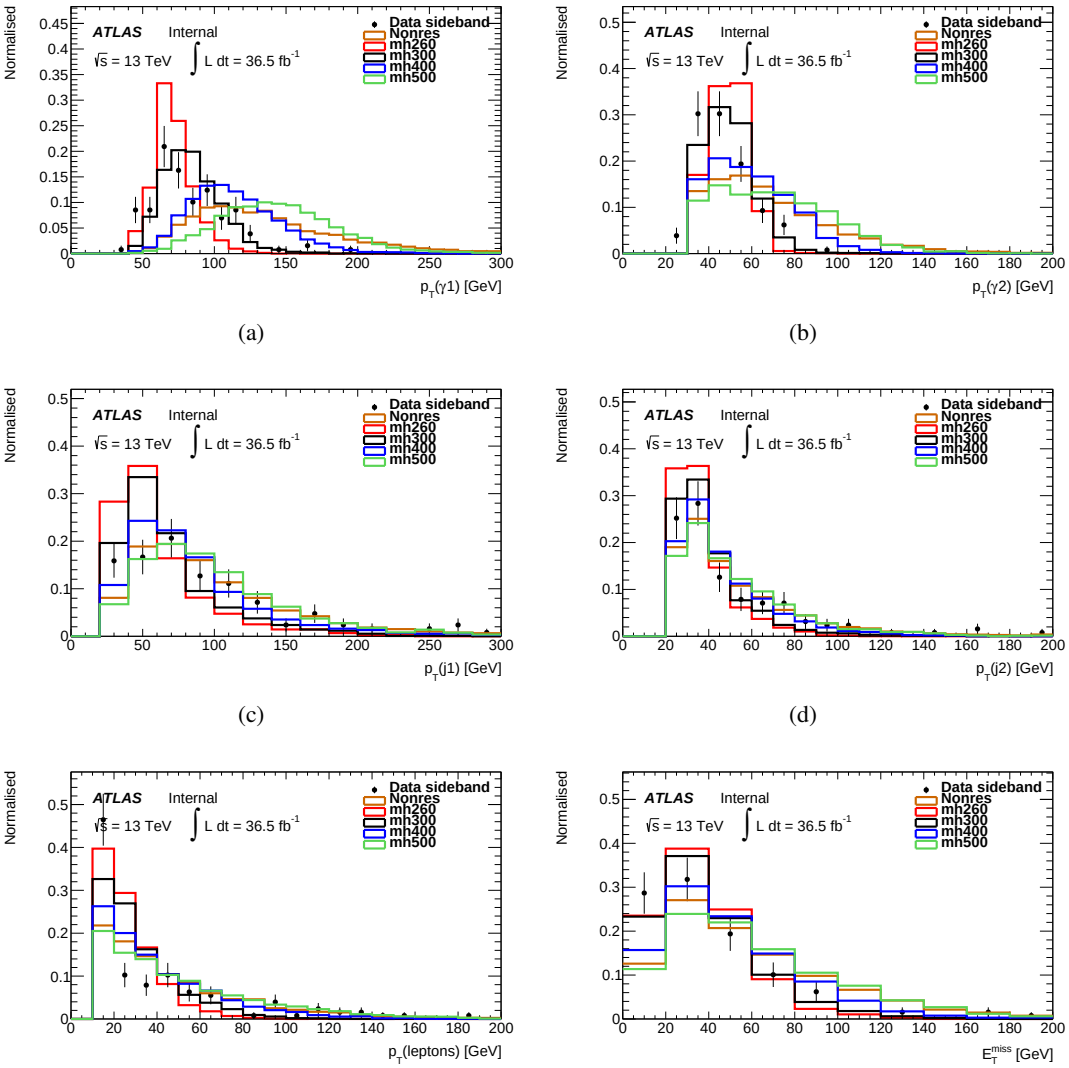

Figure 3: (a) p_T of leading photon, (b) p_T of sub-leading photon, (c) p_T of leading jet, (d) p_T of sub-leading jet, (e) p_T of leading lepton. (f) missing transverse energy. Events pass all selections defined in signal region.

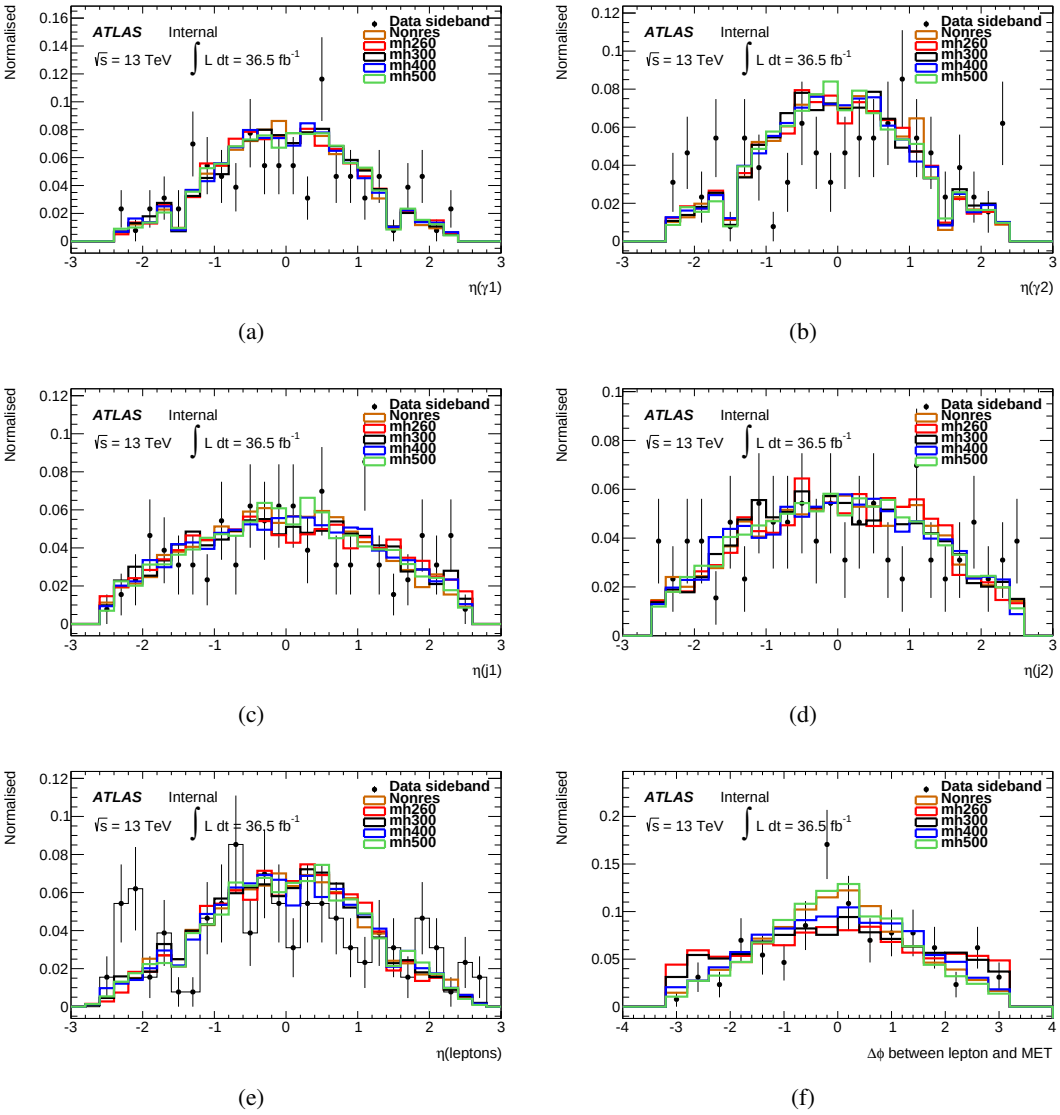

(a) (b) (c) (d) (e) (f)

Figure 4: (a) η of leading photon, (b) η of sub-leading photon, (c) η of leading jet, (d) η of sub-leading jet, (e) η of leading lepton, (f) $\Delta\phi$ between leading lepton and MET. Events pass all selections defined in signal region.

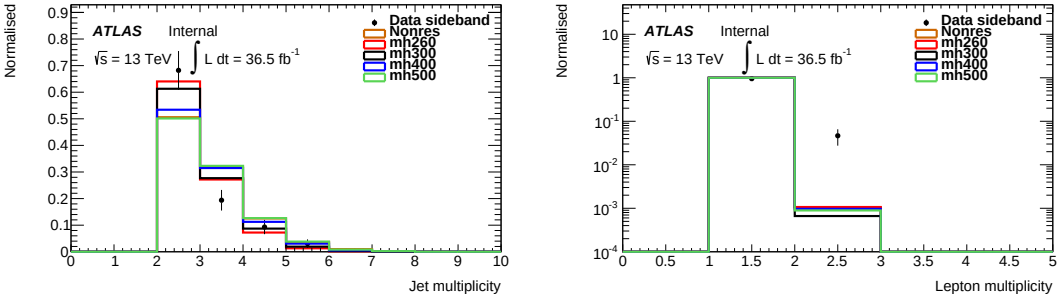

(a) (b)

Figure 5: (a) jet multiplicity, (b) lepton multiplicity. Events pass all selections defined in signal region.

7.2 Single Higgs background estimation

Backgrounds with final states similar to signal are considered including SM single Higgs boson production and continuum photon background. SM single Higgs production is estimated using MC samples. The cut efficiencies and events yields are summarized in Table 8 and Table 9. The tth production contributes the most among all SM single Higgs productions due to its higher jet multiplicity in the central region and real leptons from top decays.

	ggh	VBF	Wh	Zh	tth
All Events	100.0%	100.0%	100.0%	100.0%	100.0%
Duplicate	100.0%	100.0%	100.0%	100.0%	100.0%
GRL	100.0%	100.0%	100.0%	100.0%	100.0%
Pass Trigger	59.6%	61.3%	56.5 %	56.0%	72.8%
Detector Quality	59.6%	61.3%	56.5 %	56.0%	72.8%
has PV	59.6%	61.3%	56.5 %	56.0%	72.8%
2 loose photons	49.8%	51.2%	44.5 %	45.2%	58.3%
Trig Match	49.7%	51.1%	44.4 %	45.1%	57.9%
Tight ID	43.4%	43.4%	38.2 %	38.9%	48.3%
Isolation	39.0%	40.2%	33.9 %	34.4%	40.0%
Rel.Pt cuts	36.1%	36.5%	31.0 %	31.4%	36.5%
$105 < m_{\gamma\gamma} < 160$ GeV	36.1%	36.4%	30.8 %	31.2%	36.0%
At least 2 central jets	5.51%	10.2%	14.9 %	15.8%	35.4%
B-veto	5.23%	9.65%	14.2 %	12.9%	6.18%
At least 1 lepton	0.00365%	0.0109%	0.533%	0.354%	1.89%
Tight mass window	0.00342%	0.00996%	0.488%	0.326%	1.76%

Table 8: Cut efficiencies for SM single Higgs processes.

Background yields	ggh	VBF	Wh	Zh	tth	SM Higgs Pair
At least one lepton	0.153	0.032	0.58	0.25	0.74	0.055
$pT_{\gamma}\gamma > 100$ GeV	0.079	0.018	0.31	0.12	0.44	0.045

Table 9: The yields for SM single Higgs and SM Higgs pair processes.

7.3 Continuum background estimation

The continuum background shape and normalization are determined sinultaneously in the final fit to the invariant mass $m_{\gamma\gamma}$. The constrain power mainly comes from the sideband by reveising tight mass window as described above. Figure **??** shows the sideband in 1-lep region requiring at least one leptons. Figure **??** shows the sideband in 0-lep region requeing exactly zero lepton. 1-lep region does not have enough statistics to determine the function form for backgroud modeling, so 0-lep region is used to stabilize the statistical fluctuation for both the shape and normalization. Similarly, Figure **??** shows $m_{\gamma\gamma}$ after $p_T(\gamma\gamma)$ cut.

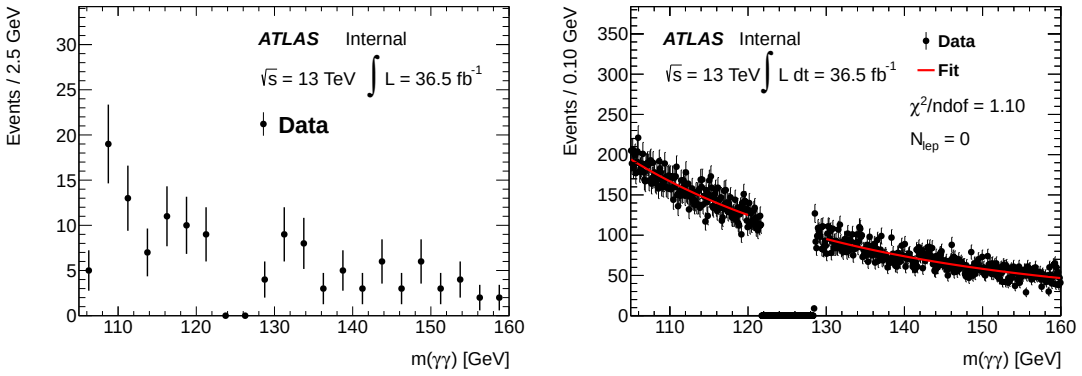

(a) (b)

Figure 6: Sideband $m_{\gamma\gamma}$ distribution with data (a) in signal-like sideband (number of leptons is larger than zero) and (b) in control region sideband (number of leptons is equal to zero) where a background fit is performed.

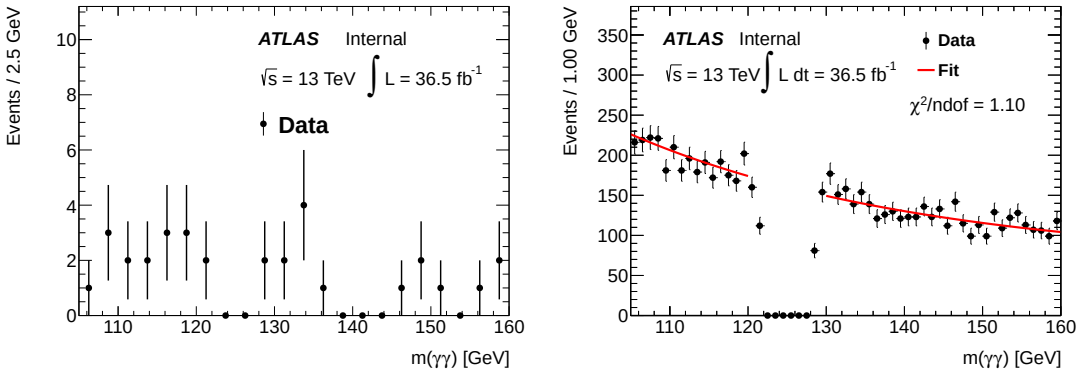

(a) (b)

Figure 7: Sideband $m_{\gamma\gamma}$ distribution with data (a) in signal-like sideband (number of leptons is larger than zero) and (b) in control region sideband (number of leptons is equal to zero) where a background fit is performed, after $p_T(\gamma\gamma)$ cut.

7.3.1 Function form

Different function forms are tested to choose the modeling of continuum background. Table 10 records the quality of fit. Figure 8 shows the fits in 0-lep region, Figure 9 in the same region with anti-ID on photons, Figure 10 with anti-ISO on photons. Here, antiID means at least one of the two leading photons fail the tight ID selection, and similarly, antiIso means at least one of the two leading photons fail the isolation criteria, as described in Section 4.1. The exponential function with a second-order polynomial is chosen given that it well accommodates all data in different background control regions.

Function	$\chi^2/ndof$
RevID	1.1
RevIso	1.1
RevID&RevIso	1.1

Table 10: NLL and $\epsilon_{\gamma\gamma}$ with different backgroumd modeling.

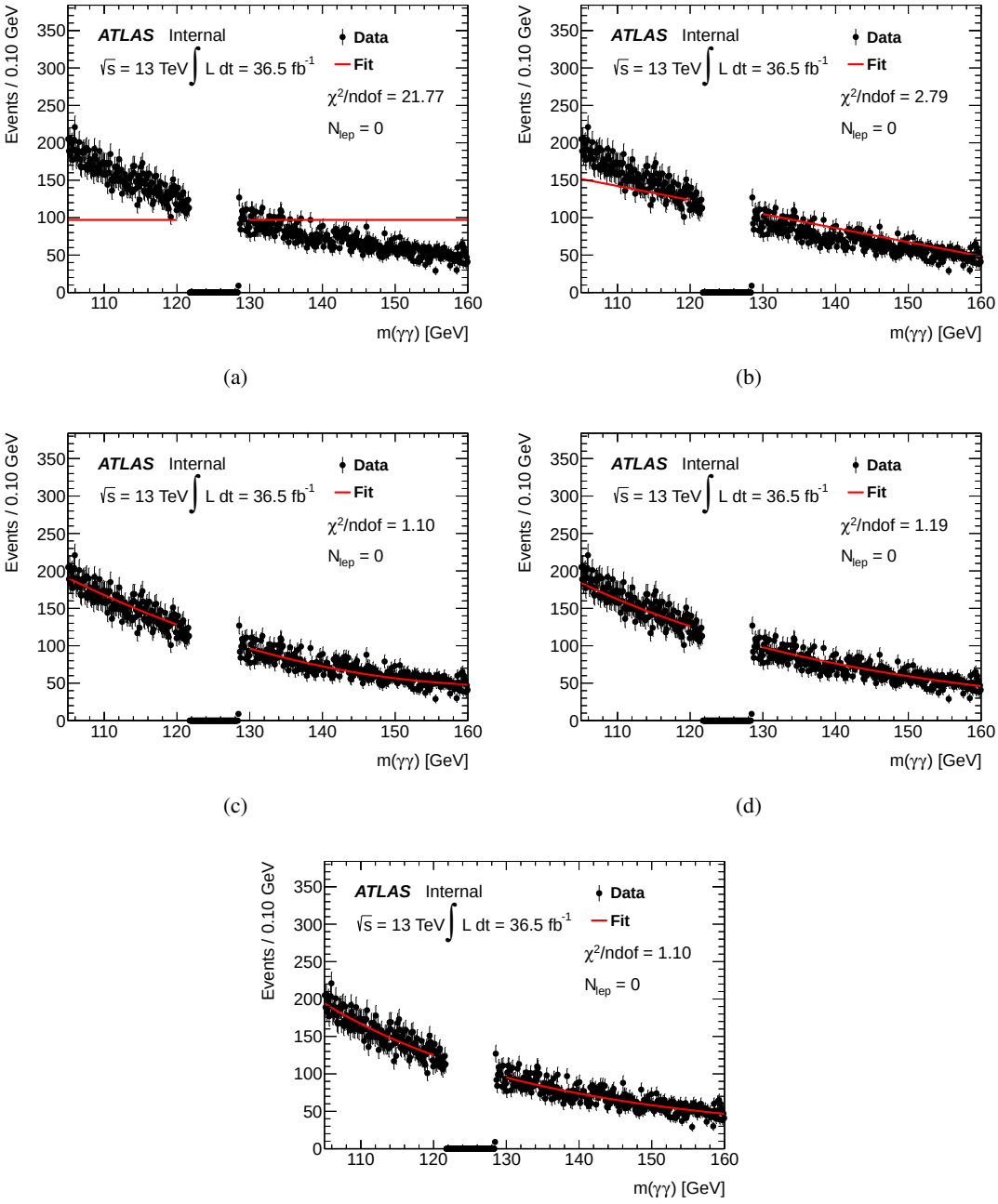

Figure 8: $m_{\gamma\gamma}$ Fits using different background modeling functions: (a) with a 0^{th}-order polynominal function; (b) with a 1^{st}-order polynominal function; (c) with a 2^{nd}-order polynominal function; (d) with an exponential function; (e) with an exponential function carrying a 2^{nd}-order polynominal.

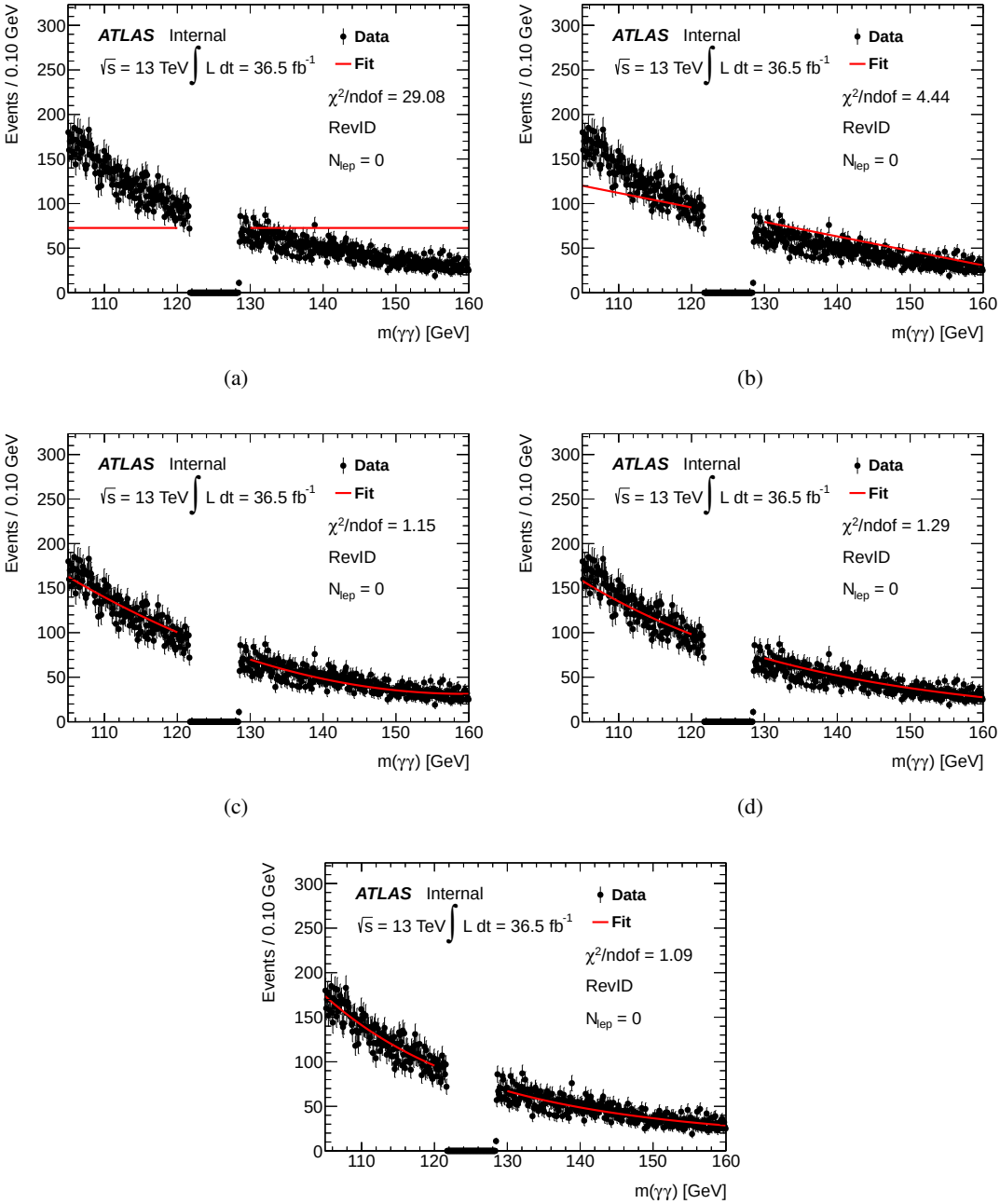

Figure 9: $m_{\gamma\gamma}$ Fits using different background modeling functions with anti-ID on photons: (a) with a 0^{th}-order polynominal function; **??** with a 1^{st}-order polynominal function; (c) with a 2^{nd}-order polynominal function; **??** with an exponential function; (e) with an exponential function carrying a 2^{nd}-order polynominal.

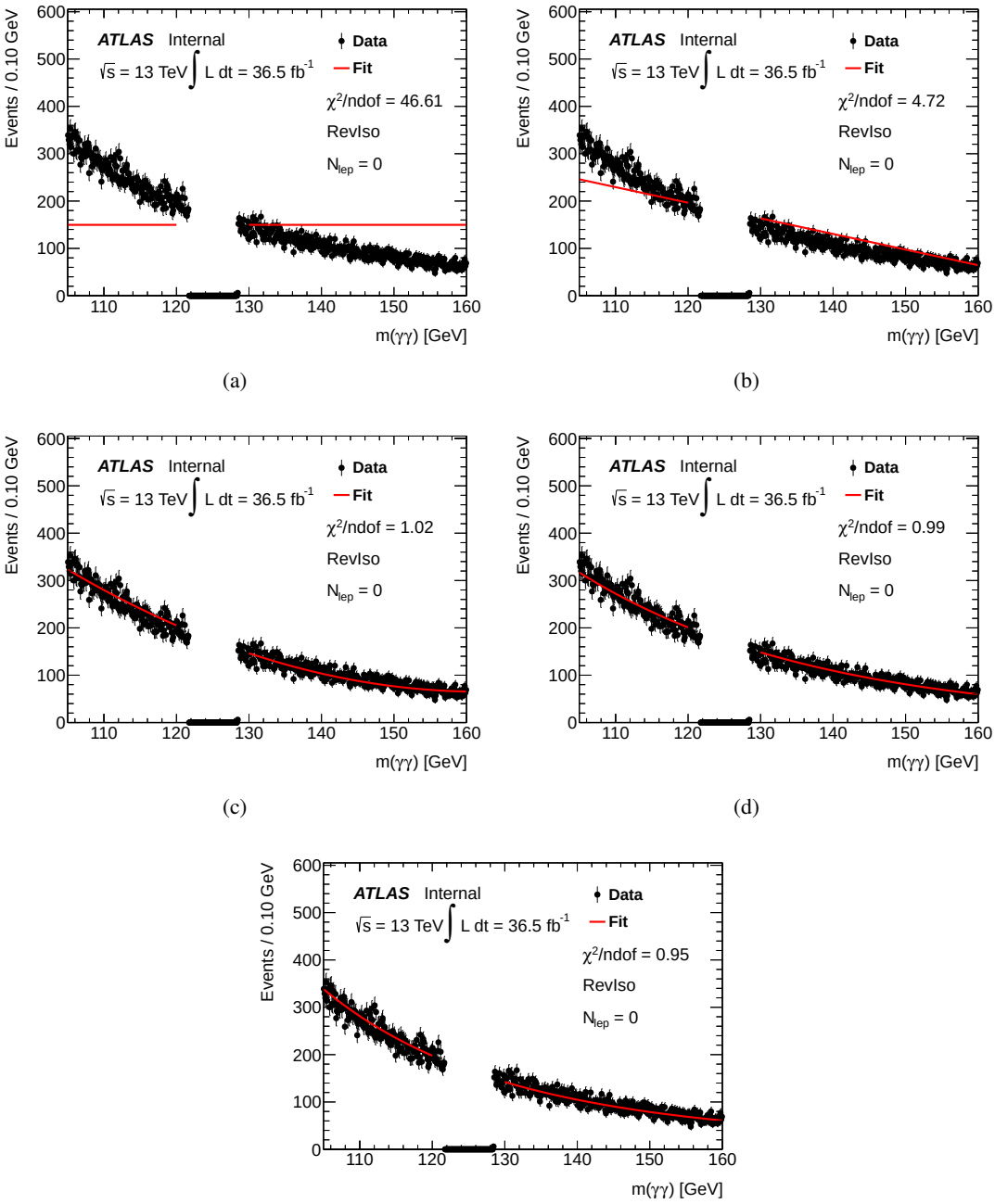

Figure 10: $m_{\gamma\gamma}$ Fits using different background modeling functions with anti-ISO on photons: (a) with a 0^{th}-order polynominal function; **??** with a 1^{st}-order polynominal function; (c) with a 2^{nd}-order polynominal function; **??** with an exponential function; (e) with an exponential function carrying a 2^{nd}-order polynominal.

7.3.2 Lepton dependence

As introduced above, 0-lep region is used to constrain the continuum background in 1-lep. A validation is performed to check the consistency of the shape in both region. Basically, the 2^{nd}-order polynominal function is freely fit to the data sideband in 0-lep region. Applying the fitted parameters to 1-lep region, the quality of fit $\chi^2/ndof$ is calculated. Effectively, the shape obtained from 0-lep is tested by $\chi^2/ndof$ in 1-lep region.

Firstly, two MC samples are used to check the consistency as shown in Figure 11 They are SM processes of $l\nu jj\gamma\gamma$ and $jjj\gamma\gamma$. The two MC samples above only mimic real photon processes whose photon purity is extremely high. This is not necessarily true in real data and the lepton dependence might vary with photon purity. Thus additional tests with antiIso photons and antiID-antiIso photons are performed as these control regions have very low photon purity. The fits are shown in Figure 12. In general, a consistent shape between 0-lep and 1-lep is seen in various scenarios.

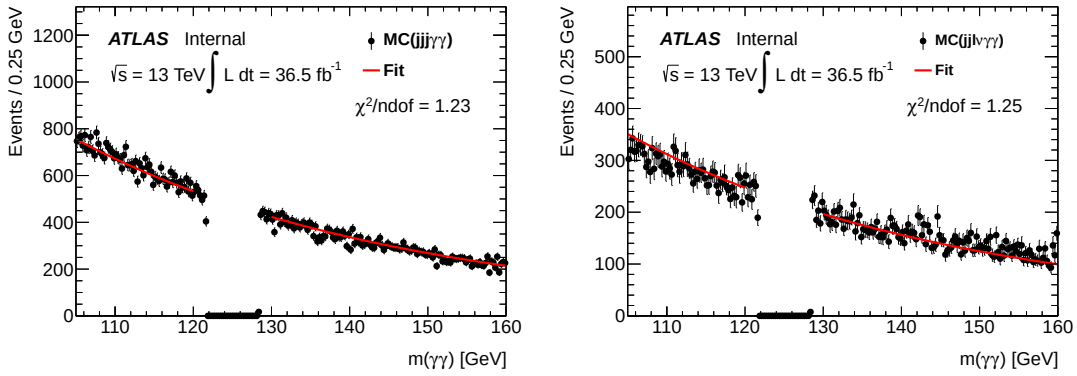

(a) (b)

Figure 11: Fits with sideband events to test lepton dependence (a) with $jjj\gamma\gamma$ MC sample and (b) with $l\nu jj\gamma\gamma$ MC sample.

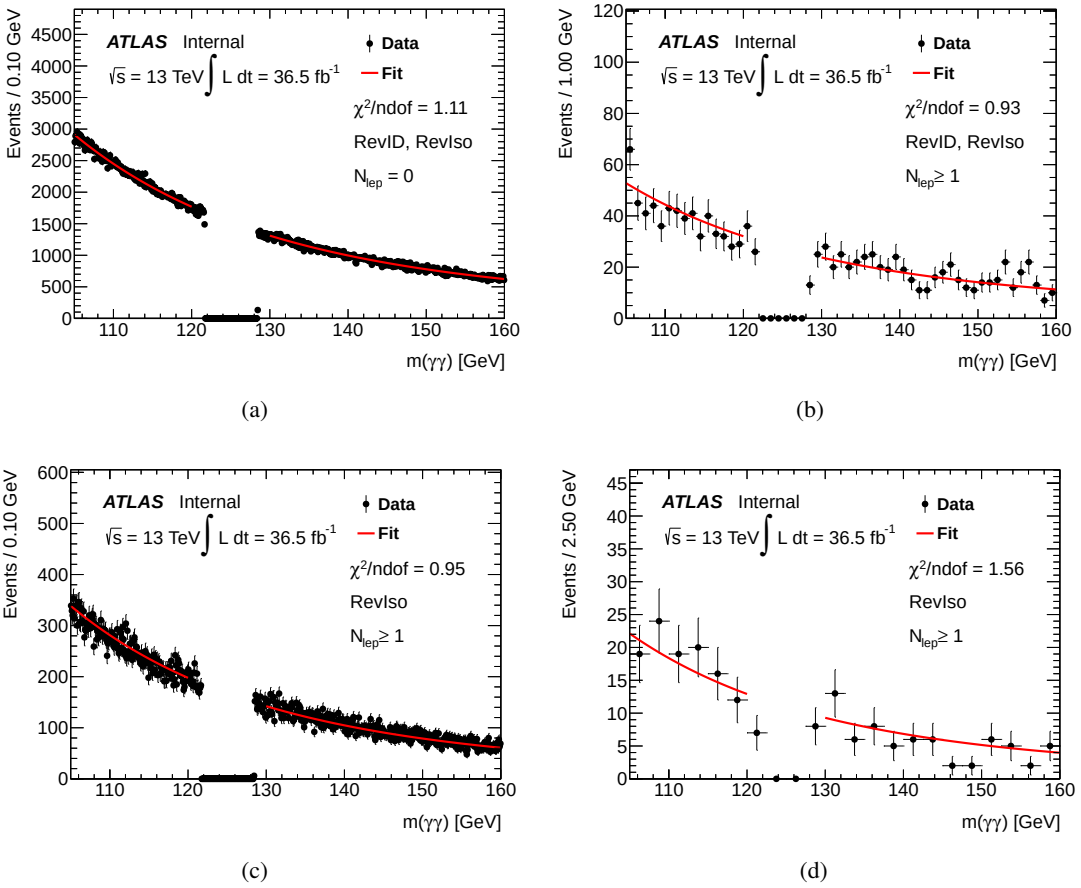

Figure 12: Fits with sideband events to test lepton dependence in reversed photon ID or isolation (a) with antiID-antiIso and zero lepton, (b) with antiID-antiIso and non-zero lepton; (c) with antiIso and zero lepton, (d) with antiIso and non-zero lepton.

Component	SR no $pT_{\gamma\gamma}$ cut	CR no $pT_{\gamma\gamma}$ cut	SR $pT_{\gamma\gamma} > 100GeV$	CR $pT_{\gamma\gamma} > 100GeV$
data	165	54762	39	8415
$\gamma\gamma$	146±15	46855±876	35.4±6.4	7829±120
$\gamma - jet$	6.25±5.08	4139±218	2.78±1.85	501±54
$jet - \gamma$	7.37±5.30	2971±129	1.00±1.00	449±42
jet-jet	5.65±2.72	780±43	0.22±0.25	46.6±9.5
purity	0.884±0.063	0.856±0.006	0.898±0.074	0.881±0.010

Table 11: The purity of diphoton in one lepton SR and zero lepton CR after different $pT_{\gamma\gamma}$ cut is shown.

Mass	Max(N_{ss})	Max($N_{ss}/\Delta S$)	Max($_{ss}/S_{ref}$)
$m_H = 260GeV$	0.845848	0.194842	1.6359
$m_H = 300GeV$	0.826406	0.189248	1.45292
$m_H = 400GeV$	-0.398046	-0.169399	-0.516232
$m_H = 500GeV$	-0.395486	-0.172747	-0.460771
non-resonant	-0.402366	-0.174128	-0.497784

Table 12: The difference between low mass and high mass is due to $pT_{\gamma\gamma}$ cut.

7.3.3 Spurious signal

The bias for a given background parametrization is estimated by fitting background MC samples with a function combining this parametrization and signal model, and measuring the fitted number of signal events N_{signal}. The fit is performed on the mass range, $m_h \in [110, 160]$ GeV, in step of 0.5 GeV. The fitted bias is evaluated as the maximum value of $|N_{signal}|$ over the fit range from 120 GeV to 130 GeV. The simultaneous fit is performed to one lepton signal region and zero lepton control region and the function of ExpPoly2 is used. The irreducible background is modeled by large statistic $l\nu\gamma\gamma jj$ MC sample and the reducible background is modeled by reverse ID or reverse ISO sample from data. They are merged according to diphoton purity.

The diphoton purity is measured by 2x2D sideband method described in Ref [20]. The result of purity mesurement with 36.1 fb^{-1} 2015+2016 data is shown in Table 11.

The Z($\rightarrow ee$)γ events are also considered as background since one of the electron could be misidentified as a photon. The yield of Zγ events could be estimated from $M_{e\gamma}$ spectrum in data sideband and the $m_{\gamma\gamma}$ shape could be obtained with events in Z peak. Figure 13 shows the m_{ey} distribution and the estimated yield is 13.7. Since the statistic is very low, the selection of at least 2 central jets is dropped to enlarge the statistic. Figure 14 shows the fit of $m_{\gamma\gamma}$ shape in Z peak. Since there is no Z peak in $M_{e\gamma}$ spectrum after $pT_{\gamma\gamma} > 100GeV$, Z$\gamma$ component is only added to the search of $m_H = 260\ GeV$ and $m_H = 300\ GeV$.

The parametrization is kept if N_{ss} satisfies at least one of the following two criteria:

- $Max(N_{ss}/N_{S.exp}) < 10\%$
- $Max(N_{ss}/\Delta N_{ss}) < 20\%$

Where $N_{S,exp}$ is the expected number of the signal events passing the "At least one lepton", and $\Delta_{N_{ss}}$ is the statistical uncertainty on the spurious signal. "Max" means the largest ratio in $m_{\gamma\gamma}$ [120, 130] GeV. The fitted spurious signal for all the mass points are shown in Figure 15 16 (The machinary is running and the plots are coming soon). The yields are summarized in Table 12.

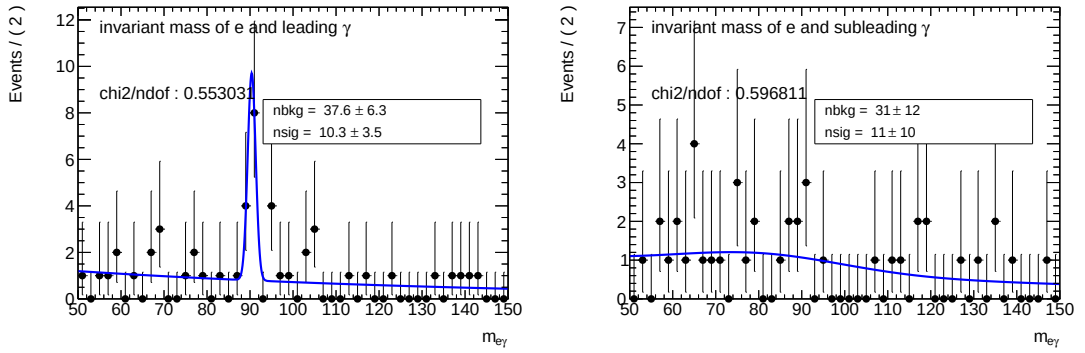

(a) (b)

(c) (d)

Figure 13: 13(a) : Invariant mass of electron and leading photon in data sideband. 13(b) : Invariant mass of electron and subleading photon. 13(c) The sum of previous two plots. 13(d) : A second order exponential fit to Z peak events in data sideband.

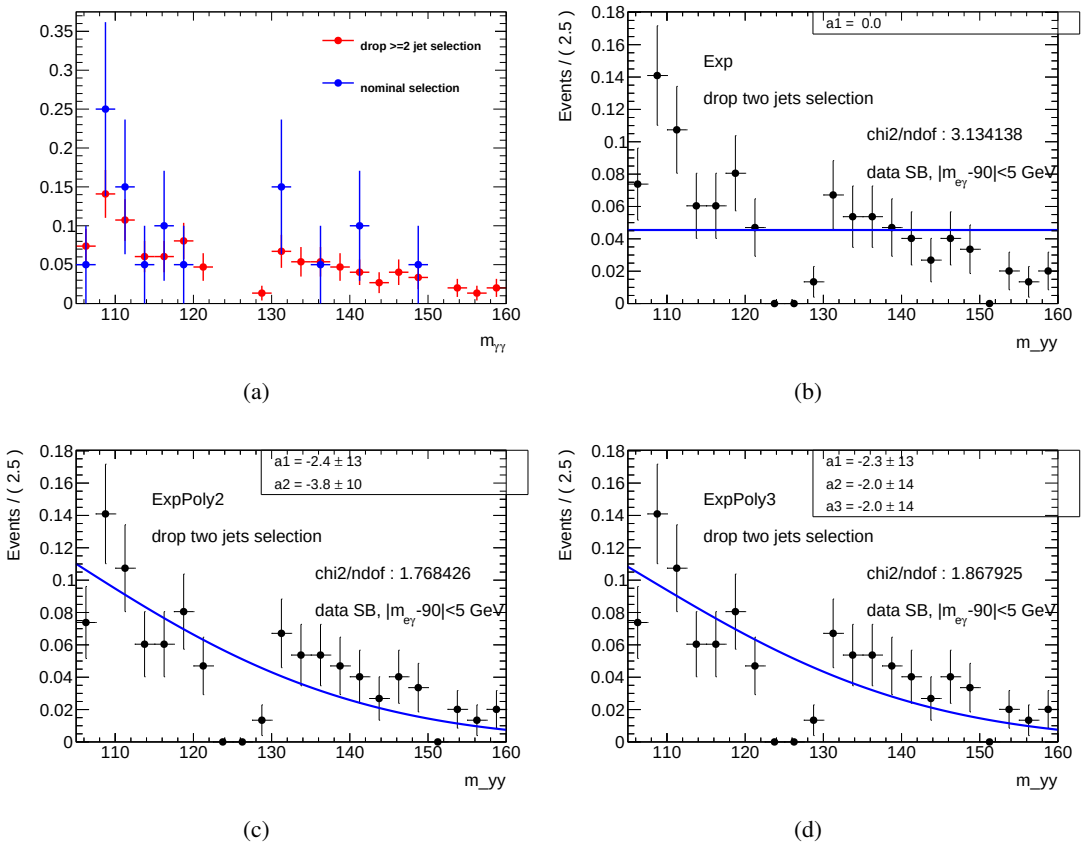

Figure 14: 14(a) shows the comparison before and after dropping 2 jets requirements to demonstrate this loose selection does not change the $m_{\gamma\gamma}$ shape. 14(b) 14(c) 14(d) show the exponential, 2nd exponential, 3rd exponential fit to $m_{\gamma\gamma}$ shape in Z peak.

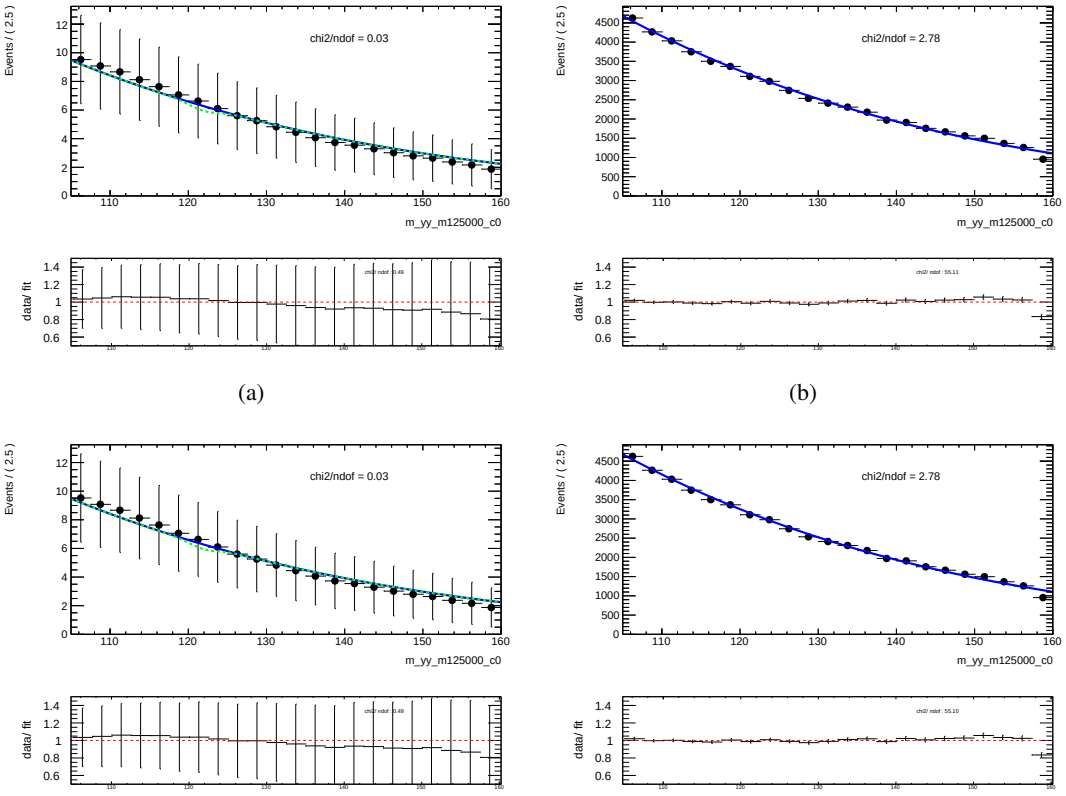

Figure 15: The fitted number of spurious signal. Left is one lepton signal region, right is zero lepton control region. The shape is constrained by control region, which has higher statistic. (a)(b) for mh260, (c)(d) for mh300,

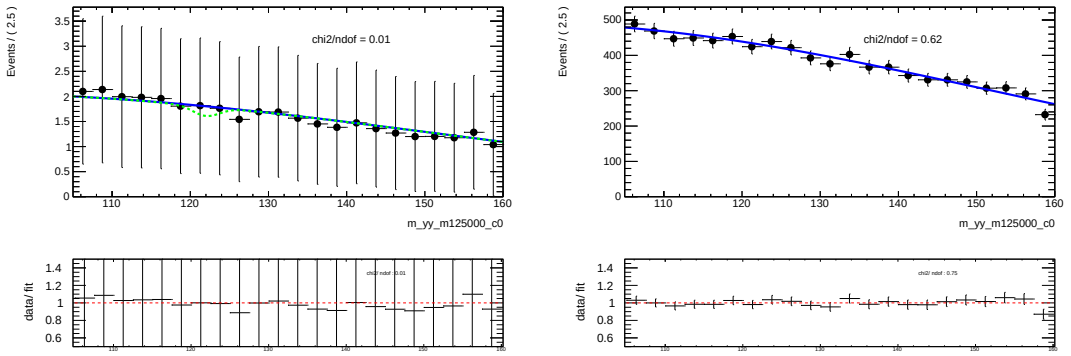

(a)

(b)

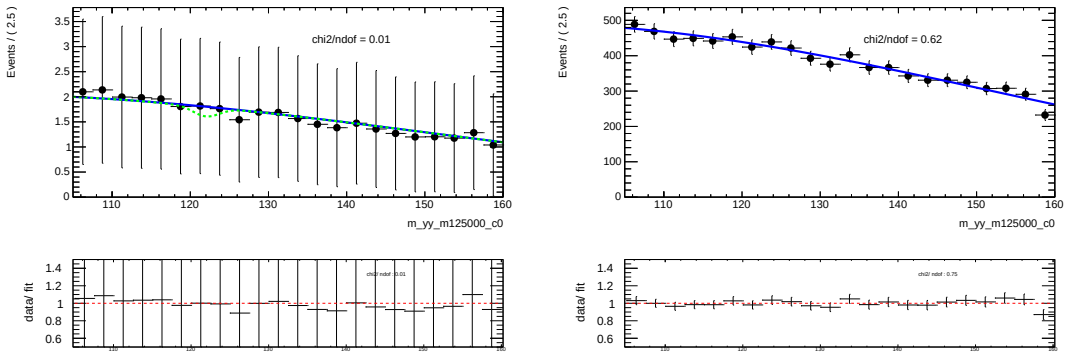

(c)

(d)

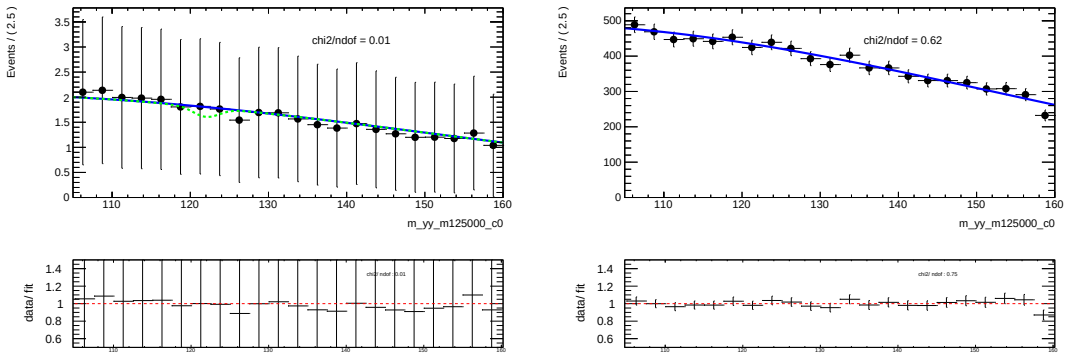

(e)

(f)

Figure 16: The fitted number of spurious signal. Left is one lepton signal region, right is zero lepton control region. The shape is constrained by control region, which has higher statistic. (a)(b) for mh400, (c)(d) for mh500, (e)(f) for non-resonant

8 Systematic uncertainties

8.1 Luminosity uncertainties

The uncertainties on the integrated luminosity that is obtained from beam separation scans taken in whole 2015 and 2016 are ±2.1% and ±4.5% [21], respectively.

8.2 Theoretical uncertainties

The LHCHXSWG recommended scale and PDF uncertainties on SM single Higgs processes are documented in Ref [22], and they are used in the analysis as presented in Table 13.

Processes	+QCD Scale %	-QCD Scale %	$\pm PDF$ %	$\pm\alpha_s$ %
ggh	+3.9	-3.9	± 1.9	± 2.6
VBF	+0.4	-0.3	± 2.1	± 0.5
Wh	+0.5	-0.7	± 1.7	± 0.9
Zh	+3.8	-3.0	± 1.3	± 0.9
tth	+5.8	-9.2	± 3.0	± 2.0

Table 13: SM single Higgs scale and PDF uncertainties.

The LHCHXSWG recommended scale and PDF uncertainties on SM Higgs pair production are used in the analysis as presented in Table 14.

$\sqrt{s}$	$\sigma^{NNLO}_{gg\to hh}$	Scale	$\pm PDF$ %	$\pm\alpha_s$ %	EFT
13 TeV	33.41 fb	+4.3% -6.0%	±2.1%	±2.3%	±5%

Table 14: SM Higgs pair process (ggF) scale and PDF uncertainties, taken from Ref [23], only applied to the non-resonant analysis

Additional uncertainty of +2.1%/-2.0% applies to the $h \to \gamma\gamma$ branching ratio, and +1.5%/-1.5% to the $h \to WW$ branching ratio according to recommendations from Ref [24], since the final upper limits is set on $\sigma(gg \to hh)$ and $\sigma(gg \to H) \times BR(X \to hh)$.

The Wh process is generated with Pythia8, which uses parton shower to model the additional jets. To take into account the uncertainties that is caused by parton-shower originated jets, we generate the $Wh+jj$ (jets from matrix element) process with MadGraph5 and compare the difference in 2-jet-inclusive bin. This results in a 37.5% uncertainty for Wh process.

8.3 Experimental Uncertainties

The uncertainties from trigger efficiency, photon energy scale, lepton efficiency, jet energy scale/resolution and b-tagging efficiency are summarized in Table 15 for signals and Table 16 for SM single Higgs backgrounds. These numbers are uncertainties on the yields and are estimated following CP and PC recommendations.

All the detailed information on uncertainties are shown in Appendix B.

Uncertainty source	Non-resonance	260 GeV	300 GeV	400 GeV	500GeV
Flavor tag (B) up	0.0650861	0.0921214	0.073844	0.0734646	0.0601294
Flavor tag (B) down	0.0646498	0.09199	0.0733022	0.0723039	0.0601101
Flavor tag (C) up	0.472762	0.362139	0.391853	0.441169	0.467811
Flavor tag (C) down	0.472293	0.361973	0.391587	0.440829	0.46736
Flavor tag (LF) up	0.423803	0.385998	0.38995	0.41174	0.424746
Flavor tag (LF) down	0.422465	0.385021	0.388903	0.410515	0.423387
Flavor tag extrapolation up	0.00803051	0.000455188	0.00221147	0.00262737	0.00722864
Flavor tag extrapolation down	0.00798505	0.000455188	0.00221147	0.00262737	0.00722648
Pileup up	0.158779	0.877376	0.169916	0.156771	1.06892
Pileup down	0.428639	0.673702	0.369119	0.514904	0.722756
Photon up	4.35908	4.3724	4.41343	4.37119	4.34523
Photon down	4.27325	4.28685	4.32613	4.28517	4.25962
Photon DD iso	0.000997	0.064722	0.0955585	0.041966	0.0237342
Electron up	0.744489	0.917579	0.834558	0.755946	0.699944
Electron down	0.744489	0.917579	0.834558	0.755946	0.699944
Egamma up	2.81932	2.59898	2.52272	3.71587	2.65252
Egamma down	6.91237	5.96987	5.19161	6.25901	7.37225
Muon up	0.34013	0.4923	0.435747	0.381803	0.330689
Muon down	0.344345	0.49397	0.430601	0.386166	0.330376
JET up	4.6672	10.418	8.14286	5.70029	3.702
JET down	4.95406	9.67426	8.32026	5.39259	3.38065
JER	0.342969	1.52351	0.335264	0.614238	0.313753

Table 15: Experimental uncertainties on the yields in percentage for signal processes.

8.4 Uncertainty on the continuum background modeling

Spurious signals are imported as a source of systematic uncertainties due to the choice of the background parametrization. These events are added to the model as signal events.

The spurious signals are calculated by doing a signal plus background fit on the background only sample with a scanning on the peak of Higgs mass in the signal PDF.

Uncertainty source	ggh	VBF	Wh	Zh	tth
Flavor tag (B) up	1.06836	0.350132	0.083865	0.468685	10.7036
Flavor tag (B) down	1.06836	0.350132	0.083865	0.467072	10.2571
Flavor tag (C) up	0.122156	0.316965	0.186938	0.257531	0.478546
Flavor tag (C) down	0.122156	0.316947	0.186617	0.256853	0.478079
Flavor tag (LF) up	0.395887	0.420928	0.390579	0.361581	0.41425
Flavor tag (LF) down	0.394873	0.419592	0.389617	0.360745	0.412758
Flavor tag extrapolation up	0	0	0.0402298	0.088111	1.48875
Flavor tag extrapolation down	0	0	0.0400921	0.088131	1.52878
Pileup up	13.8733	4.76491	0.974677	1.57804	1.56557
Pileup down	9.74485	3.69482	0.836758	0.525316	1.71323
Photon up	4.31217	4.4389	4.51596	4.43344	4.41042
Photon down	4.22909	4.34985	4.42458	4.34531	4.32298
Photon DD iso	0	1.42252	0.038109	0	0
Electron up	0.281956	0.614818	0.671288	0.66722	0.728369
Electron down	0.281956	0.614818	0.671288	0.66722	0.728368
Egamma up	5.96617	2.06907	1.87162	2.72589	1.47049
Egamma down	5.9341	2.90573	2.09111	3.27575	2.39543
Muon up	1.27993	1.15012	0.372511	0.376371	0.353962
Muon down	1.27994	1.95057	0.35458	0.386865	0.391932
JET up	5.61672	7.67473	13.28	11.7479	2.79255
JET down	5.02181	7.19362	10.5476	7.48568	2.62342
JER	0.917808	6.02256	5.51179	3.22629	2.39804

Table 16: Experimental uncertainties on the yields in percentage for background processes.

9 Statistical interpretation

(SO FAR THE FOLLOW STATISTICAL RESULTS ARE OBTAINED WITH EVENT NUMBER COUNTING, TO BE UPDATED TO SHAPE FIT IN THE NEXT ROUND)

The statistical model is built up with an unbinned likelihood function. Its formula is shown below.

$$\mathcal{L}(\mu,\theta) = \prod_i (n_{BSM}(\mu,\theta)\times f_{DSCB}(m^i_{\gamma\gamma},\theta)+n_{SM}(\theta)\times f_{DSCB}(m^i_{\gamma\gamma},\theta)+n_{Cont}\times f_{Cont}(m^i_{\gamma\gamma},\theta))) \prod Norm(\theta|0,1) \quad (2)$$

where i stands for the event index, n_{BSM} the number of expected signal events, n_{SM} the number of expected single Higgs events, n_B the number of expected continuum background events, f_{DSBC} the pdf of a double-sided crystal ball function shared by both BSM signal and SM Higgs, f_{Cont} the pdf of the continuum background i.e. the second order exponential, μ the cross section (time the branching ratio of $X \to hh$) of non-resonant (resonant) production, and $Norm$ the probability density function of a Gaussian distribution used for constraining the nuisance paramters. The systematic uncertainties are introduced by a set of nuisance parameters θ which can vary the acceptance of signal and single Higgs processes as well as the function paramters of either f_{DSBC} or f_{Cont}.

To make sure that the statistical model are properly built up, checks on the pull of nuisance parameters $(\theta_{fit} - \theta_0)/\Delta\theta$ are performed with an unconditional fit to the amount of expected backgrounds, as shown in Figure 17, 18, 19, 20 and 21. The values of the pull of nuisance parameteres are always close to 0, which suggests a correct implementation of the staistical model. Similar checkes are done with the observed data in order to check the data constraints on nuisance parameters, as shown in Figure 22, 23, 24, 25 and 26.

Meanwhile, checks on the correlation between all parameters in the statistical model are performed, as shown in Figure 27, 28, 29, 30 and 31, with an unconditional fit to the amount of expected backgrounds, and in Figure 32, 33, 34, 35 and 36, with an unconditional fit to observed data.

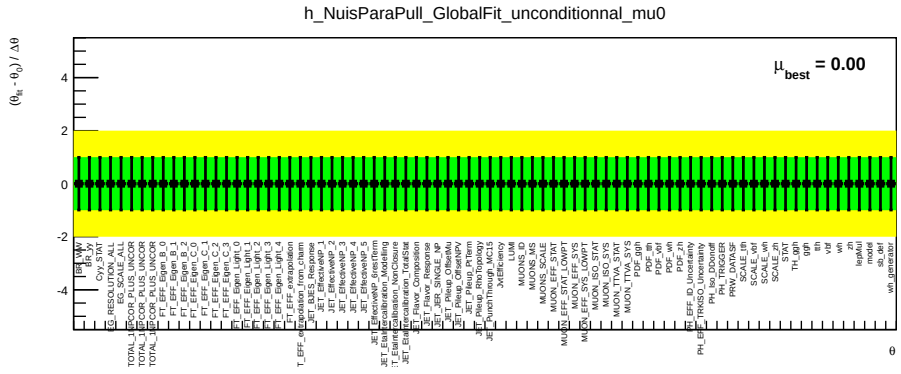

Figure 17: Nuisance parameter pull checks for non-resonance with a fit to expected backgrounds only.

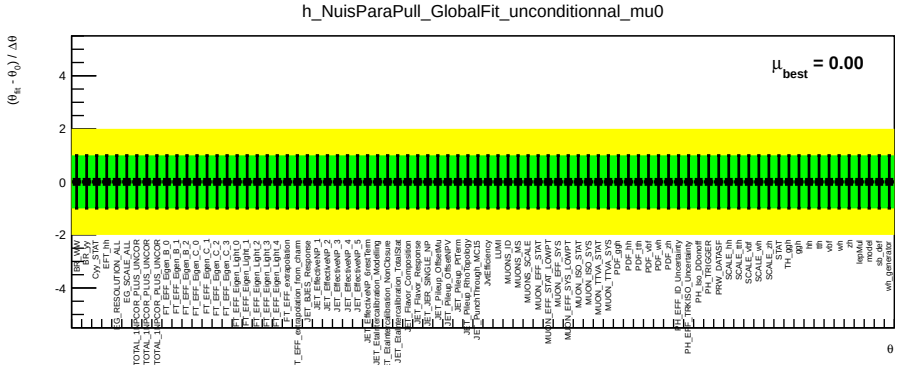

Figure 18: Nuisance parameter pull checks for resonance $m_H = 260$ GeV with a fit to expected backgrounds only.

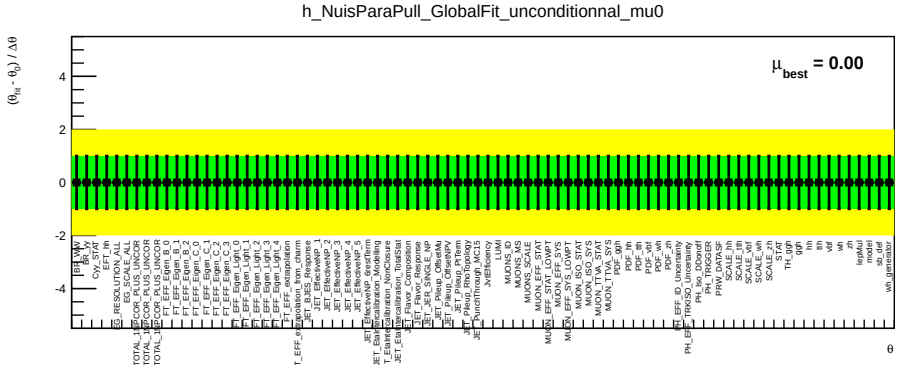

Figure 19: Nuisance parameter pull checks for resonance $m_H = 300$ GeV with a fit to expected backgrounds only.

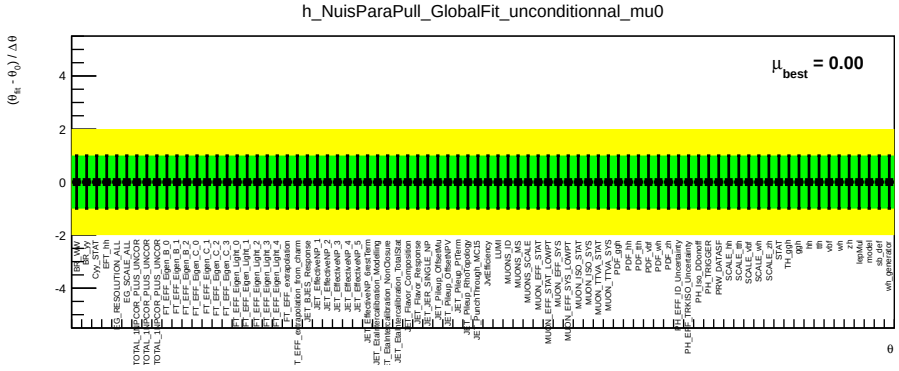

Figure 20: Nuisance parameter pull checks for resonance $m_H = 400$ GeV with a fit to expected backgrounds only.

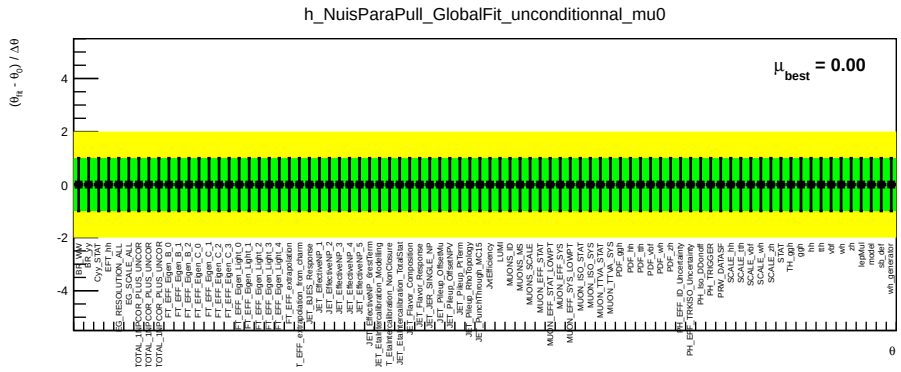

Figure 21: Nuisance parameter pull checks for resonance $m_H = 500$ GeV with a fit to expected backgrounds only.

IMAGE COMING SOON

Figure 22: Nuisance parameter pull checks for non-resonance with a fit to observed data.

Figure 23: Nuisance parameter pull checks for resonance m_H = 260 GeV with a fit to observed data.

Figure 24: Nuisance parameter pull checks for resonance m_H = 300 GeV with a fit to observed data.

Figure 25: Nuisance parameter pull checks for resonance m_H = 400 GeV with a fit to observed data.

Figure 26: Nuisance parameter pull checks for resonance m_H = 500 GeV with a fit to observed data.

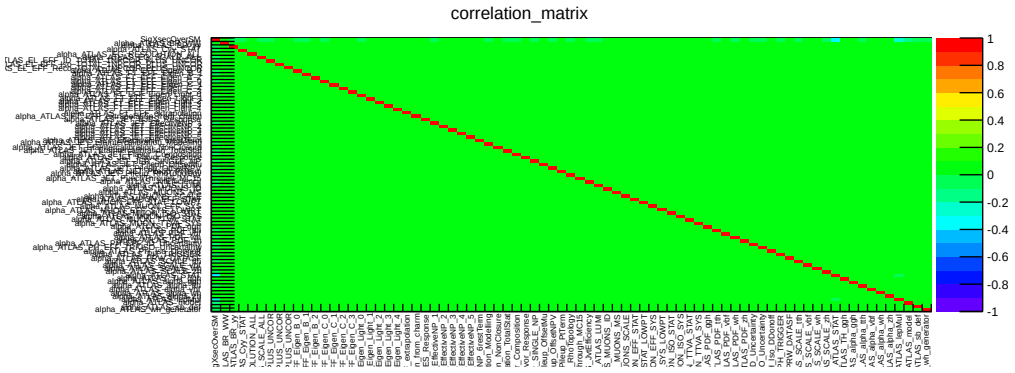

Figure 27: Correlation matrix for nuisance parameters for non-resonance with a fit to expected backgrounds only.

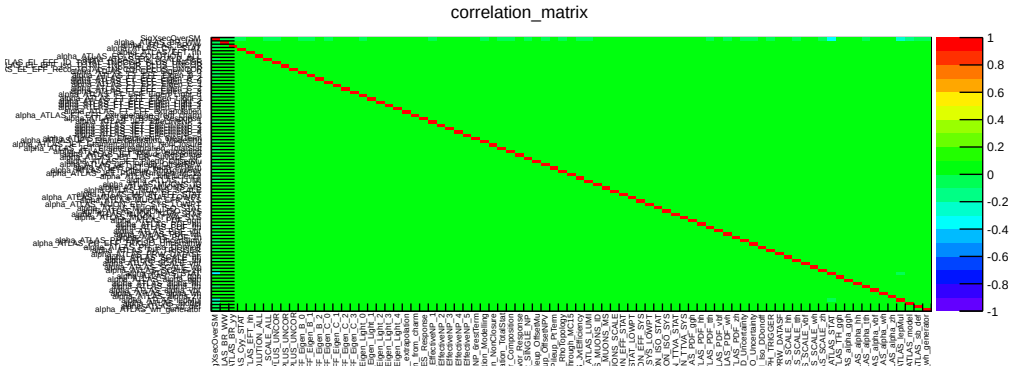

Figure 28: Correlation matrix for nuisance parameters for resonance $m_H = 260$ GeV with a fit to expected backgrounds only.

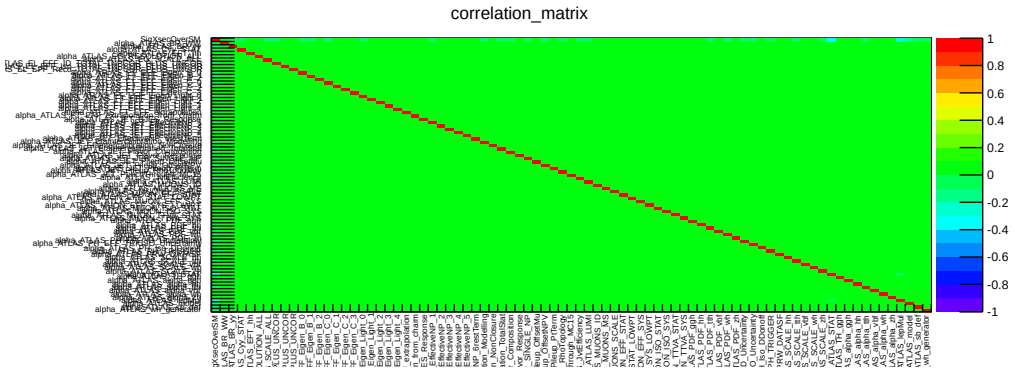

Figure 29: Correlation matrix for nuisance parameters for resonance $m_H = 300$ GeV with a fit to expected backgrounds only.

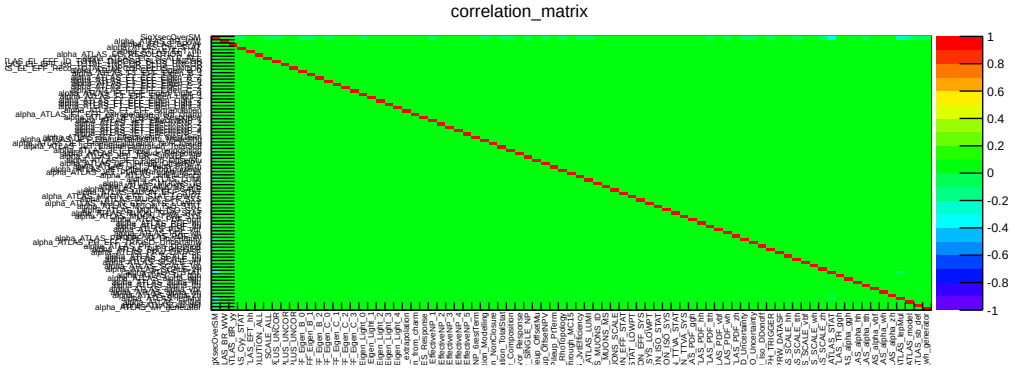

Figure 30: Correlation matrix for nuisance parameters for resonance $m_H = 400$ GeV with a fit to expected backgrounds only.

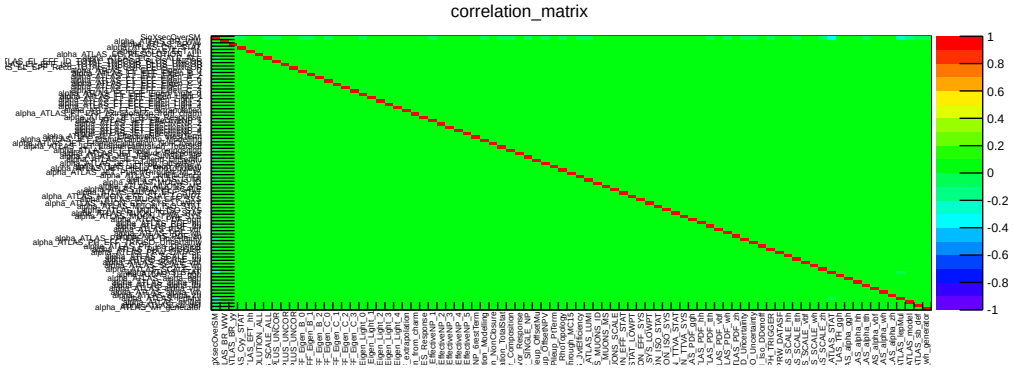

Figure 31: Correlation matrix for nuisance parameters for resonance $m_H = 500$ GeV with a fit to expected backgrounds only.

Figure 32: Correlation matrix for nuisance parameters for non-resonance with a fit to observed data.

Figure 33: Correlation matrix for nuisance parameters for resonance $m_H = 260$ GeV with a fit to observed data.

Figure 34: Correlation matrix for nuisance parameters for resonance $m_H = 300$ GeV with a fit to observed data.

Figure 35: Correlation matrix for nuisance parameters for resonance $m_H = 400$ GeV with a fit to observed data.

Figure 36: Correlation matrix for nuisance parameters for resonance $m_H = 500$ GeV with a fit to observed data.

A likelihood ratio based test statistic is used in the statistical analysis. It is defined as follows:

$$\tilde{q}_\mu = \begin{cases} -2\ln\frac{\mathcal{L}(\mu,\hat{\hat{\theta}}(\mu))}{\mathcal{L}(0,\hat{\hat{\theta}}(0))} & \text{if } \hat{\mu} < 0 \\ -2\ln\frac{\mathcal{L}(\mu,\hat{\hat{\theta}}(\mu))}{\mathcal{L}(\hat{\mu},\hat{\theta})} & \text{if } 0 \le \hat{\mu} \le \mu \\ 0 & \text{if } \hat{\mu} > \mu \end{cases} \quad (3)$$

where $\mathcal{L}$ stands for the likelihood function for the statisticl model of the analysis, θ a set of nuisance parameters through which the systematic uncertainties are introduced, and the parameter of interest (POI) μ the cross section of non-resonant production or the cross section of resonant production times the branching ratio of $X \to hh$. Single hat stands for unconditional fit and double hat for conditional fit, i.e., POI μ is fixed to a certain value. With this test statistic, one derives the upper limits of the cross section for non-resonant production and the cross section times the branching ratio of $X \to hh$ for resonant production at 95% confidence level by using the CL_s method [25] under the asymptotic approximation [26]. The results are shown in Figure 37 and the numbers are summarized in Table 17.

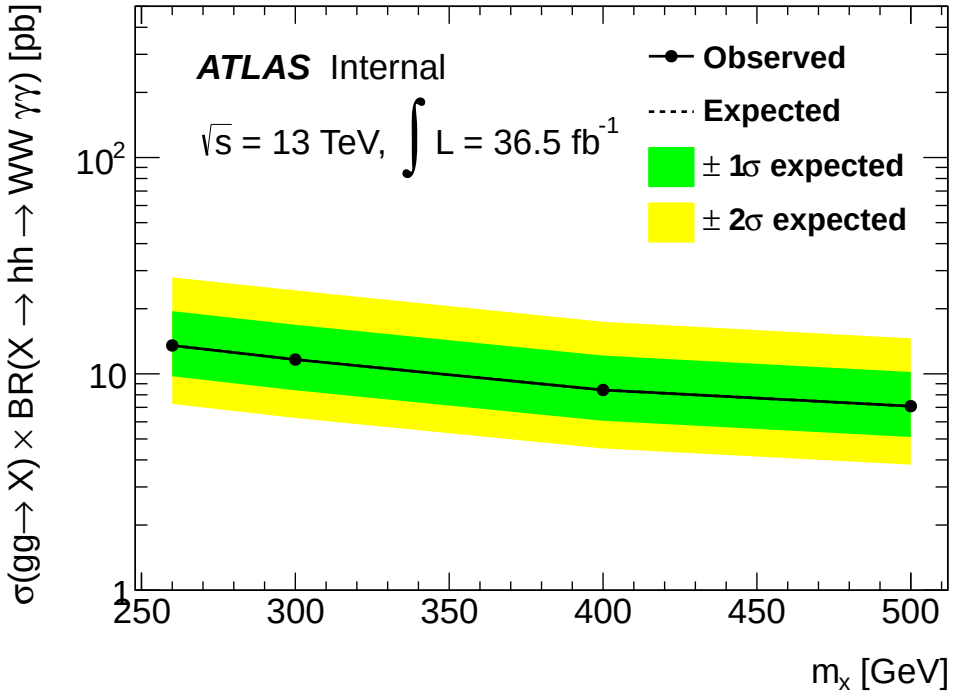

Figure 37: Upper limits at the 95% confidence level for resonance as a function of the mass of the heavy scalar.

	Higgs pair	260 GeV	300 GeV	400 GeV	500 GeV
$+2\sigma$	16.071	27.9317	24.305	17.4098	14.5864
$+1\sigma$	11.2084	19.4905	16.8559	12.1447	10.1997
-1σ	5.60365	9.74654	8.39283	6.06772	5.10635
-2σ	4.17403	7.25999	6.25163	4.51971	3.80361
Median	7.77684	13.5264	11.6477	8.4209	7.08669
Observed	7.77491	13.5237	11.6423	8.41989	7.08776

Table 17: Upper limits at the 95% confidence level for the cross section of the gluon fusion production of the non-resonance and the cross section of the gluon fusion production of the resonance times the branching ratio of $X \to hh$.

References

[1] ATLAS Collaboration, *Observation of a new particle in the search for the Standard Model Higgs boson with the ATLAS detector at the LHC*, Phys. Lett. B **716** (2012) 1–29. http://www.sciencedirect.com/science/article/pii/S037026931200857X.

[2] CMS Collaboration, *Observation of a new boson at a mass of 125 GeV with the CMS experiment at the LHC*, Phys. Lett. B **716** (2012) 30–61. http://www.sciencedirect.com/science/article/pii/S0370269312008581.

[3] ATLAS Collaboration, *Measurements of Higgs boson production and couplings in diboson final states with the ATLAS detector at the LHC*, Phys.Lett. **B726** (2013) 88–119.

[4] The CMS Collaboration, *Combination of standard model Higgs boson searches and measurements of the properties of the new boson with a mass near 125 GeV*, CMS-PAS-HIG-13-005, CERN, Geneva, 2013. http://cdsweb.cern.ch/record/1542387.

[5] ATLAS and CMS Collaborations ATLAS-CONF-2015-044, Sep, 2015. https://atlas.web.cern.ch/Atlas/GROUPS/PHYSICS/CONFNOTES/ATLAS-CONF-2015-044/.

[6] *LHC Higgs Cross Section HH Sub-group*, https://twiki.cern.ch/twiki/bin/view/LHCPhysics/LHCHXSWGHH.

[7] J. Baglio, A. Djouadi, R. Gröber, M.M. Mühlleitner, J. Quevillon et al., *The measurement of the Higgs self-coupling at the LHC: theoretical status*, JHEP **1304** (2013) 151.

[8] G. C. Branco, P. M. Ferreira, L. Lavoura, M. N. Rebelo, M. Sher, and J. P. Silva, *Theory and phenomenology of two-Higgs-doublet models*, Phys. Rept. **516** (2012) 1–102, arXiv:1106.0034 [hep-ph].

[9] ATLAS Collaboration, G. Aad et al., *Search For Higgs Boson Pair Production in the $\gamma\gamma b\bar{b}$ Final State using pp Collision Data at $\sqrt{s} = 8$ TeV from the ATLAS Detector*, Phys. Rev. Lett. **114** (2015) no. 8, 081802, arXiv:1406.5053 [hep-ex].

[10] ATLAS Collaboration, G. Aad et al., *Search for Higgs boson pair production in the $b\bar{b}b\bar{b}$ final state from pp collisions at $\sqrt{s} = 8$ TeVwith the ATLAS detector*, Eur. Phys. J. **C75** (2015) no. 9, 412, arXiv:1506.00285 [hep-ex].

[11] ATLAS Collaboration, G. Aad et al., *Searches for Higgs boson pair production in the $hh \to bb\tau\tau, \gamma\gamma WW^*, \gamma\gamma bb, bbbb$ channels with the ATLAS detector*, Phys. Rev. **D92** (2015) 092004, arXiv:1509.04670 [hep-ex].

[12] J. Alwall, M. Herquet, F. Maltoni, O. Mattelaer, and T. Stelzer, *MadGraph 5 : Going Beyond*, JHEP **06** (2011) 128, arXiv:1106.0522 [hep-ph].

[13] Web pages. F. Maltoni, Higgs pair production. https://cp3.irmp.ucl.ac.be/projects/madgraph/wiki/HiggsPairProduction, Dec 2013.

[14] S. Frixione and B. R. Webber, *Matching NLO QCD computations and parton shower simulations*, JHEP **06** (2002) 029, arXiv:hep-ph/0204244 [hep-ph].

[15] J. Grigo, J. Hoff, and M. Steinhauser, *Higgs boson pair production: top quark mass effects at NLO and NNLO*, Nucl. Phys. **B900** (2015) 412–430, arXiv:1508.00909 [hep-ph].

[16] J. Bellm et al., *Herwig++ 2.7 Release Note*, arXiv:1310.6877 [hep-ph].

[17] S. Gieseke, C. Rohr, and A. Siodmok, *Colour reconnections in Herwig++*, Eur. Phys. J. **C72** (2012) 2225, arXiv:1206.0041 [hep-ph].

[18] P. M. Nadolsky, H.-L. Lai, Q.-H. Cao, J. Huston, J. Pumplin, D. Stump, W.-K. Tung, and C. P. Yuan, *Implications of CTEQ global analysis for collider observables*, Phys. Rev. **D78** (2008) 013004, arXiv:0802.0007 [hep-ph].

[19] M. Cacciari, G. P. Salam, and G. Soyez, *The anti- k t jet clustering algorithm*, Journal of High Energy Physics **2008** (2008) no. 04, 063.

[20] L. C. et al., *Measurement of the isolated di-photon cross section in 4.9 fb1 of pp collisions at ps = 7 TeV with the ATLAS detecto*, ATL-COM-PHYS-2012-592, CERN, 2012. https://cds.cern.ch/record/1450063.

[21] *LuminosityForPhysics*, https://twiki.cern.ch/twiki/bin/viewauth/Atlas/LuminosityForPhysics.

[22] *CERN Yellow Report 4*, https://twiki.cern.ch/twiki/bin/view/LHCPhysics/CERNYellowReportPageAt13TeV.

[23] *LHC Higgs Cross Section HH Sub-group*, https://twiki.cern.ch/twiki/bin/view/LHCPhysics/LHCHXSWGHH#Current_recommendations_for_di_H.

[24] *LHC Higgs Cross Section Working Group*, https://twiki.cern.ch/twiki/bin/view/LHCPhysics/CERNYellowReportPageBR#Higgs_2_fermions.

[25] A. L. Read, *Presentation of search results: The CL(s) technique*, J.Phys. **G28** (2002) 2693–2704.

[26] G. Cowan et al., *Asymptotic formulae for likelihood-based tests of new physics*, Eur. Phys. J. **C71** (2011) 1554, arXiv:1007.1727 [physics.data-an].

Appendices

A MadGraphs5 cards used for signals

Here, the cards used for generating heavy scalar resonant at the mass point of 300 GeV are given. The cards for other mass points are basically the same except the mass setting.

```
#*********************************************************************
#                        MadGraph5_aMC@NLO                           *
#                                                                    *
#                      run_card.dat aMC@NLO                          *
#                                                                    *
#  This file is used to set the parameters of the run.               *
#                                                                    *
#  Some notation/conventions:                                        *
#                                                                    *
#   Lines starting with a hash (#) are info or comments              *
#                                                                    *
#   mind the format:   value    = variable     ! comment             *
#*********************************************************************
#
#*******************
# Running parameters
#*******************
#
#*********************************************************************
# Tag name for the run (one word)                                    *
#*********************************************************************
  tag_1     = run_tag ! name of the run
#*********************************************************************
# Number of LHE events (and their normalization) and the required    *
# (relative) accuracy on the Xsec.                                   *
# These values are ignored for fixed order runs                      *
#*********************************************************************
  15000       = nevents ! Number of unweighted events requested
    -1 = req_acc ! Required accuracy (-1=auto determined from nevents)
    -1 = nevt_job! Max number of events per job in event generation.
                 !  (-1= no split).
#*********************************************************************
# Normalize the weights of LHE events such that they sum or average to *
# the total cross section                                            *
#*********************************************************************
 average = event_norm      ! average or sum
#*********************************************************************
# Number of points per itegration channel (ignored for aMC@NLO runs)   *
#*********************************************************************
 0.01   = req_acc_FO       ! Required accuracy (-1=ignored, and use the
                           ! number of points and iter. below)
```

```
# These numbers are ignored except if req_acc_FO is equal to -1
 5000   = npoints_FO_grid  ! number of points to setup grids
 4      = niters_FO_grid   ! number of iter. to setup grids
 10000  = npoints_FO       ! number of points to compute Xsec
 6      = niters_FO        ! number of iter. to compute Xsec
#*********************************************************************
# Random number seed                                                 *
#*********************************************************************
   234      = iseed   ! rnd seed (0=assigned automatically=default))
#*********************************************************************
# Collider type and energy                                           *
#*********************************************************************
    1   = lpp1    ! beam 1 type (0 = no PDF)
    1   = lpp2    ! beam 2 type (0 = no PDF)
   6500      = ebeam1  ! beam 1 energy in GeV
   6500      = ebeam2  ! beam 2 energy in GeV
#*********************************************************************
# PDF choice: this automatically fixes also alpha_s(MZ) and its evol.  *
#*********************************************************************
 lhapdf    = pdlabel   ! PDF set
 11000    = lhaid     ! if pdlabel=lhapdf, this is the lhapdf number
#*********************************************************************
# Include the NLO Monte Carlo subtr. terms for the following parton    *
# shower (HERWIG6 | HERWIGPP | PYTHIA6Q | PYTHIA6PT | PYTHIA8)         *
# WARNING: PYTHIA6PT works only for processes without FSR!!!!          *
#*********************************************************************
 HERWIGPP    = parton_shower
#*********************************************************************
# Renormalization and factorization scales                           *
# (Default functional form for the non-fixed scales is the sum of      *
# the transverse masses of all final state particles and partons. This *
# can be changed in SubProcesses/set_scales.f)                       *
#*********************************************************************
 .true.   = fixed_ren_scale  ! if .true. use fixed ren scale
 .true.   = fixed_fac_scale  ! if .true. use fixed fac scale
 150.0    = muR_ref_fixed    ! fixed ren reference scale
 150.0    = muF1_ref_fixed   ! fixed fact reference scale for pdf1
 150.0    = muF2_ref_fixed   ! fixed fact reference scale for pdf2
#*********************************************************************
# Renormalization and factorization scales (advanced and NLO options)  *
#*********************************************************************
 .true.   = fixed_QES_scale  ! if .true. use fixed Ellis-Sexton scale
 150.0    = QES_ref_fixed    ! fixed Ellis-Sexton reference scale
 1        = muR_over_ref     ! ratio of current muR over reference muR
 1        = muF1_over_ref    ! ratio of current muF1 over reference muF1
 1        = muF2_over_ref    ! ratio of current muF2 over reference muF2
 1        = QES_over_ref     ! ratio of current QES over reference QES
#*********************************************************************
```

```
# Reweight flags to get scale dependence and PDF uncertainty          *
# For scale dependence: factor rw_scale_up/down around central scale  *
# For PDF uncertainty: use LHAPDF with supported set                  *
#*********************************************************************
 .true.   = reweight_scale   ! reweight to get scale dependence
  0.5     = rw_Rscale_down   ! lower bound for ren scale variations
  2.0     = rw_Rscale_up     ! upper bound for ren scale variations
  0.5     = rw_Fscale_down   ! lower bound for fact scale variations
  2.0     = rw_Fscale_up     ! upper bound for fact scale variations
 .false.  = reweight_PDF     ! reweight to get PDF uncertainty
 11001    = PDF_set_min      ! First of the error PDF sets
 11052    = PDF_set_max      ! Last of the error PDF sets
#*********************************************************************
# Merging - WARNING! Applies merging only at the hard-event level.    *
# After showering an MLM-type merging should be applied as well.      *
# See http://amcatnlo.cern.ch/FxFx_merging.htm for more details.      *
#*********************************************************************
 0        = ickkw            ! 0 no merging, 3 FxFx merging, 4 UNLOPS
#*********************************************************************
#
#*********************************************************************
# BW cutoff (M+/-bwcutoff*Gamma)                                      *
#*********************************************************************
 15  = bwcutoff
#*********************************************************************
# Cuts on the jets                                                    *
# Jet clustering is performed by FastJet.
# When matching to a parton shower, these generation cuts should be   *
# considerably softer than the analysis cuts.                         *
# (more specific cuts can be specified in SubProcesses/cuts.f)        *
#*********************************************************************
  -1  = jetalgo   ! FastJet jet algorithm (1=kT, 0=C/A, -1=anti-kT)
 0.4  = jetradius ! The radius parameter for the jet algorithm
  10  = ptj       ! Min jet transverse momentum
  -1  = etaj      ! Max jet abs(pseudo-rap) (a value .lt.0 means no cut)
#*********************************************************************
# Cuts on the charged leptons (e+, e-, mu+, mu-, tau+ and tau-)       *
# (more specific gen cuts can be specified in SubProcesses/cuts.f)    *
#*********************************************************************
   0  = ptl     ! Min lepton transverse momentum
  -1  = etal    ! Max lepton abs(pseudo-rap) (a value .lt.0 means no cut)
   0  = drll    ! Min distance between opposite sign lepton pairs
   0  = drll_sf ! Min distance between opp. sign same-flavor lepton pairs
   0  = mll     ! Min inv. mass of all opposite sign lepton pairs
  30  = mll_sf  ! Min inv. mass of all opp. sign same-flavor lepton pairs
#*********************************************************************
# Photon-isolation cuts, according to hep-ph/9801442                  *
# When ptgmin=0, all the other parameters are ignored                 *
```

```
#*********************************************************************
  20  = ptgmin    ! Min photon transverse momentum
  -1  = etagamma  ! Max photon abs(pseudo-rap)
 0.4  = R0gamma   ! Radius of isolation code
 1.0  = xn        ! n parameter of eq.(3.4) in hep-ph/9801442
 1.0  = epsgamma  ! epsilon_gamma parameter of eq.(3.4) in hep-ph/9801442
 .true.  = isoEM  ! isolate photons from EM energy (photons and leptons)
#*********************************************************************
# Maximal PDG code for quark to be considered a jet when applying cuts.*
# At least all massless quarks of the model should be included here.   *
#*********************************************************************
 4 = maxjetflavor
#*********************************************************************
# For aMCfast+APPLGRID use in PDF fitting (http://amcfast.hepforge.org)*
#*********************************************************************
 0 = iappl   ! aMCfast switch (0=OFF, 1=prepare APPLgrids, 2=fill grids)
#*********************************************************************
```

B Systematic uncertainties in details

Uncertainty Source	Relative Variations
$EG\_RESOLUTION\_ALL\_\_1down$	-0.137961
$EG\_RESOLUTION\_ALL\_\_1up$	-1.18221
$EG\_SCALE\_ALL\_\_1down$	-2.39145
$EG\_SCALE\_ALL\_\_1up$	-0.874492
$EL\_EFF\_ID\_TOTAL\_1NPCOR\_PLUS\_UNCOR\_\_1down$	-0.657327
$EL\_EFF\_ID\_TOTAL\_1NPCOR\_PLUS\_UNCOR\_\_1up$	0.657327
$EL\_EFF\_Iso\_TOTAL\_1NPCOR\_PLUS\_UNCOR\_\_1down$	-0.174149
$EL\_EFF\_Iso\_TOTAL\_1NPCOR\_PLUS\_UNCOR\_\_1up$	0.17415
$EL\_EFF\_Reco\_TOTAL\_1NPCOR\_PLUS\_UNCOR\_\_1down$	-0.260986
$EL\_EFF\_Reco\_TOTAL\_1NPCOR\_PLUS\_UNCOR\_\_1up$	0.260987
$MUONS\_ID\_\_1down$	0.0917129
$MUONS\_ID\_\_1up$	0.0612452
$MUONS\_MS\_\_1down$	0.153867
$MUONS\_MS\_\_1up$	-0.000134826
$MUONS\_SCALE\_\_1down$	-0.000187282
$MUONS\_SCALE\_\_1up$	0.000114101
$MUON\_EFF\_STAT\_LOWPT\_\_1down$	-0.0308792
$MUON\_EFF\_STAT\_LOWPT\_\_1up$	0.0308792
$MUON\_EFF\_STAT\_\_1down$	-0.122007
$MUON\_EFF\_STAT\_\_1up$	0.122007
$MUON\_EFF\_SYS\_LOWPT\_\_1down$	-0.0280802
$MUON\_EFF\_SYS\_LOWPT\_\_1up$	0.0280802
$MUON\_EFF\_SYS\_\_1down$	-0.208108
$MUON\_EFF\_SYS\_\_1up$	0.208142
$MUON\_ISO\_STAT\_\_1down$	-0.0172122
$MUON\_ISO\_STAT\_\_1up$	0.0172122
$MUON\_ISO\_SYS\_\_1down$	-0.115447
$MUON\_ISO\_SYS\_\_1up$	0.115447
$MUON\_TTVA\_STAT\_\_1down$	-0.0790578
$MUON\_TTVA\_STAT\_\_1up$	0.0790579
$MUON\_TTVA\_SYS\_\_1down$	-0.204239
$MUON\_TTVA\_SYS\_\_1up$	0.204239
$PH\_EFF\_ID\_Uncertainty\_\_1down$	-4.17194
$PH\_EFF\_ID\_Uncertainty\_\_1up$	4.26067
$PH\_EFF\_TRKISO\_Uncertainty\_\_1down$	-1.13272
$PH\_EFF\_TRKISO\_Uncertainty\_\_1up$	1.13951
$PH\_Iso\_DDonoff$	0
$PRW\_DATASF\_\_1down$	1.71323
$PRW\_DATASF\_\_1up$	-1.56557

Table 18: Systematic uncertainties for *tth* in percent.

Uncertainty Source	Relative Variations
$JET\_BJES\_Response\_\_1up$	-0.158368
$JET\_BJES\_Response\_\_1down$	1.21216
$JET\_EffectiveNP\_1\_\_1up$	-0.567856
$JET\_EffectiveNP\_1\_\_1down$	1.91092
$JET\_EffectiveNP\_2\_\_1up$	0.327808
$JET\_EffectiveNP\_2\_\_1down$	-0.19533
$JET\_EffectiveNP\_3\_\_1up$	-0.0428545
$JET\_EffectiveNP\_3\_\_1down$	0.38271
$JET\_EffectiveNP\_4\_\_1up$	0.246797
$JET\_EffectiveNP\_4\_\_1down$	-0.0150673
$JET\_EffectiveNP\_5\_\_1up$	0.00378298
$JET\_EffectiveNP\_5\_\_1down$	-0.00607099
$JET\_EffectiveNP\_6restTerm\_\_1up$	0.0106005
$JET\_EffectiveNP\_6restTerm\_\_1down$	0.129305
$JET\_EtaIntercalibration\_Modelling\_\_1up$	0.773632
$JET\_EtaIntercalibration\_Modelling\_\_1down$	0.29923
$JET\_EtaIntercalibration\_NonClosure\_\_1up$	-0.0022013
$JET\_EtaIntercalibration\_NonClosure\_\_1down$	-0.0003448
$JET\_EtaIntercalibration\_TotalStat\_\_1up$	-0.0534712
$JET\_EtaIntercalibration\_TotalStat\_\_1down$	0.105292
$JET\_Flavor\_Composition\_\_1up$	0.767915
$JET\_Flavor\_Composition\_\_1down$	-0.683071
$JET\_Flavor\_Response\_\_1up$	-0.415142
$JET\_Flavor\_Response\_\_1down$	0.0999425
$JET\_JER\_SINGLE\_NP\_\_1up$	2.39804
$JET\_Pileup\_OffsetMu\_\_1up$	-0.130591
$JET\_Pileup\_OffsetMu\_\_1down$	0.33675
$JET\_Pileup\_OffsetNPV\_\_1up$	0.23825
$JET\_Pileup\_OffsetNPV\_\_1down$	0.290904
$JET\_Pileup\_PtTerm\_\_1up$	0.00600941
$JET\_Pileup\_PtTerm\_\_1down$	0.0689693
$JET\_Pileup\_RhoTopology\_\_1up$	0.304264
$JET\_Pileup\_RhoTopology\_\_1down$	0.883056
$JET\_PunchThrough\_MC15\_\_1up$	-4.92251e-06
$JET\_PunchThrough\_MC15\_\_1down$	1.87617e-05
$JET\_SingleParticle\_HighPt\_\_1up$	0
$JET\_SingleParticle\_HighPt\_\_1down$	0
$JvtEfficiencyDown$	-3.62616
$JvtEfficiencyUp$	3.74445

Table 19: Systematic uncertainties for *tth* in percent.

Uncertainty Source	Relative Variations
$FT\_EFF\_Eigen\_B\_0\_\_1down$	-9.58011
$FT\_EFF\_Eigen\_B\_0\_\_1up$	10.0348
$FT\_EFF\_Eigen\_B\_1\_\_1down$	-3.50262
$FT\_EFF\_Eigen\_B\_1\_\_1up$	3.56904
$FT\_EFF\_Eigen\_B\_2\_\_1down$	1.07806
$FT\_EFF\_Eigen\_B\_2\_\_1up$	-1.06382
$FT\_EFF\_Eigen\_C\_0\_\_1down$	-0.464646
$FT\_EFF\_Eigen\_C\_0\_\_1up$	0.465142
$FT\_EFF\_Eigen\_C\_1\_\_1down$	0.0870532
$FT\_EFF\_Eigen\_C\_1\_\_1up$	-0.0869841
$FT\_EFF\_Eigen\_C\_2\_\_1down$	0.0699073
$FT\_EFF\_Eigen\_C\_2\_\_1up$	-0.0698937
$FT\_EFF\_Eigen\_C\_3\_\_1down$	0.0140752
$FT\_EFF\_Eigen\_C\_3\_\_1up$	-0.0140722
$FT\_EFF\_Eigen\_Light\_0\_\_1down$	-0.412255
$FT\_EFF\_Eigen\_Light\_0\_\_1up$	0.413749
$FT\_EFF\_Eigen\_Light\_1\_\_1down$	0.0100785
$FT\_EFF\_Eigen\_Light\_1\_\_1up$	-0.0100734
$FT\_EFF\_Eigen\_Light\_2\_\_1down$	-0.0118959
$FT\_EFF\_Eigen\_Light\_2\_\_1up$	0.0118966
$FT\_EFF\_Eigen\_Light\_3\_\_1down$	-0.0129796
$FT\_EFF\_Eigen\_Light\_3\_\_1up$	0.012981
$FT\_EFF\_Eigen\_Light\_4\_\_1down$	-0.00175263
$FT\_EFF\_Eigen\_Light\_4\_\_1up$	0.00175239
$FT\_EFF\_extrapolation\_\_1down$	1.52862
$FT\_EFF\_extrapolation\_\_1up$	-1.48859
$FT\_EFF\_extrapolation\_from\_charm\_\_1down$	0.0222475
$FT\_EFF\_extrapolation\_from\_charm\_\_1up$	-0.0222475

Table 20: Systematic uncertainties for *tth* in percent.

Uncertainty Source	Relative Variations
$EG\_RESOLUTION\_ALL\_\_1down$	1.21376
$EG\_RESOLUTION\_ALL\_\_1up$	-1.72337
$EG\_SCALE\_ALL\_\_1down$	-1.7028
$EG\_SCALE\_ALL\_\_1up$	-0.730029
$EL\_EFF\_ID\_TOTAL\_1NPCOR\_PLUS\_UNCOR\_\_1down$	-0.610964
$EL\_EFF\_ID\_TOTAL\_1NPCOR\_PLUS\_UNCOR\_\_1up$	0.610964
$EL\_EFF\_Iso\_TOTAL\_1NPCOR\_PLUS\_UNCOR\_\_1down$	-0.163813
$EL\_EFF\_Iso\_TOTAL\_1NPCOR\_PLUS\_UNCOR\_\_1up$	0.163813
$EL\_EFF\_Reco\_TOTAL\_1NPCOR\_PLUS\_UNCOR\_\_1down$	-0.224757
$EL\_EFF\_Reco\_TOTAL\_1NPCOR\_PLUS\_UNCOR\_\_1up$	0.224756
$MUONS\_ID\_\_1down$	0.0647234
$MUONS\_ID\_\_1up$	0.195078
$MUONS\_MS\_\_1down$	0.13214
$MUONS\_MS\_\_1up$	-0.0266703
$MUONS\_SCALE\_\_1down$	0.0646208
$MUONS\_SCALE\_\_1up$	-0.00225471
$MUON\_EFF\_STAT\_LOWPT\_\_1down$	-0.028785
$MUON\_EFF\_STAT\_LOWPT\_\_1up$	0.0287851
$MUON\_EFF\_STAT\_\_1down$	-0.112113
$MUON\_EFF\_STAT\_\_1up$	0.112113
$MUON\_EFF\_SYS\_LOWPT\_\_1down$	-0.0262831
$MUON\_EFF\_SYS\_LOWPT\_\_1up$	0.0262832
$MUON\_EFF\_SYS\_\_1down$	-0.206836
$MUON\_EFF\_SYS\_\_1up$	0.207057
$MUON\_ISO\_STAT\_\_1down$	-0.0193073
$MUON\_ISO\_STAT\_\_1up$	0.0193074
$MUON\_ISO\_SYS\_\_1down$	-0.112182
$MUON\_ISO\_SYS\_\_1up$	0.112182
$MUON\_TTVA\_STAT\_\_1down$	-0.0775207
$MUON\_TTVA\_STAT\_\_1up$	0.0775208
$MUON\_TTVA\_SYS\_\_1down$	-0.155127
$MUON\_TTVA\_SYS\_\_1up$	0.155127
$PH\_EFF\_ID\_Uncertainty\_\_1down$	-4.26645
$PH\_EFF\_ID\_Uncertainty\_\_1up$	4.35919
$PH\_EFF\_TRKISO\_Uncertainty\_\_1down$	-1.17229
$PH\_EFF\_TRKISO\_Uncertainty\_\_1up$	1.17954
$PH\_Iso\_DDonoff$	0.0381094
$PRW\_DATASF\_\_1down$	0.836758
$PRW\_DATASF\_\_1up$	-0.974677

Table 21: Systematic uncertainties for *wh* in percent.

Uncertainty Source	Relative Variations
$JET\_BJES\_Response\_\_1up$	-0.00115719
$JET\_BJES\_Response\_\_1down$	0.0656272
$JET\_EffectiveNP\_1\_\_1up$	7.66735
$JET\_EffectiveNP\_1\_\_1down$	-6.55696
$JET\_EffectiveNP\_2\_\_1up$	-0.94654
$JET\_EffectiveNP\_2\_\_1down$	1.29033
$JET\_EffectiveNP\_3\_\_1up$	0.119814
$JET\_EffectiveNP\_3\_\_1down$	-0.509574
$JET\_EffectiveNP\_4\_\_1up$	-0.391922
$JET\_EffectiveNP\_4\_\_1down$	0.146153
$JET\_EffectiveNP\_5\_\_1up$	-0.00234222
$JET\_EffectiveNP\_5\_\_1down$	0.00374885
$JET\_EffectiveNP\_6restTerm\_\_1up$	0.002143
$JET\_EffectiveNP\_6restTerm\_\_1down$	-0.304331
$JET\_EtaIntercalibration\_Modelling\_\_1up$	1.92833
$JET\_EtaIntercalibration\_Modelling\_\_1down$	-2.6824
$JET\_EtaIntercalibration\_NonClosure\_\_1up$	0.0743784
$JET\_EtaIntercalibration\_NonClosure\_\_1down$	-0.000127677
$JET\_EtaIntercalibration\_TotalStat\_\_1up$	1.26364
$JET\_EtaIntercalibration\_TotalStat\_\_1down$	-0.982873
$JET\_Flavor\_Composition\_\_1up$	8.31149
$JET\_Flavor\_Composition\_\_1down$	-6.87355
$JET\_Flavor\_Response\_\_1up$	-2.10876
$JET\_Flavor\_Response\_\_1down$	1.82069
$JET\_JER\_SINGLE\_NP\_\_1up$	5.51179
$JET\_Pileup\_OffsetMu\_\_1up$	1.19827
$JET\_Pileup\_OffsetMu\_\_1down$	-0.899808
$JET\_Pileup\_OffsetNPV\_\_1up$	1.20396
$JET\_Pileup\_OffsetNPV\_\_1down$	-1.22362
$JET\_Pileup\_PtTerm\_\_1up$	0.00491128
$JET\_Pileup\_PtTerm\_\_1down$	-0.00295458
$JET\_Pileup\_RhoTopology\_\_1up$	2.09596
$JET\_Pileup\_RhoTopology\_\_1down$	-2.2774
$JET\_PunchThrough\_MC15\_\_1up$	5.24735e-06
$JET\_PunchThrough\_MC15\_\_1down$	8.63089e-07
$JET\_SingleParticle\_HighPt\_\_1up$	0
$JET\_SingleParticle\_HighPt\_\_1down$	0
$JvtEfficiencyDown$	-3.06354
$JvtEfficiencyUp$	3.12314

Table 22: Systematic uncertainties for *wh* in percent.

Uncertainty Source	Relative Variations
$FT\_EFF\_Eigen\_B\_0\_\_1down$	-0.0825357
$FT\_EFF\_Eigen\_B\_0\_\_1up$	0.0825356
$FT\_EFF\_Eigen\_B\_1\_\_1down$	-0.0148612
$FT\_EFF\_Eigen\_B\_1\_\_1up$	0.0148612
$FT\_EFF\_Eigen\_B\_2\_\_1down$	-0.000575812
$FT\_EFF\_Eigen\_B\_2\_\_1up$	0.000575795
$FT\_EFF\_Eigen\_C\_0\_\_1down$	-0.177569
$FT\_EFF\_Eigen\_C\_0\_\_1up$	0.177925
$FT\_EFF\_Eigen\_C\_1\_\_1down$	0.0559542
$FT\_EFF\_Eigen\_C\_1\_\_1up$	-0.0558976
$FT\_EFF\_Eigen\_C\_2\_\_1down$	0.00697363
$FT\_EFF\_Eigen\_C\_2\_\_1up$	-0.00697883
$FT\_EFF\_Eigen\_C\_3\_\_1down$	0.0107446
$FT\_EFF\_Eigen\_C\_3\_\_1up$	-0.0107403
$FT\_EFF\_Eigen\_Light\_0\_\_1down$	-0.388024
$FT\_EFF\_Eigen\_Light\_0\_\_1up$	0.38899
$FT\_EFF\_Eigen\_Light\_1\_\_1down$	-0.002429
$FT\_EFF\_Eigen\_Light\_1\_\_1up$	0.00242845
$FT\_EFF\_Eigen\_Light\_2\_\_1down$	-0.0313901
$FT\_EFF\_Eigen\_Light\_2\_\_1up$	0.0313965
$FT\_EFF\_Eigen\_Light\_3\_\_1down$	-0.0156775
$FT\_EFF\_Eigen\_Light\_3\_\_1up$	0.0156786
$FT\_EFF\_Eigen\_Light\_4\_\_1down$	-0.00118379
$FT\_EFF\_Eigen\_Light\_4\_\_1up$	0.00118366
$FT\_EFF\_extrapolation\_\_1down$	0.0400921
$FT\_EFF\_extrapolation\_\_1up$	-0.0402298
$FT\_EFF\_extrapolation\_from\_charm\_\_1down$	0
$FT\_EFF\_extrapolation\_from\_charm\_\_1up$	0

Table 23: Systematic uncertainties for *wh* in percent.

Uncertainty Source	Relative Variations
$EG\_RESOLUTION\_ALL\_\_1down$	1.9386
$EG\_RESOLUTION\_ALL\_\_1up$	-2.07198
$EG\_SCALE\_ALL\_\_1down$	-2.64052
$EG\_SCALE\_ALL\_\_1up$	-1.77126
$EL\_EFF\_ID\_TOTAL\_1NPCOR\_PLUS\_UNCOR\_\_1down$	-0.601386
$EL\_EFF\_ID\_TOTAL\_1NPCOR\_PLUS\_UNCOR\_\_1up$	0.601386
$EL\_EFF\_Iso\_TOTAL\_1NPCOR\_PLUS\_UNCOR\_\_1down$	-0.156837
$EL\_EFF\_Iso\_TOTAL\_1NPCOR\_PLUS\_UNCOR\_\_1up$	0.156837
$EL\_EFF\_Reco\_TOTAL\_1NPCOR\_PLUS\_UNCOR\_\_1down$	-0.242733
$EL\_EFF\_Reco\_TOTAL\_1NPCOR\_PLUS\_UNCOR\_\_1up$	0.242733
$MUONS\_ID\_\_1down$	-4.27935e-05
$MUONS\_ID\_\_1up$	0.000758504
$MUONS\_MS\_\_1down$	0.0900961
$MUONS\_MS\_\_1up$	5.2808e-05
$MUONS\_SCALE\_\_1down$	1.78936e-05
$MUONS\_SCALE\_\_1up$	2.69368e-05
$MUON\_EFF\_STAT\_LOWPT\_\_1down$	-0.0421647
$MUON\_EFF\_STAT\_LOWPT\_\_1up$	0.0421647
$MUON\_EFF\_STAT\_\_1down$	-0.119478
$MUON\_EFF\_STAT\_\_1up$	0.119478
$MUON\_EFF\_SYS\_LOWPT\_\_1down$	-0.0325375
$MUON\_EFF\_SYS\_LOWPT\_\_1up$	0.0325375
$MUON\_EFF\_SYS\_\_1down$	-0.226253
$MUON\_EFF\_SYS\_\_1up$	0.226489
$MUON\_ISO\_STAT\_\_1down$	-0.0210473
$MUON\_ISO\_STAT\_\_1up$	0.0210474
$MUON\_ISO\_SYS\_\_1down$	-0.120378
$MUON\_ISO\_SYS\_\_1up$	0.120378
$MUON\_TTVA\_STAT\_\_1down$	-0.0849405
$MUON\_TTVA\_STAT\_\_1up$	0.0849405
$MUON\_TTVA\_SYS\_\_1down$	-0.226047
$MUON\_TTVA\_SYS\_\_1up$	0.226047
$PH\_EFF\_ID\_Uncertainty\_\_1down$	-4.18193
$PH\_EFF\_ID\_Uncertainty\_\_1up$	4.27131
$PH\_EFF\_TRKISO\_Uncertainty\_\_1down$	-1.18033
$PH\_EFF\_TRKISO\_Uncertainty\_\_1up$	1.18799
$PH\_Iso\_DDonoff$	0
$PRW\_DATASF\_\_1down$	-0.525316
$PRW\_DATASF\_\_1up$	1.57804

Table 24: Systematic uncertainties for *zh* in percent.

Uncertainty Source	Relative Variations
$JET\_BJES\_Response\_\_1up$	0.00150674
$JET\_BJES\_Response\_\_1down$	0.123321
$JET\_EffectiveNP\_1\_\_1up$	7.04752
$JET\_EffectiveNP\_1\_\_1down$	-4.48328
$JET\_EffectiveNP\_2\_\_1up$	-0.0838889
$JET\_EffectiveNP\_2\_\_1down$	0.281898
$JET\_EffectiveNP\_3\_\_1up$	0.0140527
$JET\_EffectiveNP\_3\_\_1down$	0.115404
$JET\_EffectiveNP\_4\_\_1up$	0.213843
$JET\_EffectiveNP\_4\_\_1down$	0.0234062
$JET\_EffectiveNP\_5\_\_1up$	0.135638
$JET\_EffectiveNP\_5\_\_1down$	0.204549
$JET\_EffectiveNP\_6restTerm\_\_1up$	0.2221
$JET\_EffectiveNP\_6restTerm\_\_1down$	0.0969101
$JET\_EtaIntercalibration\_Modelling\_\_1up$	2.43627
$JET\_EtaIntercalibration\_Modelling\_\_1down$	-1.41586
$JET\_EtaIntercalibration\_NonClosure\_\_1up$	-0.00118227
$JET\_EtaIntercalibration\_NonClosure\_\_1down$	0.142621
$JET\_EtaIntercalibration\_TotalStat\_\_1up$	0.410464
$JET\_EtaIntercalibration\_TotalStat\_\_1down$	-0.304751
$JET\_Flavor\_Composition\_\_1up$	8.08862
$JET\_Flavor\_Composition\_\_1down$	-5.4182
$JET\_Flavor\_Response\_\_1up$	-1.1575
$JET\_Flavor\_Response\_\_1down$	1.25189
$JET\_JER\_SINGLE\_NP\_\_1up$	3.22629
$JET\_Pileup\_OffsetMu\_\_1up$	0.712334
$JET\_Pileup\_OffsetMu\_\_1down$	-0.566704
$JET\_Pileup\_OffsetNPV\_\_1up$	1.32666
$JET\_Pileup\_OffsetNPV\_\_1down$	-0.968783
$JET\_Pileup\_PtTerm\_\_1up$	0.183124
$JET\_Pileup\_PtTerm\_\_1down$	0.0963329
$JET\_Pileup\_RhoTopology\_\_1up$	1.62673
$JET\_Pileup\_RhoTopology\_\_1down$	-1.21029
$JET\_PunchThrough\_MC15\_\_1up$	-1.07583e-07
$JET\_PunchThrough\_MC15\_\_1down$	4.79312e-08
$JET\_SingleParticle\_HighPt\_\_1up$	0
$JET\_SingleParticle\_HighPt\_\_1down$	0
$JvtEfficiencyDown$	-2.7055
$JvtEfficiencyUp$	2.75324

Table 25: Systematic uncertainties for *zh* in percent.

Uncertainty Source	Relative Variations
$FT\_EFF\_Eigen\_B\_0\_\_1down$	-0.451588
$FT\_EFF\_Eigen\_B\_0\_\_1up$	0.453261
$FT\_EFF\_Eigen\_B\_1\_\_1down$	-0.0765213
$FT\_EFF\_Eigen\_B\_1\_\_1up$	0.0764674
$FT\_EFF\_Eigen\_B\_2\_\_1down$	0.0914844
$FT\_EFF\_Eigen\_B\_2\_\_1up$	-0.0915032
$FT\_EFF\_Eigen\_C\_0\_\_1down$	-0.246179
$FT\_EFF\_Eigen\_C\_0\_\_1up$	0.24691
$FT\_EFF\_Eigen\_C\_1\_\_1down$	0.0710084
$FT\_EFF\_Eigen\_C\_1\_\_1up$	-0.0709322
$FT\_EFF\_Eigen\_C\_2\_\_1down$	0.012023
$FT\_EFF\_Eigen\_C\_2\_\_1up$	-0.0120083
$FT\_EFF\_Eigen\_C\_3\_\_1down$	0.0135073
$FT\_EFF\_Eigen\_C\_3\_\_1up$	-0.0135049
$FT\_EFF\_Eigen\_Light\_0\_\_1down$	-0.359154
$FT\_EFF\_Eigen\_Light\_0\_\_1up$	0.359993
$FT\_EFF\_Eigen\_Light\_1\_\_1down$	-0.0103481
$FT\_EFF\_Eigen\_Light\_1\_\_1up$	0.010348
$FT\_EFF\_Eigen\_Light\_2\_\_1down$	-0.0265961
$FT\_EFF\_Eigen\_Light\_2\_\_1up$	0.0266006
$FT\_EFF\_Eigen\_Light\_3\_\_1down$	-0.0181142
$FT\_EFF\_Eigen\_Light\_3\_\_1up$	0.0181157
$FT\_EFF\_Eigen\_Light\_4\_\_1down$	-0.00171785
$FT\_EFF\_Eigen\_Light\_4\_\_1up$	0.00171786
$FT\_EFF\_extrapolation\_\_1down$	0.00507104
$FT\_EFF\_extrapolation\_\_1up$	-0.00507104
$FT\_EFF\_extrapolation\_from\_charm\_\_1down$	0.0879849
$FT\_EFF\_extrapolation\_from\_charm\_\_1up$	-0.087965

Table 26: Systematic uncertainties for *zh* in percent.

Uncertainty Source	Relative Variations
$EG\_RESOLUTION\_ALL\_\_1down$	2.6637
$EG\_RESOLUTION\_ALL\_\_1up$	0.00164145
$EG\_SCALE\_ALL\_\_1down$	-1.16102
$EG\_SCALE\_ALL\_\_1up$	-2.06907
$EL\_EFF\_ID\_TOTAL\_1NPCOR\_PLUS\_UNCOR\_\_1down$	-0.563929
$EL\_EFF\_ID\_TOTAL\_1NPCOR\_PLUS\_UNCOR\_\_1up$	0.563929
$EL\_EFF\_Iso\_TOTAL\_1NPCOR\_PLUS\_UNCOR\_\_1down$	-0.0434629
$EL\_EFF\_Iso\_TOTAL\_1NPCOR\_PLUS\_UNCOR\_\_1up$	0.0434627
$EL\_EFF\_Reco\_TOTAL\_1NPCOR\_PLUS\_UNCOR\_\_1down$	-0.241032
$EL\_EFF\_Reco\_TOTAL\_1NPCOR\_PLUS\_UNCOR\_\_1up$	0.241031
$MUONS\_ID\_\_1down$	1.00447
$MUONS\_ID\_\_1up$	0
$MUONS\_MS\_\_1down$	-1.21367
$MUONS\_MS\_\_1up$	0
$MUONS\_SCALE\_\_1down$	0
$MUONS\_SCALE\_\_1up$	0
$MUON\_EFF\_STAT\_LOWPT\_\_1down$	-0.304771
$MUON\_EFF\_STAT\_LOWPT\_\_1up$	0.304771
$MUON\_EFF\_STAT\_\_1down$	-0.140135
$MUON\_EFF\_STAT\_\_1up$	0.140135
$MUON\_EFF\_SYS\_LOWPT\_\_1down$	-0.347394
$MUON\_EFF\_SYS\_LOWPT\_\_1up$	0.347394
$MUON\_EFF\_SYS\_\_1down$	-0.0906169
$MUON\_EFF\_SYS\_\_1up$	0.090617
$MUON\_ISO\_STAT\_\_1down$	-0.0144171
$MUON\_ISO\_STAT\_\_1up$	0.0144169
$MUON\_ISO\_SYS\_\_1down$	-0.149246
$MUON\_ISO\_SYS\_\_1up$	0.149243
$MUON\_TTVA\_STAT\_\_1down$	-0.113866
$MUON\_TTVA\_STAT\_\_1up$	0.113866
$MUON\_TTVA\_SYS\_\_1down$	-1.0227
$MUON\_TTVA\_SYS\_\_1up$	1.0227
$PH\_EFF\_ID\_Uncertainty\_\_1down$	-4.20193
$PH\_EFF\_ID\_Uncertainty\_\_1up$	4.29231
$PH\_EFF\_TRKISO\_Uncertainty\_\_1down$	-1.12475
$PH\_EFF\_TRKISO\_Uncertainty\_\_1up$	1.13134
$PH\_Iso\_DDonoff$	1.42252
$PRW\_DATASF\_\_1down$	-3.69482
$PRW\_DATASF\_\_1up$	4.76491

Table 27: Systematic uncertainties for VBF in percent.

Uncertainty Source	Relative Variations
$JET\_BJES\_Response\_\_1up$	-0.00662922
$JET\_BJES\_Response\_\_1down$	0.000870889
$JET\_EffectiveNP\_1\_\_1up$	2.75682
$JET\_EffectiveNP\_1\_\_1down$	-2.86996
$JET\_EffectiveNP\_2\_\_1up$	0.0892752
$JET\_EffectiveNP\_2\_\_1down$	0.010756
$JET\_EffectiveNP\_3\_\_1up$	0.000221807
$JET\_EffectiveNP\_3\_\_1down$	-0.00939269
$JET\_EffectiveNP\_4\_\_1up$	0.0299136
$JET\_EffectiveNP\_4\_\_1down$	0.000181095
$JET\_EffectiveNP\_5\_\_1up$	9.29501e-05
$JET\_EffectiveNP\_5\_\_1down$	0.0299969
$JET\_EffectiveNP\_6restTerm\_\_1up$	-0.000103931
$JET\_EffectiveNP\_6restTerm\_\_1down$	0.0301913
$JET\_EtaIntercalibration\_Modelling\_\_1up$	0.0362756
$JET\_EtaIntercalibration\_Modelling\_\_1down$	-1.95447
$JET\_EtaIntercalibration\_NonClosure\_\_1up$	-0.0401175
$JET\_EtaIntercalibration\_NonClosure\_\_1down$	4.57402e-05
$JET\_EtaIntercalibration\_TotalStat\_\_1up$	0.0231144
$JET\_EtaIntercalibration\_TotalStat\_\_1down$	0.0899624
$JET\_Flavor\_Composition\_\_1up$	3.70375
$JET\_Flavor\_Composition\_\_1down$	-6.18461
$JET\_Flavor\_Response\_\_1up$	0.076121
$JET\_Flavor\_Response\_\_1down$	0.773404
$JET\_JER\_SINGLE\_NP\_\_1up$	6.02256
$JET\_Pileup\_OffsetMu\_\_1up$	0.109994
$JET\_Pileup\_OffsetMu\_\_1down$	-0.01008
$JET\_Pileup\_OffsetNPV\_\_1up$	0.864563
$JET\_Pileup\_OffsetNPV\_\_1down$	-0.0150318
$JET\_Pileup\_PtTerm\_\_1up$	0.0136493
$JET\_Pileup\_PtTerm\_\_1down$	0.000153914
$JET\_Pileup\_RhoTopology\_\_1up$	0.731116
$JET\_Pileup\_RhoTopology\_\_1down$	-0.912974
$JET\_PunchThrough\_MC15\_\_1up$	5.15827e-06
$JET\_PunchThrough\_MC15\_\_1down$	1.35728e-06
$JET\_SingleParticle\_HighPt\_\_1up$	0
$JET\_SingleParticle\_HighPt\_\_1down$	0
$JvtEfficiencyDown$	-2.21584
$JvtEfficiencyUp$	2.25378

Table 28: Systematic uncertainties for VBF in percent.

Uncertainty Source	Relative Variations
$FT\_EFF\_Eigen\_B\_0\_\_1down$	-0.345555
$FT\_EFF\_Eigen\_B\_0\_\_1up$	0.345555
$FT\_EFF\_Eigen\_B\_1\_\_1down$	0.0137502
$FT\_EFF\_Eigen\_B\_1\_\_1up$	-0.0137503
$FT\_EFF\_Eigen\_B\_2\_\_1down$	0.054726
$FT\_EFF\_Eigen\_B\_2\_\_1up$	-0.0547261
$FT\_EFF\_Eigen\_C\_0\_\_1down$	-0.307862
$FT\_EFF\_Eigen\_C\_0\_\_1up$	0.307881
$FT\_EFF\_Eigen\_C\_1\_\_1down$	0.0557558
$FT\_EFF\_Eigen\_C\_1\_\_1up$	-0.0557518
$FT\_EFF\_Eigen\_C\_2\_\_1down$	0.0504749
$FT\_EFF\_Eigen\_C\_2\_\_1up$	-0.050471
$FT\_EFF\_Eigen\_C\_3\_\_1down$	-0.00448329
$FT\_EFF\_Eigen\_C\_3\_\_1up$	0.00448285
$FT\_EFF\_Eigen\_Light\_0\_\_1down$	-0.417865
$FT\_EFF\_Eigen\_Light\_0\_\_1up$	0.419206
$FT\_EFF\_Eigen\_Light\_1\_\_1down$	-0.0242747
$FT\_EFF\_Eigen\_Light\_1\_\_1up$	0.024288
$FT\_EFF\_Eigen\_Light\_2\_\_1down$	-0.0176219
$FT\_EFF\_Eigen\_Light\_2\_\_1up$	0.0176226
$FT\_EFF\_Eigen\_Light\_3\_\_1down$	-0.0232225
$FT\_EFF\_Eigen\_Light\_3\_\_1up$	0.0232264
$FT\_EFF\_Eigen\_Light\_4\_\_1down$	-0.00257081
$FT\_EFF\_Eigen\_Light\_4\_\_1up$	0.00257166
$FT\_EFF\_extrapolation\_\_1down$	0
$FT\_EFF\_extrapolation\_\_1up$	0
$FT\_EFF\_extrapolation\_from\_charm\_\_1down$	0
$FT\_EFF\_extrapolation\_from\_charm\_\_1up$	0

Table 29: Systematic uncertainties for VBF in percent.

Uncertainty Source	Relative Variations
$EG\_RESOLUTION\_ALL\_\_1down$	1.17047
$EG\_RESOLUTION\_ALL\_\_1up$	5.96617
$EG\_SCALE\_ALL\_\_1down$	5.81752
$EG\_SCALE\_ALL\_\_1up$	0
$EL\_EFF\_ID\_TOTAL\_1NPCOR\_PLUS\_UNCOR\_\_1down$	-0.220943
$EL\_EFF\_ID\_TOTAL\_1NPCOR\_PLUS\_UNCOR\_\_1up$	0.220943
$EL\_EFF\_Iso\_TOTAL\_1NPCOR\_PLUS\_UNCOR\_\_1down$	-0.0208027
$EL\_EFF\_Iso\_TOTAL\_1NPCOR\_PLUS\_UNCOR\_\_1up$	0.0208026
$EL\_EFF\_Reco\_TOTAL\_1NPCOR\_PLUS\_UNCOR\_\_1down$	-0.173926
$EL\_EFF\_Reco\_TOTAL\_1NPCOR\_PLUS\_UNCOR\_\_1up$	0.173926
$MUONS\_ID\_\_1down$	0
$MUONS\_ID\_\_1up$	-0.00109619
$MUONS\_MS\_\_1down$	0.00574966
$MUONS\_MS\_\_1up$	0.00218528
$MUONS\_SCALE\_\_1down$	0
$MUONS\_SCALE\_\_1up$	0
$MUON\_EFF\_STAT\_LOWPT\_\_1down$	-0.30145
$MUON\_EFF\_STAT\_LOWPT\_\_1up$	0.30145
$MUON\_EFF\_STAT\_\_1down$	-0.195803
$MUON\_EFF\_STAT\_\_1up$	0.195803
$MUON\_EFF\_SYS\_LOWPT\_\_1down$	-0.263718
$MUON\_EFF\_SYS\_LOWPT\_\_1up$	0.263717
$MUON\_EFF\_SYS\_\_1down$	-0.202774
$MUON\_EFF\_SYS\_\_1up$	0.202775
$MUON\_ISO\_STAT\_\_1down$	-0.0163906
$MUON\_ISO\_STAT\_\_1up$	0.0163913
$MUON\_ISO\_SYS\_\_1down$	-0.173216
$MUON\_ISO\_SYS\_\_1up$	0.173212
$MUON\_TTVA\_STAT\_\_1down$	-0.138066
$MUON\_TTVA\_STAT\_\_1up$	0.138064
$MUON\_TTVA\_SYS\_\_1down$	-1.16147
$MUON\_TTVA\_SYS\_\_1up$	1.16147
$PH\_EFF\_ID\_Uncertainty\_\_1down$	-4.06059
$PH\_EFF\_ID\_Uncertainty\_\_1up$	4.14473
$PH\_EFF\_TRKISO\_Uncertainty\_\_1down$	-1.18187
$PH\_EFF\_TRKISO\_Uncertainty\_\_1up$	1.18996
$PH\_Iso\_DDonoff$	0
$PRW\_DATASF\_\_1down$	-9.74485
$PRW\_DATASF\_\_1up$	13.8733

Table 30: Systematic uncertainties for *ggh* in percent.

Uncertainty Source	Relative Variations
$JET\_BJES\_Response\_\_1up$	-0.0126832
$JET\_BJES\_Response\_\_1down$	0.00302192
$JET\_EffectiveNP\_1\_\_1up$	2.70315
$JET\_EffectiveNP\_1\_\_1down$	-2.85184
$JET\_EffectiveNP\_2\_\_1up$	0.00486663
$JET\_EffectiveNP\_2\_\_1down$	0.00253794
$JET\_EffectiveNP\_3\_\_1up$	0.0106255
$JET\_EffectiveNP\_3\_\_1down$	0.00448421
$JET\_EffectiveNP\_4\_\_1up$	-0.0005469
$JET\_EffectiveNP\_4\_\_1down$	0.00035593
$JET\_EffectiveNP\_5\_\_1up$	0.00025637
$JET\_EffectiveNP\_5\_\_1down$	0.0102421
$JET\_EffectiveNP\_6restTerm\_\_1up$	0.010319
$JET\_EffectiveNP\_6restTerm\_\_1down$	0.000207613
$JET\_EtaIntercalibration\_Modelling\_\_1up$	2.78956
$JET\_EtaIntercalibration\_Modelling\_\_1down$	0.0554407
$JET\_EtaIntercalibration\_NonClosure\_\_1up$	6.38938e-05
$JET\_EtaIntercalibration\_NonClosure\_\_1down$	-0.00028761
$JET\_EtaIntercalibration\_TotalStat\_\_1up$	0.0161144
$JET\_EtaIntercalibration\_TotalStat\_\_1down$	-0.00865801
$JET\_Flavor\_Composition\_\_1up$	2.77447
$JET\_Flavor\_Composition\_\_1down$	-2.87123
$JET\_Flavor\_Response\_\_1up$	-0.00982476
$JET\_Flavor\_Response\_\_1down$	0.611316
$JET\_JER\_SINGLE\_NP\_\_1up$	-0.917808
$JET\_Pileup\_OffsetMu\_\_1up$	0.00640314
$JET\_Pileup\_OffsetMu\_\_1down$	0.00105705
$JET\_Pileup\_OffsetNPV\_\_1up$	0.592709
$JET\_Pileup\_OffsetNPV\_\_1down$	0.00139711
$JET\_Pileup\_PtTerm\_\_1up$	0.00476628
$JET\_Pileup\_PtTerm\_\_1down$	0.0109456
$JET\_Pileup\_RhoTopology\_\_1up$	2.75077
$JET\_Pileup\_RhoTopology\_\_1down$	-2.90937
$JET\_PunchThrough\_MC15\_\_1up$	0
$JET\_PunchThrough\_MC15\_\_1down$	4.11851e-07
$JET\_SingleParticle\_HighPt\_\_1up$	0
$JET\_SingleParticle\_HighPt\_\_1down$	0
$JvtEfficiencyDown$	-3.53627
$JvtEfficiencyUp$	3.62881

Table 31: Systematic uncertainties for *ggh* in percent.

Uncertainty Source	Relative Variations
$FT\_EFF\_Eigen\_B\_0\_\_1down$	-1.03221
$FT\_EFF\_Eigen\_B\_0\_\_1up$	1.03221
$FT\_EFF\_Eigen\_B\_1\_\_1down$	-0.0747759
$FT\_EFF\_Eigen\_B\_1\_\_1up$	0.0747758
$FT\_EFF\_Eigen\_B\_2\_\_1down$	0.265232
$FT\_EFF\_Eigen\_B\_2\_\_1up$	-0.265232
$FT\_EFF\_Eigen\_C\_0\_\_1down$	-0.109277
$FT\_EFF\_Eigen\_C\_0\_\_1up$	0.109277
$FT\_EFF\_Eigen\_C\_1\_\_1down$	0.0517932
$FT\_EFF\_Eigen\_C\_1\_\_1up$	-0.0517932
$FT\_EFF\_Eigen\_C\_2\_\_1down$	0.00174222
$FT\_EFF\_Eigen\_C\_2\_\_1up$	-0.00174198
$FT\_EFF\_Eigen\_C\_3\_\_1down$	0.0171775
$FT\_EFF\_Eigen\_C\_3\_\_1up$	-0.0171775
$FT\_EFF\_Eigen\_Light\_0\_\_1down$	-0.392775
$FT\_EFF\_Eigen\_Light\_0\_\_1up$	0.393794
$FT\_EFF\_Eigen\_Light\_1\_\_1down$	0.0109541
$FT\_EFF\_Eigen\_Light\_1\_\_1up$	-0.010951
$FT\_EFF\_Eigen\_Light\_2\_\_1down$	-0.0370579
$FT\_EFF\_Eigen\_Light\_2\_\_1up$	0.0370669
$FT\_EFF\_Eigen\_Light\_3\_\_1down$	-0.0123862
$FT\_EFF\_Eigen\_Light\_3\_\_1up$	0.0123879
$FT\_EFF\_Eigen\_Light\_4\_\_1down$	-0.00234555
$FT\_EFF\_Eigen\_Light\_4\_\_1up$	0.00234824
$FT\_EFF\_extrapolation\_\_1down$	0
$FT\_EFF\_extrapolation\_\_1up$	0
$FT\_EFF\_extrapolation\_from\_charm\_\_1down$	0
$FT\_EFF\_extrapolation\_from\_charm\_\_1up$	0

Table 32: Systematic uncertainties for *ggh* in percent.

Uncertainty Source	Relative Variations
$EG\_RESOLUTION\_ALL\_\_1down$	1.71139
$EG\_RESOLUTION\_ALL\_\_1up$	-1.95952
$EG\_SCALE\_ALL\_\_1down$	-6.69717
$EG\_SCALE\_ALL\_\_1up$	2.02703
$EL\_EFF\_ID\_TOTAL\_1NPCOR\_PLUS\_UNCOR\_\_1down$	-0.685876
$EL\_EFF\_ID\_TOTAL\_1NPCOR\_PLUS\_UNCOR\_\_1up$	0.685877
$EL\_EFF\_Iso\_TOTAL\_1NPCOR\_PLUS\_UNCOR\_\_1down$	-0.10985
$EL\_EFF\_Iso\_TOTAL\_1NPCOR\_PLUS\_UNCOR\_\_1up$	0.10985
$EL\_EFF\_Reco\_TOTAL\_1NPCOR\_PLUS\_UNCOR\_\_1down$	-0.2679
$EL\_EFF\_Reco\_TOTAL\_1NPCOR\_PLUS\_UNCOR\_\_1up$	0.2679
$MUONS\_ID\_\_1down$	-0.0461005
$MUONS\_ID\_\_1up$	0.000261598
$MUONS\_MS\_\_1down$	0.0227497
$MUONS\_MS\_\_1up$	0.0124257
$MUONS\_SCALE\_\_1down$	0.0228554
$MUONS\_SCALE\_\_1up$	-0.010915
$MUON\_EFF\_STAT\_LOWPT\_\_1down$	-0.0380427
$MUON\_EFF\_STAT\_LOWPT\_\_1up$	0.0380428
$MUON\_EFF\_STAT\_\_1down$	-0.0992024
$MUON\_EFF\_STAT\_\_1up$	0.0992026
$MUON\_EFF\_SYS\_LOWPT\_\_1down$	-0.0378615
$MUON\_EFF\_SYS\_LOWPT\_\_1up$	0.0378615
$MUON\_EFF\_SYS\_\_1down$	-0.155326
$MUON\_EFF\_SYS\_\_1up$	0.155347
$MUON\_ISO\_STAT\_\_1down$	-0.0121117
$MUON\_ISO\_STAT\_\_1up$	0.0121117
$MUON\_ISO\_SYS\_\_1down$	-0.104744
$MUON\_ISO\_SYS\_\_1up$	0.104744
$MUON\_TTVA\_STAT\_\_1down$	-0.0675451
$MUON\_TTVA\_STAT\_\_1up$	0.0675452
$MUON\_TTVA\_SYS\_\_1down$	-0.250759
$MUON\_TTVA\_SYS\_\_1up$	0.250759
$PH\_EFF\_ID\_Uncertainty\_\_1down$	-4.12842
$PH\_EFF\_ID\_Uncertainty\_\_1up$	4.21551
$PH\_EFF\_TRKISO\_Uncertainty\_\_1down$	-1.10311
$PH\_EFF\_TRKISO\_Uncertainty\_\_1up$	1.10951
$PH\_Iso\_DDonoff$	-0.000997416
$PRW\_DATASF\_\_1down$	0.428639
$PRW\_DATASF\_\_1up$	0.158779

Table 33: Systematic uncertainties for non-resonance in percent.

Uncertainty Source	Relative Variations
$JET\_BJES\_Response\_\_1up$	-0.00684266
$JET\_BJES\_Response\_\_1down$	0.0083952
$JET\_EffectiveNP\_1\_\_1up$	2.83622
$JET\_EffectiveNP\_1\_\_1down$	-3.11529
$JET\_EffectiveNP\_2\_\_1up$	-0.542736
$JET\_EffectiveNP\_2\_\_1down$	0.412979
$JET\_EffectiveNP\_3\_\_1up$	0.219524
$JET\_EffectiveNP\_3\_\_1down$	-0.16048
$JET\_EffectiveNP\_4\_\_1up$	-0.0897192
$JET\_EffectiveNP\_4\_\_1down$	0.139604
$JET\_EffectiveNP\_5\_\_1up$	0.0366352
$JET\_EffectiveNP\_5\_\_1down$	-0.0301525
$JET\_EffectiveNP\_6restTerm\_\_1up$	0.0465731
$JET\_EffectiveNP\_6restTerm\_\_1down$	-0.0413724
$JET\_EtaIntercalibration\_Modelling\_\_1up$	1.20163
$JET\_EtaIntercalibration\_Modelling\_\_1down$	-0.868363
$JET\_EtaIntercalibration\_NonClosure\_\_1up$	-0.0235237
$JET\_EtaIntercalibration\_NonClosure\_\_1down$	0.0825272
$JET\_EtaIntercalibration\_TotalStat\_\_1up$	0.395489
$JET\_EtaIntercalibration\_TotalStat\_\_1down$	-0.529012
$JET\_Flavor\_Composition\_\_1up$	3.00821
$JET\_Flavor\_Composition\_\_1down$	-3.32219
$JET\_Flavor\_Response\_\_1up$	-1.03319
$JET\_Flavor\_Response\_\_1down$	0.893771
$JET\_JER\_SINGLE\_NP\_\_1up$	-0.342969
$JET\_Pileup\_OffsetMu\_\_1up$	0.484703
$JET\_Pileup\_OffsetMu\_\_1down$	-0.548056
$JET\_Pileup\_OffsetNPV\_\_1up$	0.558076
$JET\_Pileup\_OffsetNPV\_\_1down$	-0.68526
$JET\_Pileup\_PtTerm\_\_1up$	0.00627371
$JET\_Pileup\_PtTerm\_\_1down$	0.0209788
$JET\_Pileup\_RhoTopology\_\_1up$	1.00122
$JET\_Pileup\_RhoTopology\_\_1down$	-0.986053
$JET\_PunchThrough\_MC15\_\_1up$	-1.05428e-07
$JET\_PunchThrough\_MC15\_\_1down$	-5.03372e-06
$JET\_SingleParticle\_HighPt\_\_1up$	0
$JET\_SingleParticle\_HighPt\_\_1down$	0
$JvtEfficiencyDown$	-3.57837
$JvtEfficiencyUp$	3.6808

Table 34: Systematic uncertainties for non-resonance in percent.

Uncertainty Source	Relative Variations
$FT\_EFF\_Eigen\_B\_0\_\_1down$	-0.0625957
$FT\_EFF\_Eigen\_B\_0\_\_1up$	0.0630371
$FT\_EFF\_Eigen\_B\_1\_\_1down$	-0.0137836
$FT\_EFF\_Eigen\_B\_1\_\_1up$	0.013793
$FT\_EFF\_Eigen\_B\_2\_\_1down$	0.00844968
$FT\_EFF\_Eigen\_B\_2\_\_1up$	-0.00850135
$FT\_EFF\_Eigen\_C\_0\_\_1down$	-0.431805
$FT\_EFF\_Eigen\_C\_0\_\_1up$	0.43235
$FT\_EFF\_Eigen\_C\_1\_\_1down$	0.182762
$FT\_EFF\_Eigen\_C\_1\_\_1up$	-0.182691
$FT\_EFF\_Eigen\_C\_2\_\_1down$	0.0525164
$FT\_EFF\_Eigen\_C\_2\_\_1up$	-0.0525013
$FT\_EFF\_Eigen\_C\_3\_\_1down$	0.0210961
$FT\_EFF\_Eigen\_C\_3\_\_1up$	-0.0210958
$FT\_EFF\_Eigen\_Light\_0\_\_1down$	-0.421214
$FT\_EFF\_Eigen\_Light\_0\_\_1up$	0.422556
$FT\_EFF\_Eigen\_Light\_1\_\_1down$	0.00579617
$FT\_EFF\_Eigen\_Light\_1\_\_1up$	-0.00579513
$FT\_EFF\_Eigen\_Light\_2\_\_1down$	-0.0272437
$FT\_EFF\_Eigen\_Light\_2\_\_1up$	0.0272498
$FT\_EFF\_Eigen\_Light\_3\_\_1down$	-0.0164459
$FT\_EFF\_Eigen\_Light\_3\_\_1up$	0.016448
$FT\_EFF\_Eigen\_Light\_4\_\_1down$	-0.00295308
$FT\_EFF\_Eigen\_Light\_4\_\_1up$	0.00295309
$FT\_EFF\_extrapolation\_\_1down$	0.00797831
$FT\_EFF\_extrapolation\_\_1up$	-0.00802381
$FT\_EFF\_extrapolation\_from\_charm\_\_1down$	0.000327955
$FT\_EFF\_extrapolation\_from\_charm\_\_1up$	-0.000327956

Table 35: Systematic uncertainties for non-resonance in percent.

Uncertainty Source	Relative Variations
$EG\_RESOLUTION\_ALL\_\_1down$	2.23119
$EG\_RESOLUTION\_ALL\_\_1up$	-2.16502
$EG\_SCALE\_ALL\_\_1down$	-5.53725
$EG\_SCALE\_ALL\_\_1up$	1.43785
$EL\_EFF\_ID\_TOTAL\_1NPCOR\_PLUS\_UNCOR\_\_1down$	-0.839205
$EL\_EFF\_ID\_TOTAL\_1NPCOR\_PLUS\_UNCOR\_\_1up$	0.839205
$EL\_EFF\_Iso\_TOTAL\_1NPCOR\_PLUS\_UNCOR\_\_1down$	-0.0687735
$EL\_EFF\_Iso\_TOTAL\_1NPCOR\_PLUS\_UNCOR\_\_1up$	0.0687736
$EL\_EFF\_Reco\_TOTAL\_1NPCOR\_PLUS\_UNCOR\_\_1down$	-0.364631
$EL\_EFF\_Reco\_TOTAL\_1NPCOR\_PLUS\_UNCOR\_\_1up$	0.36463
$MUONS\_ID\_\_1down$	0.0208774
$MUONS\_ID\_\_1up$	-0.00572065
$MUONS\_MS\_\_1down$	-0.00454632
$MUONS\_MS\_\_1up$	-0.000461713
$MUONS\_SCALE\_\_1down$	0.0390073
$MUONS\_SCALE\_\_1up$	-0.0172664
$MUON\_EFF\_STAT\_LOWPT\_\_1down$	-0.070324
$MUON\_EFF\_STAT\_LOWPT\_\_1up$	0.0703241
$MUON\_EFF\_STAT\_\_1down$	-0.0837466
$MUON\_EFF\_STAT\_\_1up$	0.0837466
$MUON\_EFF\_SYS\_LOWPT\_\_1down$	-0.0723673
$MUON\_EFF\_SYS\_LOWPT\_\_1up$	0.0723674
$MUON\_EFF\_SYS\_\_1down$	-0.126044
$MUON\_EFF\_SYS\_\_1up$	0.126044
$MUON\_ISO\_STAT\_\_1down$	-0.00912301
$MUON\_ISO\_STAT\_\_1up$	0.00912293
$MUON\_ISO\_SYS\_\_1down$	-0.111086
$MUON\_ISO\_SYS\_\_1up$	0.111085
$MUON\_TTVA\_STAT\_\_1down$	-0.0687485
$MUON\_TTVA\_STAT\_\_1up$	0.0687485
$MUON\_TTVA\_SYS\_\_1down$	-0.437944
$MUON\_TTVA\_SYS\_\_1up$	0.437944
$PH\_EFF\_ID\_Uncertainty\_\_1down$	-4.12674
$PH\_EFF\_ID\_Uncertainty\_\_1up$	4.2136
$PH\_EFF\_TRKISO\_Uncertainty\_\_1down$	-1.16065
$PH\_EFF\_TRKISO\_Uncertainty\_\_1up$	1.16767
$PH\_Iso\_DDonoff$	0.0647221
$PRW\_DATASF\_\_1down$	0.673702
$PRW\_DATASF\_\_1up$	-0.877376

Table 36: Systematic uncertainties for resonance m_H=260 GeV in percent.

Uncertainty Source	Relative Variations
$JET\_BJES\_Response\_\_1up$	0.0575611
$JET\_BJES\_Response\_\_1down$	0.0347171
$JET\_EffectiveNP\_1\_\_1up$	6.36006
$JET\_EffectiveNP\_1\_\_1down$	-5.60478
$JET\_EffectiveNP\_2\_\_1up$	-1.20666
$JET\_EffectiveNP\_2\_\_1down$	1.2558
$JET\_EffectiveNP\_3\_\_1up$	0.334804
$JET\_EffectiveNP\_3\_\_1down$	-0.433423
$JET\_EffectiveNP\_4\_\_1up$	-0.196006
$JET\_EffectiveNP\_4\_\_1down$	0.135669
$JET\_EffectiveNP\_5\_\_1up$	0.103835
$JET\_EffectiveNP\_5\_\_1down$	-0.0455967
$JET\_EffectiveNP\_6restTerm\_\_1up$	0.0761899
$JET\_EffectiveNP\_6restTerm\_\_1down$	-0.0159399
$JET\_EtaIntercalibration\_Modelling\_\_1up$	2.00245
$JET\_EtaIntercalibration\_Modelling\_\_1down$	-1.18177
$JET\_EtaIntercalibration\_NonClosure\_\_1up$	-0.116869
$JET\_EtaIntercalibration\_NonClosure\_\_1down$	0.0200544
$JET\_EtaIntercalibration\_TotalStat\_\_1up$	1.16849
$JET\_EtaIntercalibration\_TotalStat\_\_1down$	-1.1877
$JET\_Flavor\_Composition\_\_1up$	6.71378
$JET\_Flavor\_Composition\_\_1down$	-6.83957
$JET\_Flavor\_Response\_\_1up$	-2.19696
$JET\_Flavor\_Response\_\_1down$	2.08465
$JET\_JER\_SINGLE\_NP\_\_1up$	1.52351
$JET\_Pileup\_OffsetMu\_\_1up$	1.11692
$JET\_Pileup\_OffsetMu\_\_1down$	-0.885739
$JET\_Pileup\_OffsetNPV\_\_1up$	1.20062
$JET\_Pileup\_OffsetNPV\_\_1down$	-0.995019
$JET\_Pileup\_PtTerm\_\_1up$	0.0372175
$JET\_Pileup\_PtTerm\_\_1down$	0.0112285
$JET\_Pileup\_RhoTopology\_\_1up$	2.48104
$JET\_Pileup\_RhoTopology\_\_1down$	-2.16402
$JET\_PunchThrough\_MC15\_\_1up$	-1.80164e-08
$JET\_PunchThrough\_MC15\_\_1down$	-1.10349e-05
$JET\_SingleParticle\_HighPt\_\_1up$	0
$JET\_SingleParticle\_HighPt\_\_1down$	0
$JvtEfficiencyDown$	-4.4129
$JvtEfficiencyUp$	4.54835

Table 37: Systematic uncertainties for resonance m_H=260 GeV in percent.

Uncertainty Source	Relative Variations
$FT\_EFF\_Eigen\_B\_0\_\_1down$	-0.0904614
$FT\_EFF\_Eigen\_B\_0\_\_1up$	0.0905958
$FT\_EFF\_Eigen\_B\_1\_\_1down$	-0.000144527
$FT\_EFF\_Eigen\_B\_1\_\_1up$	0.000138814
$FT\_EFF\_Eigen\_B\_2\_\_1down$	0.0166996
$FT\_EFF\_Eigen\_B\_2\_\_1up$	-0.0166951
$FT\_EFF\_Eigen\_C\_0\_\_1down$	-0.298177
$FT\_EFF\_Eigen\_C\_0\_\_1up$	0.298447
$FT\_EFF\_Eigen\_C\_1\_\_1down$	0.197958
$FT\_EFF\_Eigen\_C\_1\_\_1up$	-0.197856
$FT\_EFF\_Eigen\_C\_2\_\_1down$	-0.0238479
$FT\_EFF\_Eigen\_C\_2\_\_1up$	0.0238457
$FT\_EFF\_Eigen\_C\_3\_\_1down$	0.0485683
$FT\_EFF\_Eigen\_C\_3\_\_1up$	-0.0485652
$FT\_EFF\_Eigen\_Light\_0\_\_1down$	-0.381249
$FT\_EFF\_Eigen\_Light\_0\_\_1up$	0.382234
$FT\_EFF\_Eigen\_Light\_1\_\_1down$	-0.00559463
$FT\_EFF\_Eigen\_Light\_1\_\_1up$	0.00559402
$FT\_EFF\_Eigen\_Light\_2\_\_1down$	-0.0496629
$FT\_EFF\_Eigen\_Light\_2\_\_1up$	0.0496788
$FT\_EFF\_Eigen\_Light\_3\_\_1down$	-0.0186918
$FT\_EFF\_Eigen\_Light\_3\_\_1up$	0.0186939
$FT\_EFF\_Eigen\_Light\_4\_\_1down$	-0.00655428
$FT\_EFF\_Eigen\_Light\_4\_\_1up$	0.0065543
$FT\_EFF\_extrapolation\_\_1down$	0
$FT\_EFF\_extrapolation\_\_1up$	0
$FT\_EFF\_extrapolation\_from\_charm\_\_1down$	0.000455188
$FT\_EFF\_extrapolation\_from\_charm\_\_1up$	-0.000455188

Table 38: Systematic uncertainties for resonance m_H=260 GeV in percent.

Uncertainty Source	Relative Variations
$EG\_RESOLUTION\_ALL\_\_1down$	1.61733
$EG\_RESOLUTION\_ALL\_\_1up$	-2.20038
$EG\_SCALE\_ALL\_\_1down$	-4.93326
$EG\_SCALE\_ALL\_\_1up$	1.23387
$EL\_EFF\_ID\_TOTAL\_1NPCOR\_PLUS\_UNCOR\_\_1down$	-0.768551
$EL\_EFF\_ID\_TOTAL\_1NPCOR\_PLUS\_UNCOR\_\_1up$	0.768551
$EL\_EFF\_Iso\_TOTAL\_1NPCOR\_PLUS\_UNCOR\_\_1down$	-0.0690452
$EL\_EFF\_Iso\_TOTAL\_1NPCOR\_PLUS\_UNCOR\_\_1up$	0.0690452
$EL\_EFF\_Reco\_TOTAL\_1NPCOR\_PLUS\_UNCOR\_\_1down$	-0.317884
$EL\_EFF\_Reco\_TOTAL\_1NPCOR\_PLUS\_UNCOR\_\_1up$	0.317883
$MUONS\_ID\_\_1down$	-0.00014874
$MUONS\_ID\_\_1up$	-0.0291081
$MUONS\_MS\_\_1down$	0.0306011
$MUONS\_MS\_\_1up$	-9.14845e-05
$MUONS\_SCALE\_\_1down$	0.000203091
$MUONS\_SCALE\_\_1up$	-0.0674328
$MUON\_EFF\_STAT\_LOWPT\_\_1down$	-0.0588329
$MUON\_EFF\_STAT\_LOWPT\_\_1up$	0.058833
$MUON\_EFF\_STAT\_\_1down$	-0.0970863
$MUON\_EFF\_STAT\_\_1up$	0.0970864
$MUON\_EFF\_SYS\_LOWPT\_\_1down$	-0.0536202
$MUON\_EFF\_SYS\_LOWPT\_\_1up$	0.0536203
$MUON\_EFF\_SYS\_\_1down$	-0.132922
$MUON\_EFF\_SYS\_\_1up$	0.132922
$MUON\_ISO\_STAT\_\_1down$	-0.00960858
$MUON\_ISO\_STAT\_\_1up$	0.00960862
$MUON\_ISO\_SYS\_\_1down$	-0.111303
$MUON\_ISO\_SYS\_\_1up$	0.111303
$MUON\_TTVA\_STAT\_\_1down$	-0.0670735
$MUON\_TTVA\_STAT\_\_1up$	0.0670736
$MUON\_TTVA\_SYS\_\_1down$	-0.366157
$MUON\_TTVA\_SYS\_\_1up$	0.366157
$PH\_EFF\_ID\_Uncertainty\_\_1down$	-4.1683
$PH\_EFF\_ID\_Uncertainty\_\_1up$	4.25692
$PH\_EFF\_TRKISO\_Uncertainty\_\_1down$	-1.15789
$PH\_EFF\_TRKISO\_Uncertainty\_\_1up$	1.16489
$PH\_Iso\_DDonoff$	0.0955585
$PRW\_DATASF\_\_1down$	0.369119
$PRW\_DATASF\_\_1up$	0.169916

Table 39: Systematic uncertainties for resonance m_H=300 GeV in percent.

Uncertainty Source	Relative Variations
$JET\_BJES\_Response\_\_1up$	0.0440813
$JET\_BJES\_Response\_\_1down$	0.000689079
$JET\_EffectiveNP\_1\_\_1up$	5.06072
$JET\_EffectiveNP\_1\_\_1down$	-4.95305
$JET\_EffectiveNP\_2\_\_1up$	-0.683635
$JET\_EffectiveNP\_2\_\_1down$	1.0067
$JET\_EffectiveNP\_3\_\_1up$	0.293234
$JET\_EffectiveNP\_3\_\_1down$	-0.146424
$JET\_EffectiveNP\_4\_\_1up$	-0.0936589
$JET\_EffectiveNP\_4\_\_1down$	0.0671801
$JET\_EffectiveNP\_5\_\_1up$	0.00793789
$JET\_EffectiveNP\_5\_\_1down$	-0.0378778
$JET\_EffectiveNP\_6restTerm\_\_1up$	-0.0127446
$JET\_EffectiveNP\_6restTerm\_\_1down$	-0.0162305
$JET\_EtaIntercalibration\_Modelling\_\_1up$	1.67384
$JET\_EtaIntercalibration\_Modelling\_\_1down$	-1.68351
$JET\_EtaIntercalibration\_NonClosure\_\_1up$	-0.0808306
$JET\_EtaIntercalibration\_NonClosure\_\_1down$	0.0231417
$JET\_EtaIntercalibration\_TotalStat\_\_1up$	1.00924
$JET\_EtaIntercalibration\_TotalStat\_\_1down$	-0.709808
$JET\_Flavor\_Composition\_\_1up$	5.23513
$JET\_Flavor\_Composition\_\_1down$	-5.64378
$JET\_Flavor\_Response\_\_1up$	-1.57255
$JET\_Flavor\_Response\_\_1down$	1.75455
$JET\_JER\_SINGLE\_NP\_\_1up$	-0.335264
$JET\_Pileup\_OffsetMu\_\_1up$	0.871142
$JET\_Pileup\_OffsetMu\_\_1down$	-0.759296
$JET\_Pileup\_OffsetNPV\_\_1up$	1.17368
$JET\_Pileup\_OffsetNPV\_\_1down$	-0.976382
$JET\_Pileup\_PtTerm\_\_1up$	0.000908042
$JET\_Pileup\_PtTerm\_\_1down$	-0.00374452
$JET\_Pileup\_RhoTopology\_\_1up$	2.0435
$JET\_Pileup\_RhoTopology\_\_1down$	-1.9631
$JET\_PunchThrough\_MC15\_\_1up$	-5.25785e-09
$JET\_PunchThrough\_MC15\_\_1down$	5.54974e-09
$JET\_SingleParticle\_HighPt\_\_1up$	0
$JET\_SingleParticle\_HighPt\_\_1down$	0
$JvtEfficiencyDown$	-4.21606
$JvtEfficiencyUp$	4.34457

Table 40: Systematic uncertainties for resonance m_H=300 GeV in percent.

Uncertainty Source	Relative Variations
$FT\_EFF\_Eigen\_B\_0\_\_1down$	-0.0720149
$FT\_EFF\_Eigen\_B\_0\_\_1up$	0.0725656
$FT\_EFF\_Eigen\_B\_1\_\_1down$	-0.00650624
$FT\_EFF\_Eigen\_B\_1\_\_1up$	0.00651125
$FT\_EFF\_Eigen\_B\_2\_\_1down$	0.0120309
$FT\_EFF\_Eigen\_B\_2\_\_1up$	-0.0120321
$FT\_EFF\_Eigen\_C\_0\_\_1down$	-0.329606
$FT\_EFF\_Eigen\_C\_0\_\_1up$	0.329978
$FT\_EFF\_Eigen\_C\_1\_\_1down$	0.206052
$FT\_EFF\_Eigen\_C\_1\_\_1up$	-0.205962
$FT\_EFF\_Eigen\_C\_2\_\_1down$	0.000289644
$FT\_EFF\_Eigen\_C\_2\_\_1up$	-0.000289022
$FT\_EFF\_Eigen\_C\_3\_\_1down$	0.0473568
$FT\_EFF\_Eigen\_C\_3\_\_1up$	-0.0473563
$FT\_EFF\_Eigen\_Light\_0\_\_1down$	-0.386019
$FT\_EFF\_Eigen\_Light\_0\_\_1up$	0.387072
$FT\_EFF\_Eigen\_Light\_1\_\_1down$	-0.000398008
$FT\_EFF\_Eigen\_Light\_1\_\_1up$	0.000398835
$FT\_EFF\_Eigen\_Light\_2\_\_1down$	-0.0431194
$FT\_EFF\_Eigen\_Light\_2\_\_1up$	0.0431329
$FT\_EFF\_Eigen\_Light\_3\_\_1down$	-0.0182926
$FT\_EFF\_Eigen\_Light\_3\_\_1up$	0.018295
$FT\_EFF\_Eigen\_Light\_4\_\_1down$	-0.00636482
$FT\_EFF\_Eigen\_Light\_4\_\_1up$	0.00636499
$FT\_EFF\_extrapolation\_\_1down$	0.00220351
$FT\_EFF\_extrapolation\_\_1up$	-0.00220351
$FT\_EFF\_extrapolation\_from\_charm\_\_1down$	0.000187416
$FT\_EFF\_extrapolation\_from\_charm\_\_1up$	-0.000187416

Table 41: Systematic uncertainties for resonance m_H=300 GeV in percent.

Uncertainty Source	Relative Variations
$EG\_RESOLUTION\_ALL\_\_1down$	2.38052
$EG\_RESOLUTION\_ALL\_\_1up$	-2.34101
$EG\_SCALE\_ALL\_\_1down$	-5.78864
$EG\_SCALE\_ALL\_\_1up$	2.88572
$EL\_EFF\_ID\_TOTAL\_1NPCOR\_PLUS\_UNCOR\_\_1down$	-0.695272
$EL\_EFF\_ID\_TOTAL\_1NPCOR\_PLUS\_UNCOR\_\_1up$	0.695272
$EL\_EFF\_Iso\_TOTAL\_1NPCOR\_PLUS\_UNCOR\_\_1down$	-0.0792117
$EL\_EFF\_Iso\_TOTAL\_1NPCOR\_PLUS\_UNCOR\_\_1up$	0.0792116
$EL\_EFF\_Reco\_TOTAL\_1NPCOR\_PLUS\_UNCOR\_\_1down$	-0.285966
$EL\_EFF\_Reco\_TOTAL\_1NPCOR\_PLUS\_UNCOR\_\_1up$	0.285966
$MUONS\_ID\_\_1down$	-6.65751e-05
$MUONS\_ID\_\_1up$	0.0124542
$MUONS\_MS\_\_1down$	0.0120978
$MUONS\_MS\_\_1up$	0.0496478
$MUONS\_SCALE\_\_1down$	0.0765172
$MUONS\_SCALE\_\_1up$	-0.0054187
$MUON\_EFF\_STAT\_LOWPT\_\_1down$	-0.0486702
$MUON\_EFF\_STAT\_LOWPT\_\_1up$	0.0486703
$MUON\_EFF\_STAT\_\_1down$	-0.100069
$MUON\_EFF\_STAT\_\_1up$	0.100069
$MUON\_EFF\_SYS\_LOWPT\_\_1down$	-0.0496635
$MUON\_EFF\_SYS\_LOWPT\_\_1up$	0.0496635
$MUON\_EFF\_SYS\_\_1down$	-0.14762
$MUON\_EFF\_SYS\_\_1up$	0.147624
$MUON\_ISO\_STAT\_\_1down$	-0.0110529
$MUON\_ISO\_STAT\_\_1up$	0.0110529
$MUON\_ISO\_SYS\_\_1down$	-0.108996
$MUON\_ISO\_SYS\_\_1up$	0.108996
$MUON\_TTVA\_STAT\_\_1down$	-0.0690108
$MUON\_TTVA\_STAT\_\_1up$	0.0690108
$MUON\_TTVA\_SYS\_\_1down$	-0.299529
$MUON\_TTVA\_SYS\_\_1up$	0.299528
$PH\_EFF\_ID\_Uncertainty\_\_1down$	-4.13366
$PH\_EFF\_ID\_Uncertainty\_\_1up$	4.22099
$PH\_EFF\_TRKISO\_Uncertainty\_\_1down$	-1.12941
$PH\_EFF\_TRKISO\_Uncertainty\_\_1up$	1.13603
$PH\_Iso\_DDonoff$	0.0419657
$PRW\_DATASF\_\_1down$	0.514904
$PRW\_DATASF\_\_1up$	-0.156771

Table 42: Systematic uncertainties for resonance m_H=400 GeV in percent.

Uncertainty Source	Relative Variations
$JET\_BJES\_Response\_\_1up$	-0.0191919
$JET\_BJES\_Response\_\_1down$	0.000842298
$JET\_EffectiveNP\_1\_\_1up$	3.5599
$JET\_EffectiveNP\_1\_\_1down$	-3.31994
$JET\_EffectiveNP\_2\_\_1up$	-0.579131
$JET\_EffectiveNP\_2\_\_1down$	0.69749
$JET\_EffectiveNP\_3\_\_1up$	0.139933
$JET\_EffectiveNP\_3\_\_1down$	-0.154411
$JET\_EffectiveNP\_4\_\_1up$	-0.0713251
$JET\_EffectiveNP\_4\_\_1down$	0.110989
$JET\_EffectiveNP\_5\_\_1up$	0.0174511
$JET\_EffectiveNP\_5\_\_1down$	0.0141711
$JET\_EffectiveNP\_6restTerm\_\_1up$	0.05949
$JET\_EffectiveNP\_6restTerm\_\_1down$	-0.0354765
$JET\_EtaIntercalibration\_Modelling\_\_1up$	1.08284
$JET\_EtaIntercalibration\_Modelling\_\_1down$	-1.00525
$JET\_EtaIntercalibration\_NonClosure\_\_1up$	-0.0307256
$JET\_EtaIntercalibration\_NonClosure\_\_1down$	0.0415638
$JET\_EtaIntercalibration\_TotalStat\_\_1up$	0.691905
$JET\_EtaIntercalibration\_TotalStat\_\_1down$	-0.533877
$JET\_Flavor\_Composition\_\_1up$	3.74891
$JET\_Flavor\_Composition\_\_1down$	-3.64132
$JET\_Flavor\_Response\_\_1up$	-1.00064
$JET\_Flavor\_Response\_\_1down$	1.2181
$JET\_JER\_SINGLE\_NP\_\_1up$	0.614238
$JET\_Pileup\_OffsetMu\_\_1up$	0.614217
$JET\_Pileup\_OffsetMu\_\_1down$	-0.309687
$JET\_Pileup\_OffsetNPV\_\_1up$	0.779765
$JET\_Pileup\_OffsetNPV\_\_1down$	-0.510067
$JET\_Pileup\_PtTerm\_\_1up$	0.0245509
$JET\_Pileup\_PtTerm\_\_1down$	-0.0158138
$JET\_Pileup\_RhoTopology\_\_1up$	1.1769
$JET\_Pileup\_RhoTopology\_\_1down$	-1.06645
$JET\_PunchThrough\_MC15\_\_1up$	-4.6315e-08
$JET\_PunchThrough\_MC15\_\_1down$	5.27753e-08
$JET\_SingleParticle\_HighPt\_\_1up$	0
$JET\_SingleParticle\_HighPt\_\_1down$	0
$JvtEfficiencyDown$	-3.86063
$JvtEfficiencyUp$	3.97448

Table 43: Systematic uncertainties for resonance m_H=400 GeV in percent.

Uncertainty Source	Relative Variations
$FT\_EFF\_Eigen\_B\_0\_\_1down$	-0.0716015
$FT\_EFF\_Eigen\_B\_0\_\_1up$	0.0727777
$FT\_EFF\_Eigen\_B\_1\_\_1down$	-0.00631027
$FT\_EFF\_Eigen\_B\_1\_\_1up$	0.00630238
$FT\_EFF\_Eigen\_B\_2\_\_1down$	0.00782721
$FT\_EFF\_Eigen\_B\_2\_\_1up$	-0.00779382
$FT\_EFF\_Eigen\_C\_0\_\_1down$	-0.382109
$FT\_EFF\_Eigen\_C\_0\_\_1up$	0.382571
$FT\_EFF\_Eigen\_C\_1\_\_1down$	0.213362
$FT\_EFF\_Eigen\_C\_1\_\_1up$	-0.213237
$FT\_EFF\_Eigen\_C\_2\_\_1down$	0.0389718
$FT\_EFF\_Eigen\_C\_2\_\_1up$	-0.0389718
$FT\_EFF\_Eigen\_C\_3\_\_1down$	0.03579
$FT\_EFF\_Eigen\_C\_3\_\_1up$	-0.035785
$FT\_EFF\_Eigen\_Light\_0\_\_1down$	-0.408701
$FT\_EFF\_Eigen\_Light\_0\_\_1up$	0.409931
$FT\_EFF\_Eigen\_Light\_1\_\_1down$	0.00140027
$FT\_EFF\_Eigen\_Light\_1\_\_1up$	-0.00139965
$FT\_EFF\_Eigen\_Light\_2\_\_1down$	-0.0332797
$FT\_EFF\_Eigen\_Light\_2\_\_1up$	0.0332879
$FT\_EFF\_Eigen\_Light\_3\_\_1down$	-0.0188859
$FT\_EFF\_Eigen\_Light\_3\_\_1up$	0.0188886
$FT\_EFF\_Eigen\_Light\_4\_\_1down$	-0.00444944
$FT\_EFF\_Eigen\_Light\_4\_\_1up$	0.00444943
$FT\_EFF\_extrapolation\_\_1down$	0.00260789
$FT\_EFF\_extrapolation\_\_1up$	-0.00260789
$FT\_EFF\_extrapolation\_from\_charm\_\_1down$	0.000319309
$FT\_EFF\_extrapolation\_from\_charm\_\_1up$	-0.000319308

Table 44: Systematic uncertainties for resonance m_H=400 GeV in percent.

Uncertainty Source	Relative Variations
$EG\_RESOLUTION\_ALL\_\_1down$	1.19109
$EG\_RESOLUTION\_ALL\_\_1up$	-2.19589
$EG\_SCALE\_ALL\_\_1down$	-7.27539
$EG\_SCALE\_ALL\_\_1up$	1.48794
$EL\_EFF\_ID\_TOTAL\_1NPCOR\_PLUS\_UNCOR\_\_1down$	-0.642961
$EL\_EFF\_ID\_TOTAL\_1NPCOR\_PLUS\_UNCOR\_\_1up$	0.642961
$EL\_EFF\_Iso\_TOTAL\_1NPCOR\_PLUS\_UNCOR\_\_1down$	-0.105524
$EL\_EFF\_Iso\_TOTAL\_1NPCOR\_PLUS\_UNCOR\_\_1up$	0.105525
$EL\_EFF\_Reco\_TOTAL\_1NPCOR\_PLUS\_UNCOR\_\_1down$	-0.255709
$EL\_EFF\_Reco\_TOTAL\_1NPCOR\_PLUS\_UNCOR\_\_1up$	0.255709
$MUONS\_ID\_\_1down$	0.00739576
$MUONS\_ID\_\_1up$	-0.0101099
$MUONS\_MS\_\_1down$	-0.0191376
$MUONS\_MS\_\_1up$	-0.0163516
$MUONS\_SCALE\_\_1down$	-0.00927138
$MUONS\_SCALE\_\_1up$	-0.0184411
$MUON\_EFF\_STAT\_LOWPT\_\_1down$	-0.0413076
$MUON\_EFF\_STAT\_LOWPT\_\_1up$	0.0413077
$MUON\_EFF\_STAT\_\_1down$	-0.100556
$MUON\_EFF\_STAT\_\_1up$	0.100556
$MUON\_EFF\_SYS\_LOWPT\_\_1down$	-0.0443808
$MUON\_EFF\_SYS\_LOWPT\_\_1up$	0.0443809
$MUON\_EFF\_SYS\_\_1down$	-0.159728
$MUON\_EFF\_SYS\_\_1up$	0.159741
$MUON\_ISO\_STAT\_\_1down$	-0.0129887
$MUON\_ISO\_STAT\_\_1up$	0.0129887
$MUON\_ISO\_SYS\_\_1down$	-0.10585
$MUON\_ISO\_SYS\_\_1up$	0.10585
$MUON\_TTVA\_STAT\_\_1down$	-0.0691934
$MUON\_TTVA\_STAT\_\_1up$	0.0691934
$MUON\_TTVA\_SYS\_\_1down$	-0.230609
$MUON\_TTVA\_SYS\_\_1up$	0.230608
$PH\_EFF\_ID\_Uncertainty\_\_1down$	-4.12358
$PH\_EFF\_ID\_Uncertainty\_\_1up$	4.21043
$PH\_EFF\_TRKISO\_Uncertainty\_\_1down$	-1.06792
$PH\_EFF\_TRKISO\_Uncertainty\_\_1up$	1.07389
$PH\_Iso\_DDonoff$	0.0237342
$PRW\_DATASF\_\_1down$	0.722756
$PRW\_DATASF\_\_1up$	-1.06892

Table 45: Systematic uncertainties for resonance m_H=500 GeV in percent.

Uncertainty Source	Relative Variations
$JET\_BJES\_Response\_\_1up$	0.000256431
$JET\_BJES\_Response\_\_1down$	-0.014022
$JET\_EffectiveNP\_1\_\_1up$	2.37117
$JET\_EffectiveNP\_1\_\_1down$	-2.08474
$JET\_EffectiveNP\_2\_\_1up$	-0.21815
$JET\_EffectiveNP\_2\_\_1down$	0.257214
$JET\_EffectiveNP\_3\_\_1up$	0.0272116
$JET\_EffectiveNP\_3\_\_1down$	-0.0814985
$JET\_EffectiveNP\_4\_\_1up$	-0.0495605
$JET\_EffectiveNP\_4\_\_1down$	0.0153503
$JET\_EffectiveNP\_5\_\_1up$	0.0021212
$JET\_EffectiveNP\_5\_\_1down$	-0.00773931
$JET\_EffectiveNP\_6restTerm\_\_1up$	0.0105241
$JET\_EffectiveNP\_6restTerm\_\_1down$	-0.034024
$JET\_EtaIntercalibration\_Modelling\_\_1up$	0.744119
$JET\_EtaIntercalibration\_Modelling\_\_1down$	-0.734607
$JET\_EtaIntercalibration\_NonClosure\_\_1up$	-0.0270339
$JET\_EtaIntercalibration\_NonClosure\_\_1down$	0.0484056
$JET\_EtaIntercalibration\_TotalStat\_\_1up$	0.301142
$JET\_EtaIntercalibration\_TotalStat\_\_1down$	-0.24202
$JET\_Flavor\_Composition\_\_1up$	2.51364
$JET\_Flavor\_Composition\_\_1down$	-2.35652
$JET\_Flavor\_Response\_\_1up$	-0.387368
$JET\_Flavor\_Response\_\_1down$	0.638017
$JET\_JER\_SINGLE\_NP\_\_1up$	-0.313753
$JET\_Pileup\_OffsetMu\_\_1up$	0.291944
$JET\_Pileup\_OffsetMu\_\_1down$	-0.3405
$JET\_Pileup\_OffsetNPV\_\_1up$	0.324114
$JET\_Pileup\_OffsetNPV\_\_1down$	-0.247961
$JET\_Pileup\_PtTerm\_\_1up$	0.0535772
$JET\_Pileup\_PtTerm\_\_1down$	-0.0033064
$JET\_Pileup\_RhoTopology\_\_1up$	0.791397
$JET\_Pileup\_RhoTopology\_\_1down$	-0.519537
$JET\_PunchThrough\_MC15\_\_1up$	-1.20311e-07
$JET\_PunchThrough\_MC15\_\_1down$	6.05641e-08
$JET\_SingleParticle\_HighPt\_\_1up$	0
$JET\_SingleParticle\_HighPt\_\_1down$	0
$JvtEfficiencyDown$	-3.55171
$JvtEfficiencyUp$	3.65112

Table 46: Systematic uncertainties for resonance m_H=500 GeV in percent.

C Cut optimizations

The cuts on the photons side are fully followed the HGam group, and the following optimizations are all on the W boson and its decay products sides. The distributions of the variables are shown in Figure 38 and

Uncertainty Source	Relative Variations
$FT\_EFF\_Eigen\_B\_0\_\_1down$	-0.0566851
$FT\_EFF\_Eigen\_B\_0\_\_1up$	0.0567041
$FT\_EFF\_Eigen\_B\_1\_\_1down$	-0.0199968
$FT\_EFF\_Eigen\_B\_1\_\_1up$	0.0200009
$FT\_EFF\_Eigen\_B\_2\_\_1down$	0.000385072
$FT\_EFF\_Eigen\_B\_2\_\_1up$	-0.000384634
$FT\_EFF\_Eigen\_C\_0\_\_1down$	-0.423624
$FT\_EFF\_Eigen\_C\_0\_\_1up$	0.424161
$FT\_EFF\_Eigen\_C\_1\_\_1down$	0.181606
$FT\_EFF\_Eigen\_C\_1\_\_1up$	-0.181515
$FT\_EFF\_Eigen\_C\_2\_\_1down$	0.0756307
$FT\_EFF\_Eigen\_C\_2\_\_1up$	-0.0756274
$FT\_EFF\_Eigen\_C\_3\_\_1down$	0.0163465
$FT\_EFF\_Eigen\_C\_3\_\_1up$	-0.0163466
$FT\_EFF\_Eigen\_Light\_0\_\_1down$	-0.422124
$FT\_EFF\_Eigen\_Light\_0\_\_1up$	0.423487
$FT\_EFF\_Eigen\_Light\_1\_\_1down$	0.00700396
$FT\_EFF\_Eigen\_Light\_1\_\_1up$	-0.00700127
$FT\_EFF\_Eigen\_Light\_2\_\_1down$	-0.02689
$FT\_EFF\_Eigen\_Light\_2\_\_1up$	0.0268958
$FT\_EFF\_Eigen\_Light\_3\_\_1down$	-0.0168426
$FT\_EFF\_Eigen\_Light\_3\_\_1up$	0.0168451
$FT\_EFF\_Eigen\_Light\_4\_\_1down$	-0.00343164
$FT\_EFF\_Eigen\_Light\_4\_\_1up$	0.00343171
$FT\_EFF\_extrapolation\_\_1down$	0.00722075
$FT\_EFF\_extrapolation\_\_1up$	-0.00722292
$FT\_EFF\_extrapolation\_from\_charm\_\_1down$	0.00028759
$FT\_EFF\_extrapolation\_from\_charm\_\_1up$	-0.000287589

Table 47: Systematic uncertainties for resonance m_H=500 GeV in percent.

Figure 39. At the left region for Figure 38(a), 38(c), 39(a), 39(c) and the right region for Figure 38(b), 39(b), the signal statistics will be low if there is a cut on these variables. The Asimov significance on the right plots is definded as Z in the Eq 1. Applying a cut on these variables doesn't improve the sensitivities too much and will decrise the signal statistics excessively. There will be not further cut besides the cuts listed in Section 5.

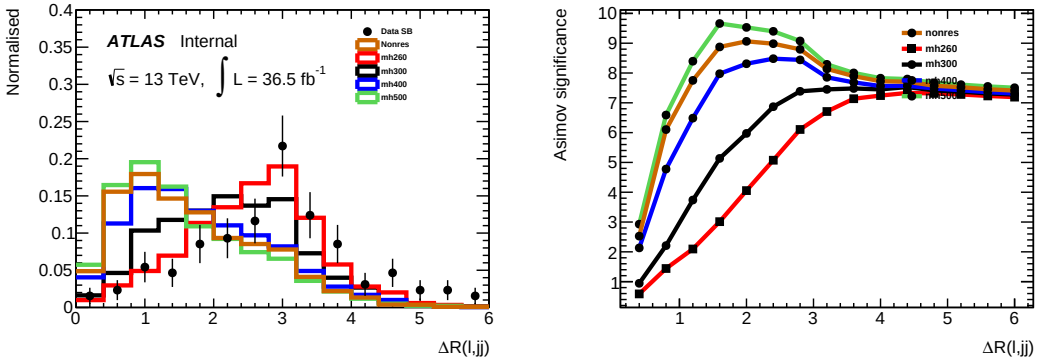

(a)

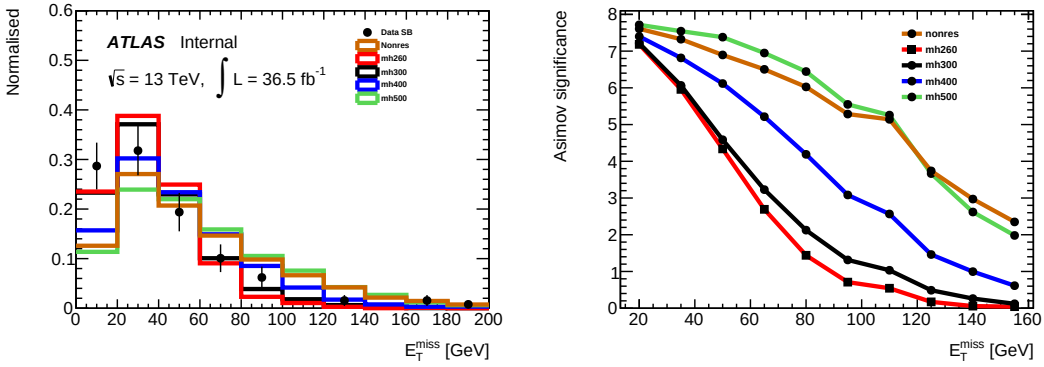

(b)

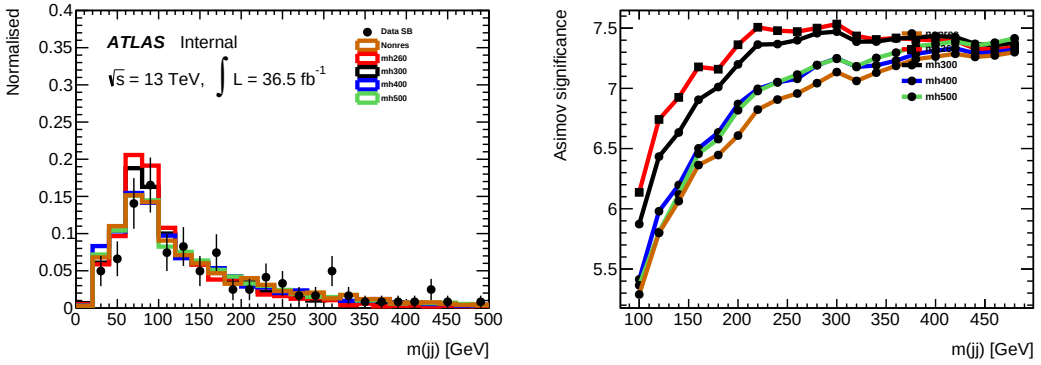

(c)

Figure 38: (a) The ΔR between the leading lepton and the di-jet system, (b) transverse missing energy, (c) the invariant mass of di-jet system.

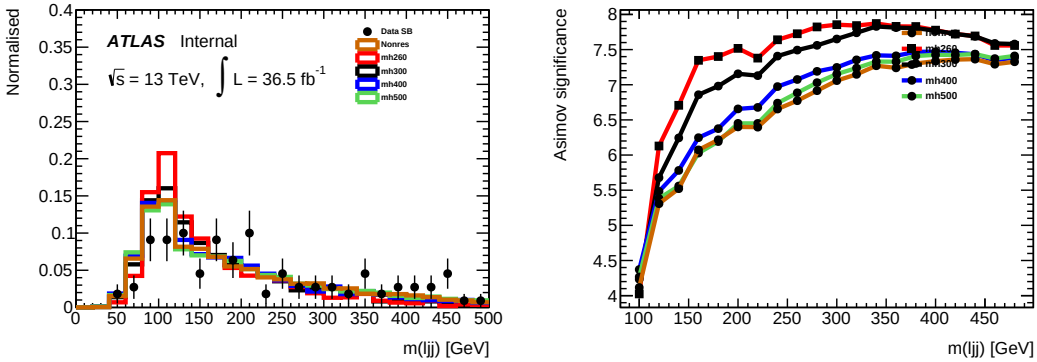

(a)

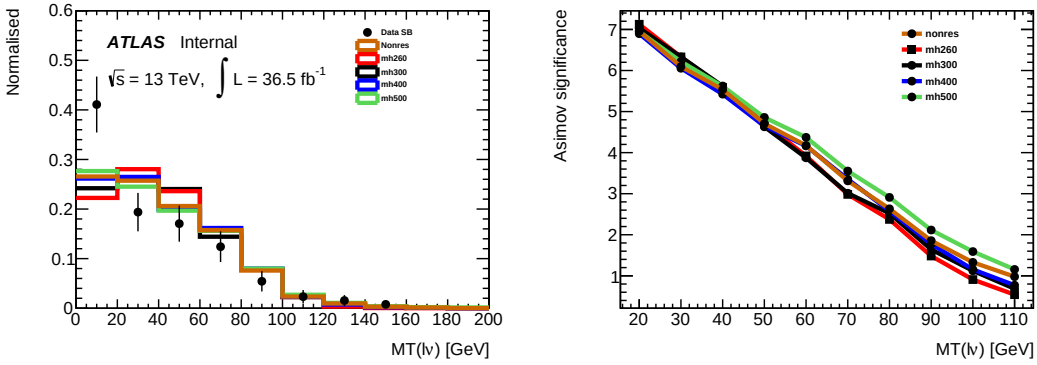

(b)

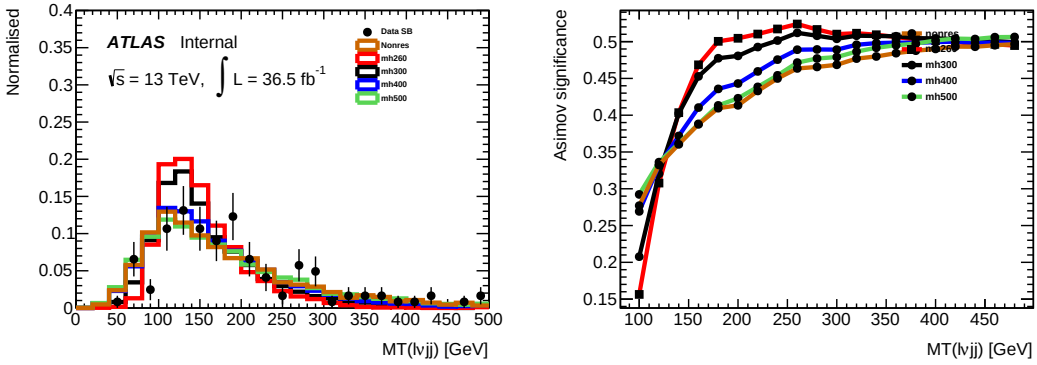

(c)

Figure 39: (a) The invatiant mass of lepton and di-jet, (b) transverse mass of the leading lepton and MET, (c) transverse mass of the leading lepton, MET and di-jet.